4167-6002-RU000

Final Report

for

Theoretical Investigation; the Scattering of Light by a Planetary Atmosphere

(1 June 1964 - 1 December 1964)

Contract No. NAS5-3891

Prepared by
TRW Space Technology Laboratories
One Space Park
Redondo Beach, California

for
Goddard Space Flight Center
Greenbelt, Maryland

4167-6002-RU-000

Final Report
for

Theoretical Investigation; the Scattering of Light by a Planetary Atmosphere

(1 June 1964 - 1 December 1964)

Contract No.: NAS5-3891

Prepared by

Robert S. Fraser

TRW Space Technology Laboratories
One Space Park
Redondo Beach, California

Robert S. Fraser
Theoretical Physics Department
Quantum Physics Laboratory

Approved:

Saul Altshuler, Manager
Theoretical Physics Department

H. C. Corben, Director
Quantum Physics Laboratory

for

Goddard Space Flight Center
Greenbelt, Maryland

ABSTRACT

20758

A theoretical-computational study is presented on how specular reflection at the ground modifies the light scattered outwards from the top of a homogeneous Rayleigh atmosphere. The computations for this model are compared with computations for a second model, which is the same, except that the ground of the second model reflects radiation according to Lambert's law. Upon comparing the corresponding radiation parameters for the two models, when their atmospheric optical thickness (τ_1) is not large ($\tau_1 < 1.0$), one sees that the relative difference is small for the flux, increases for the specific intensity, becomes large for the maximum degree of polarization, and is still larger for the neutral point positions. The neutral point characteristics for the two models are quite different for optical thickness smaller than 0.25. The flow of the radiation is divided into several streams that have physical significance and can be calculated separately. Under certain conditions some of these streams can be neglected.

Author ↑

TABLE OF CONTENTS

LIST OF ILLUSTRATIONS

Page

Page

Page

LIST OF TABLES

I. INTRODUCTION

The characteristics of radiation scattered from a planetary atmosphere depend on how the radiation is reflected from a surface at the lower boundary of the atmosphere. One extreme type of reflection from a surface occurs when the incident and reflected radiation are uncorrelated to the extent that the reflected radiation is unpolarized and of equal intensity in all directions towards the upward hemisphere, independent of the character of the incident radiation. This type of reflection, referred to as Lambert reflection, has generally been used in studies of radiative transfer in planetary atmospheres because of its simplicity.[1,4,5,6,11,13,23]* Another extreme type of surface reflection occurs when the radiation reflected from the surface is perfectly correlated with the incident radiation, as occurs when radiation is specularly reflected from a smooth, plane surface according to Fresnel's law. The purpose of this study is to compute the effect on the radiation field of Frensel reflection from the lower boundary, or ground.

Fraser and Sekera[14] commenced the study of the effect of Fresnel reflection by deriving the equations for the intensity matrix that gives the Stokes parameters of the radiation that falls on the ground, when the atmosphere is externally illuminated on top by parallel radiation and scatters the radiation according to Rayleigh's law. Later, Professor Sekera used these equations to compute the radiation parameters.[24] The

---

* The superscript refers to the reference number. Because there will be many references to Chandrasekhar's Radiative Transfer, it will be designated by R.T.

computations showed that the degree of polarization and the intensity of the radiation falling on the ground for the Fresnel model are nearly the same for corresponding parameters for the Lambert model of reflection. However, the locations of the neutral points in the degree of polarization field differ significantly for the two models.

Dave and Sekera[8] derived most of the equations that are required to compute the parameters that characterize the radiation leaving the upper surface of a Rayleigh atmosphere. Fraser independently derived equations for the same parameters. The two sets of analyses agreed with each other. The equations for the radiation parameters at the upper boundary of the atmosphere will be derived in the next section. This analysis will depend on the characteristics of the radiation at the lower boundary. Although the equations for the radiation parameters at the ground are given in a report[14], the report is not obtained easily. Hence, the equations for the ground parameters are included in this report.

The section following the theory presents details of the computational routine. The accuracy of the data is discussed, also. Then the results of the computations are given in another section.

The effect of Fresnel ground reflection on the radiation leaving the top of a Rayleigh atmosphere will be shown by comparing the radiation parameters for the model with Fresnel ground reflection and the parameters for the same model, except that the Fresnel law is replaced by the Lambert law. The albedo at the ground is the same for both models. The radiation

parameters that will be used are the flux, total intensity, degree of polarization and the neutral points. The data for the Fresnel model can be applied to planetary atmospheres that have a small aerosol content and lie above extensive bodies of water that are not too rough, since such water reflects light according to approximately Fresnel's law.[7,18]

The flow of radiation for the Fresnel model is separated into several streams, which have physical significance and whose properties can be computed separately. The radiation characteristics of these streams are studied as a function of the ground albedo in order to find the conditions for which the characteristics of a stream can be neglected and thereby simplify the computations.

II. THEORY

The following analyses will be based on Chandrasekhar's[4] solution of the planetary problem. The only difference between the problem solved by Chandrasekhar and the one solved here is that Chandrasekhar assumed that the ground reflected radiation according to Lambert's law, and here the assumption is that the ground reflects according to Fresnel's law. However, the reader need not be familiar with Chandrasekhar's R.T. to follow the analysis given here. Before the equations for the radiation parameters are derived, the radiation parameters that will be used are introduced. Then the radiation characteristics of the atmospheric model are presented. Finally, the description of the planetary atmosphere model is completed with a review of Fresnel's law of reflection from a dielectric ground.

A. Model

1. Radiation parameters

The intensity and polarization characteristics of a quasi-monochromatic pencil of light in a scattering atmosphere are conveniently represented by four Stokes parameters. The Stokes parameters are defined and discussed in R.T., Chapt. 1. The matrix of the Stokes parameters that is used in this report will be called the intensity matrix and is

$$\underline{I}\,(\tau;\mu,\phi) = \begin{pmatrix} I_\ell \\ I_r \\ U \\ V \end{pmatrix} \quad . \qquad (2.1)$$

Each of the four parameters has the same functional dependence that is shown on the left-hand side of the equation. The matrix is independent of time for the particular models used here, but the matrix depends on position, which is customarily given by only the normal optical thickness (τ) for the type of model atmosphere that will be used. The normal optical thickness of a plane layer of atmosphere between the top and a level at distance z above the lower boundary can be defined in terms of a scattering cross-section per particle, σ, and the number of particles per unit volume, N, by the relation

$$\tau(z,\lambda) = \int_z^\infty \sigma(z,\lambda)\, N(z)\, dz \quad , \qquad (2.2)$$

where λ represents the radiation wave length. The optical thickness increases from zero at the top of the atmosphere to the maximum value τ_1 at the lower boundary, where z = 0. The optical thickness is defined in Eq. (2.2) for a single wave length, but usually τ does not change appreciably over the small spectral bandwidth for which the intensity matrix (2.1) applies. The intensity matrix also depends on the direction that the radiation is flowing; ϕ represents the azimuth and $\mu = \cos\theta$, where θ is the angle measured

from the positive z-axis. Since it is convenient to use the absolute value of μ in many equations that will be given, μ will be restricted to positive values: $0 \leq \mu \leq 1$. To do this, radiation flowing from the upper to the lower boundary, inwards, will depend on $-\mu$, and radiation flowing outwards will depend on μ.

The Stokes parameters have a physical significance that depends on a local coordinate system. A useful coordinate system is constructed as follows: consider an arbitrary pencil of radiation. Pass a plane perpendicular to the lower boundary of the atmosphere through the pencil. Such a plane will be called a vertical plane. Introduce two unit vectors $\underset{\sim}{\ell}$ and $\underset{\sim}{r}$, which are parallel and perpendicular, respectively, to the vertical plane. Furthermore, let the vector cross-product $\underset{\sim}{r} \times \underset{\sim}{\ell}$ point in the direction that the radiation is flowing. Then the Stokes parameters I_ℓ and I_r are the values of the intensities in the two planes containing the pencil of radiation and $\underset{\sim}{\ell}$ and $\underset{\sim}{r}$, respectively. The total intensity is obtained by adding I_ℓ and I_r:

$$I = I_r + I_\ell \quad . \tag{2.3}$$

The inclination of the plane of polarization (χ) from $\underset{\sim}{\ell}$ is given by the equation

$$\tan 2\chi = \frac{U}{I_\ell - I_r} \quad . \tag{2.4}$$

The ellipticity of the light depends on the parameter V. However, V = 0 for the models of atmosphere and ground reflection that are used here, if the external source of radiation falling on the atmosphere is unpolarized, as will be assumed in these computations. Therefore, the parameter V will not be needed.

The degree of polarization (P') is defined in terms of the Stokes parameters by the following equation:

$$P' = \frac{\left[(I_r - I_\ell)^2 + U^2 + V^2 \right]^{1/2}}{I} \quad . \qquad (2.5)$$

In some important cases U = V = 0; then another quantity, given by the relation

$$P = \frac{I_r - I_\ell}{I} \quad , \qquad (2.6)$$

is more useful. The absolute value of P equals the degree of polarization. The advantage of using P rather than P' is that the sign of P gives the orientation of the plane of polarization. Since Eq. (2.6) is used only when U = 0, on these occasions the plane of polarization is either perpendicular or parallel to the vertical plane that passes through the pencil of radiation being considered. P is positive or negative according to whether the plane of polarization is perpendicular or parallel, respectively, to the vertical

plane. The quantity P will be called the degree of polarization; and the degree of polarization will be called negative when P is negative.

2. Atmosphere

The model atmosphere that is used for the computations is composed of non-absorbing particles that scatter light according to the Rayleigh law. All characteristics of the Rayleigh law can be obtained from the following relation between the intensity matrices of the scattered ($\underline{I}^{(s)}$) and incident pencils ($\underline{I}$) (see R.T., p. 37-39):

$$\underline{I}^{(s)} = \begin{pmatrix} I_{\ell}^{(s)} \\ I_{r}^{(s)} \\ U^{(s)} \\ V^{(s)} \end{pmatrix} = \frac{3}{8\pi} \frac{d\tau}{\mu} d\omega \begin{pmatrix} \cos^2 \Theta & 0 & 0 & 0 \\ 0 & 1 & 0 & 0 \\ 0 & 0 & \cos \Theta & 0 \\ 0 & 0 & 0 & \cos \Theta \end{pmatrix} \underline{I}, \quad (2.7)$$

where the incident pencil is confined to the solid angle $d\omega$, and Θ is the angle between the directions of propagation of the pencils of the incident and scattered light. In Eq. (2.7) only, the $\underset{\sim}{\ell}$ and $\underset{\sim}{r}$ vectors are parallel and perpendicular, respectively, to the scattering plane, which contains the two pencils of incident and scattered light. In order to review the characteristics of light scattered according to the Rayleigh law, let the incident light be unpolarized, that is, $\underline{I} = \frac{1}{2}(1, 1, 0, 0)$. Since $U^{(s)} = 0$, the plane of polarization of the scattered light is either parallel or

perpendicular to the scattering plane. The plane of polarization is perpendicular to the scattering plane; since $I_{\ell}^{(s)} \sim \cos^2 \Theta$ and $I_r^{(s)} \sim 1$, then $I_{\ell}^{(s)} \leq I_r^{(s)}$. The degree of polarization of the scattered light is given by the expression $P = \sin^2 \Theta \ (1 + \cos^2 \Theta)^{-1}$; the degree of polarization is zero for forward and backward scattering and is 100 percent in a direction perpendicular to the incident pencil. The total intensity of the scattered light ($I^{(s)}$) is proportional to $1 + \cos^2 \Theta$; hence, the intensity of the light scattered perpendicularly to the incident pencil is one-half of the maximum intensity, which occurs in the forward and backward directions.

The intensities of Rayleigh scattering ($I_{\ell}^{(s)}$, $I_r^{(s)}$, $I^{(s)}$) depend on wave length, which enters into Eq. (2.7) through the optical thickness $d\tau(\lambda)$. According to Eq. (2.7), the intensities are directly proportional to the optical thickness, whose equation for a gaseous, non-absorbing atmosphere is

$$d\tau(\lambda) = \frac{8\pi^3}{3} \frac{(m^2 - 1)^2}{\lambda^4 N} \, dz \quad , \qquad (2.8)$$

where m is the index of refraction of the gas (R.T., p. 38). (The Rayleigh theory need not be restricted to gases, but is valid also for small spheres whose index of refraction is near one.) If the index of refraction is independent of wave length, the optical thickness, and therefore the intensities, are inversely proportional to the fourth power of the wave length, a well-known characteristic of Rayleigh scattering. In the case of the gaseous part of the earth's atmosphere, for example, the index of refraction depends

only slightly on wave length.[12] Hence, the intensities of the light that is scattered from a small mass of the earth's atmosphere are very nearly proportional to the inverse fourth power of the wave length.

Other specifications of the model atmosphere are introduced now. The model atmosphere is assumed to be plane-parallel; that is, the physical properties vary only in the vertical (z) direction. The radiation parameters do not depend on horizontal coordinates, but only on the optical thickness, which is a function of height. Furthermore, the model atmosphere is homogeneous, because the phase matrix and absorption cross-section, which equals zero, are independent of height. Each particle of the model atmosphere is assumed to scatter light independently of the others in order to add the Stokes parameters. The model atmosphere is bounded on the top by a vacuum, and on the bottom by a surface that reflects the light incident on it according to Fresnel's law. Only light from above is incident on the lower boundary. If the light incident on the lower boundary is not reflected up into the atmosphere, it is lost to the radiation field.

The model atmosphere that has just been given deviates more or less from those planetary atmospheres whose compositions are known to some extent, even when the sphericity of the true atmosphere can be neglected. First, the known planetary atmospheres are believed to contain particles that do not scatter light according to Rayleigh's law. The phase matrix for such particles is more complex than the Rayleigh phase matrix and make the computations for the characteristics of the scattered light more difficult. Second, true planetary atmospheres are not homogeneous, even in the vertical direction: the phase

matrix, scattering and absorption cross-sections vary with respect to height. The techniques that will be used later to find a solution for the intensity matrix of the planetary problem can not be applied to inhomogeneous atmospheres.

3. Reflection laws at the lower boundary

The computed radiation parameters will be compared for the two cases that the ground reflects the incident light according to Fresnel's and to Lambert's law.

Light is reflected from a surface according to Lambert's law, when the reflected light is unpolarized and of equal intensity (I) in all directions towards the outward hemisphere, regardless of the state of polarization of the light incident on the surface.

Fresnel's law of reflection will be used here only when the medium below the boundary is a dielectric with an index of refraction m. The atmosphere has already been given the properties of a dielectric, whose index of refraction is now assigned the value of one. The deviation from the true value is less than 3×10^{-4} for the earth's atmosphere and the visible spectrum. When light is incident from above onto the lower boundary, the characteristics of the light reflected according to Fresnel's law are: the pencils of incident and reflected light lie in the same vertical plane; the zenith angle of the reflected light equals the supplement of the zenith angle of the incident light; and the matrices of the reflected light ($\uparrow\underline{I}_g$) and incident light ($\downarrow\underline{I}$) are related by a reflection matrix ($\underline{R}$) as follows:

$$\uparrow \underline{I}_g(\tau_1;\mu,\phi) = \begin{pmatrix} I_{g,\ell} \\ I_{g,r} \\ U_g \\ V_g \end{pmatrix} = \underline{R}(\mu) \downarrow \underline{I}(\tau_1;-\mu,\phi) \quad , \tag{2.9}$$

$$\underline{R}(\mu) = R(\mu) \begin{pmatrix} q^2(\mu) & 0 & 0 & 0 \\ 0 & 1 & 0 & 0 \\ 0 & 0 & q(\mu) & 0 \\ 0 & 0 & 0 & q(\mu) \end{pmatrix} , \tag{2.10}$$

$$R(\mu) = \left[\frac{\mu - (m^2 - 1 + \mu^2)^{1/2}}{\mu + (m^2 - 1 + \mu^2)^{1/2}} \right]^2 , \tag{2.11}$$

$$q(\mu) = \frac{1 - \mu^2 - \mu(m^2 - 1 + \mu^2)^{1/2}}{1 - \mu^2 + \mu(m^2 - 1 + \mu^2)^{1/2}} . \tag{2.12}$$

The arrows that are introduced in Eq. (2.9) are redundant, but they eliminate any uncertainty about whether the radiation is flowing upwards or downwards.

The intensities and degree of polarization of light that would be reflected upwards from a surface according to Fresnel's laws (Eq. (2.9) are shown on Fig. 1. The ratio of the indices of refraction of the lower to the upper medium is m = 1.346, which is the index of refraction of some sea waters at the wave length λ4364 Å. The light incident on the lower medium is unpolarized and of intensity I = 1. For nearly normal incidence, only

two percent of the incident light is reflected, and it is nearly neutral. As the angle of incidence increases, the reflected light becomes partially, plane polarized, and eventually becomes completely polarized at the Brewster angle;* but only 4 percent of the incident radiation is reflected at the Brewster angle. As the angle of incidence increases beyond the Brewster angle, the total intensity rapidly increases to one and the degree of polarization decreases to zero at $i = 90^{\circ}$.

---

* The Brewster angle occurs at the angle of incidence where $\uparrow I_{g,\ell} = 0$. On Fig. 1 the Brewster angle = 53.4° .

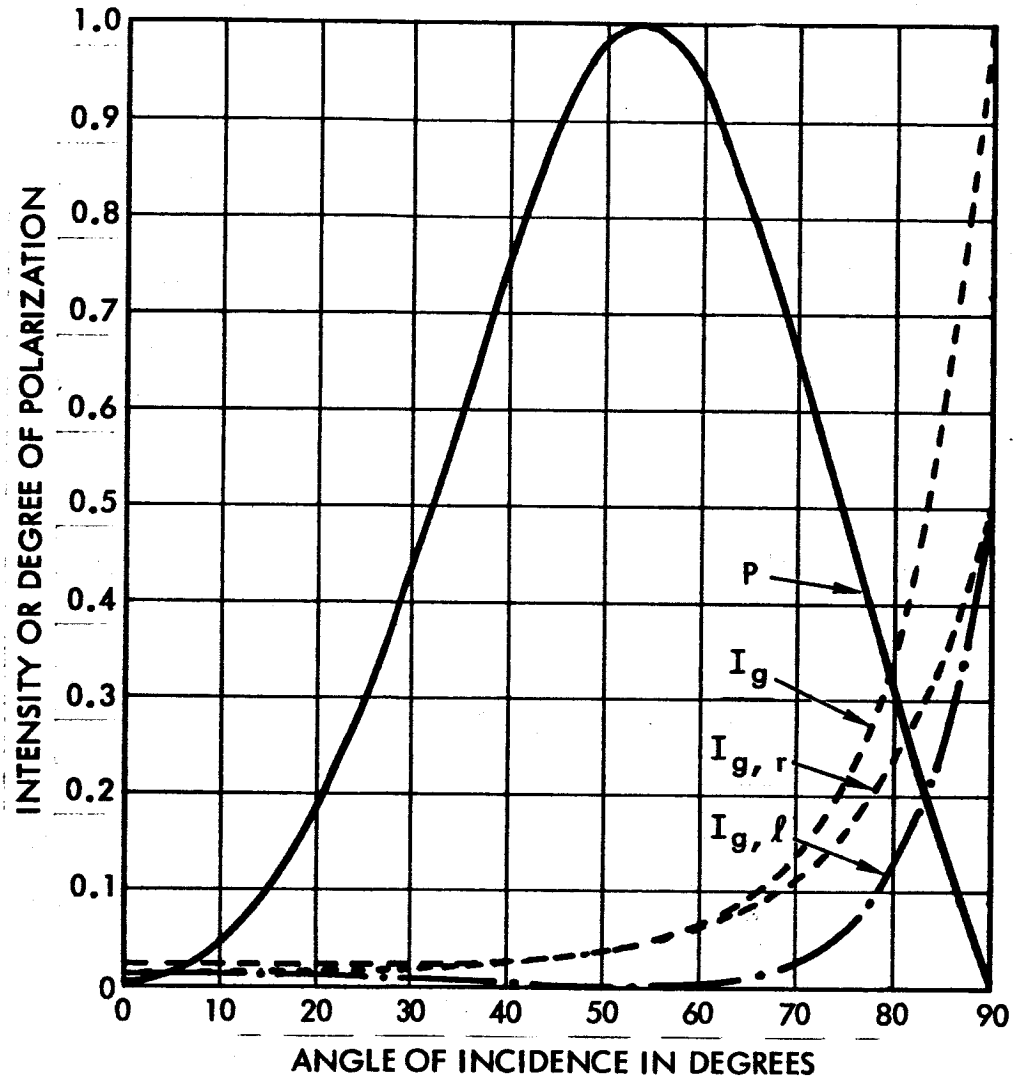

Figure 1. Intensities and degree of polarization of light reflected upward from a plane surface according to Fresnel's law. The ratio of the indices of refraction of the lower to the upper medium is m = 1.346. The light incident on the lower medium is unpolarized and of total intensity I = 1.

B. Equations for Radiation

1. Boundary conditions

The model atmosphere is illuminated by an external source of parallel, unpolarized radiation that is incident on top of the atmosphere in the direction $-\mu_o, \phi_o$. The matrix of the incident flux is given by

$$\pi \underline{F}(-\mu_o,\phi_o) = \frac{\pi F_o}{2} \begin{pmatrix} 1 \\ 1 \\ 0 \\ 0 \end{pmatrix} . \qquad (3.1)$$

Hence, $\pi F_o \mu_o$ units of flux flow through a horizontal surface at the top of the atmosphere. The reduced incident flux, $e^{-\tau_1/\mu_o} \pi \underline{F}(-\mu_o,\phi_o)$, will be distinguished from the diffuse radiation, or airlight, which arises as a result of one or more scatterings. Since no diffuse radiation flows into the top of the atmosphere, the boundary condition on the diffuse radiation is

$$\downarrow \underline{I}(0;-\mu,\phi_o-\phi) = 0 , \qquad (3.2)$$

where $\phi_o-\phi$ indicates the azimuth relative to the azimuth (ϕ_o) of the incident flux.

The bottom of the atmosphere is illuminated from below by the radiation that is reflected from the lower boundary. Therefore, the lower boundary condition is specified by the matrix $\uparrow \underline{I}(\tau_1;\mu,\phi_o-\phi) \equiv \uparrow \underline{I}_g(\tau_1;\mu,\phi_o-\phi)$ which has already been given by Eq. (2.9).

The intensity matrices of the radiation passing outwards from the upper boundary, or flowing downwards at the lower boundary, are simply related to the boundary conditions by means of reflection ($\underline{S}$) and transmission ($\underline{T}$) matrices, which were first introduced in R.T., Chapt. 1. At the upper boundary, the equation for the intensity matrix of the upward flowing radiation is

$$\begin{aligned}\uparrow\underline{I}^{*}(0;\mu,\phi_o-\phi) = \frac{1}{4\mu}\ \underline{S}(\tau_1;\mu,\phi;\mu_o\phi_o)\ \underline{F}\ (-\mu_o\phi_o) \\ + \uparrow\underline{I}_g(\tau_1;\mu,\phi_o-\phi)\ e^{-\tau_1/\mu} \\ + \frac{1}{4\pi\mu}\int_0^1\int_0^{2\pi}\underline{T}(\tau_1;\mu,\phi;\mu',\phi') \\ x\ \uparrow\underline{I}_g(\tau_1;\mu',\phi')d\mu'd\phi' \quad .\end{aligned} \tag{3.3}$$

The first term on the right of the equation represents the Stokes parameters of the incident radiation that is scattered out of the atmosphere through the upper boundary before the radiation reaches the lower boundary. (The dependent variable notation of the $\underline{S}$ matrix, and similarly for the $\underline{T}$ matrix, indicates that the incident radiation is coming from the direction $-\mu_o,\phi_o$ and leaves the upper boundary in the direction μ,ϕ; the $\underline{S}$ and $\underline{T}$ matrices also depend on the total optical thickness of the atmosphere (τ_1) .) The second term on the right of Eq. (3.3) represents the characteristics of the radiation that passes directly from the lower boundary to the upper boundary

and experiences no change other than attenuation. The last term represents the characteristics of the radiation that leaves the lower boundary and is scattered at least once by the atmosphere before it finally emerges from the upper surface in the direction, μ,ϕ.

At the bottom of the atmosphere the intensity matrix for the inward flowing radiation is given by the equation

$$\downarrow\underline{I}^{*}(\tau_1;-\mu,\phi_o-\phi) = \frac{1}{4\mu}\,\underline{T}\,(\tau_1;\mu,\phi;\mu_o\phi_o)\,\underline{F}(-\mu_o,\phi_o) + \frac{1}{4\pi\mu}\int_o^1\int_o^{2\pi}\underline{S}(\tau_1;\mu,\phi;\mu',\phi') \times \uparrow\underline{I}_g\,(\tau_1;\mu',\phi_o-\phi')\,d\mu'd\phi' \quad . \tag{3.4}$$

The reduced solar flux, $\pi\,\underline{F}(-\mu_o\phi_o)e^{-\tau_1/\mu_o}$, augments the radiation when the direction $-\mu,\phi = -\mu_o,\phi_o$. The first term on the right of Eq. (3.4) represents the direct sunlight that has been scattered at least once, and only by the atmosphere, before it reaches the lower boundary. This term, and also the first term of Eq. (3.3), are independent of the reflectivity at the lower boundary. The second term of Eq. (3.4) represents the radiation reflected from the ground, or the illumination of the atmosphere from below, that is reflected back to the lower boundary by the atmosphere.

2. Analysis of radiation at the lower boundary

This section is subdivided into three subsections. In the first section an equation that can be used to compute the first term on the right

side of Eq. (3.4) is given. An equation for the second term is given in the second section. The equations for the albedo and fluxes are given in the third section.

a. First term

Introduce the following matrix for the first term:

$$\downarrow\underline{I}(\tau_1;-\mu,\phi_o-\phi) = \frac{1}{4\pi\mu}\,\underline{T}(\tau_1;\mu,\phi;\mu_o,\phi_o)\underline{F}(-\mu_o,\phi_o) \quad . \tag{3.5}$$

The $\underline{T}$ matrix is given in R.T., p 253, Eq. (122). When the $\underline{T}$ and $\underline{F}$ (Eq. (3.1)) matrices are substituted into Eq. (3.5), it becomes

$$\downarrow\underline{I}(\tau_1;-\mu,\phi_o-\phi) = \begin{pmatrix} I_\ell^{(o)}(\mu,\mu_o;1) \\ I_r^{(o)}(\mu,\mu_o;1) \\ 0 \end{pmatrix} - \mu_o\, I_\ell^{(1)}(\mu,\mu_o)\underline{P}^{(1)\,\prime}(-\mu,\phi_o-\phi) + (1-\mu_o^2)\underline{I}_r^{(2)}(\mu,\mu_o)\underline{P}^{(2)\,\prime}(-\mu,\phi_o-\phi) \quad . \tag{3.6}$$

The matrices that give the azimuthal dependence are defined by the following expressions:

$$\underline{P}^{(1)\,\prime}(\mu,\phi_o-\phi) = \begin{pmatrix} \mu\cos(\phi_o-\phi) \\ 0 \\ -\sin(\phi_o-\phi) \end{pmatrix} \quad , \tag{3.7}$$

$$\underline{P}^{(2)\,\prime}(\mu,\phi_o-\phi) = \begin{pmatrix} -\mu^2\cos 2(\phi_o-\phi) \\ \cos 2(\phi_o-\phi) \\ 2\mu\sin 2(\phi_o-\phi) \end{pmatrix} \quad . \tag{3.8}$$

The $I_{\ell}^{(o)}$, $I_{r}^{(o)}$, $I_{\ell}^{(1)}$, $I_{r}^{(1)}$ functions are not the same as those that appear in R.T. The definitions of these functions are as follows:

$$\begin{pmatrix} I_{\ell}^{(o)}\left[\mu,\mu_o;q(\mu_o)\right] \\ I_{r}^{(o)}\left[\mu,\mu_o;q(\mu_o)\right] \end{pmatrix} = \frac{3F_o\mu_o}{32(\mu-\mu_o)}\left[\underline{S}_2(\mu)\underline{S}_1'\left[\mu_o,q(\mu_o)\right] - \underline{S}_1(\mu)\underline{S}_2'\left[\mu_o,q(\mu_o)\right]\right] \quad ; \tag{3.9}$$

$$\underline{S}_1(\mu) = \begin{pmatrix} \psi(\mu) & \sqrt{2}\,\phi(\mu) \\ \chi(\mu) & \sqrt{2}\,\zeta(\mu) \end{pmatrix} \quad , \quad \underline{S}_2(\mu) = \begin{pmatrix} \xi(\mu) & \sqrt{2}\,\eta(\mu) \\ \sigma(\mu) & \sqrt{2}\,\theta(\mu) \end{pmatrix} ; \tag{3.10}$$

$$\underline{S}_1'\left[\mu,q(\mu)\right] = \begin{pmatrix} q^2(\mu)\,\psi(\mu) + \chi(\mu) \\ \sqrt{2}\left[q^2(\mu)\phi(\mu) + \zeta(\mu)\right] \end{pmatrix} \quad ,$$

$$\underline{S}_2'\left[\mu,q(\mu)\right] = \begin{pmatrix} q^2(\mu)\;\xi(\mu) + \sigma(\mu) \\ \sqrt{2}\left[q^2(\mu)\eta(\mu) + \theta(\mu)\right] \end{pmatrix} \quad . \tag{3.11}$$

The quantity q can have the value given by Eq. (2.12), or it can be assigned the value one, independent of μ, as in Eq. (3.6). Later, beginning with Eq. (3.26), a tilda appears over the matrices that are given by Eq. (3.10) and indicates their transpose. The eight functions that are introduced in Eq. (3.10) are defined in R.T., p. 269. The equations for the two other functions that appear in Eq. (3.6) are

$$I_{\ell}^{(o)}(\mu,\mu_o) = \frac{3\,F_o\mu_o}{8(\mu-\mu_o)}\left[(1-\mu^2)(1-\mu_o^2)\right]^{1/2}\left[Y^{(1)}(\mu)X^{(1)}(\mu_o) - X^{(1)}(\mu)Y^{(1)}(\mu_o)\right] , \tag{3.12}$$

$$I_{r}^{(2)}(\mu,\mu_o) = \frac{3\,F_o\mu_o}{32(\mu-\mu_o)}\left[Y^{(2)}(\mu)X^{(2)}(\mu_o) - X^{(2)}(\mu)Y^{(2)}(\mu_o)\right] . \tag{3.13}$$

The $X^{(i)}, Y^{(i)}$ functions ($i = 1,2$) are defined in R.T., p. 253, Eq. (124). The twelve scattering functions introduced into Eqs.(3.10),(3.12), and (3.13) are also dependent on the total optical thickness of the atmosphere (τ_1). Equations using the $\underline{T}$ matrix, such as Eqs. (3.9), (3.12), and (3.13) are indeterminate in the direction $\mu = \mu_o$. Wherever this indeterminancy appears in this analysis, the quantities can be evaluated by using L'Hospital's rule and taking just the first derivatives of the numerator and denominator.

b. Second term

The second term of Eq. (3.4) represents the radiation that is reflected from the lower boundary and then scattered by the atmosphere back down to the lower boundary. This term will be represented by the following intensity matrix:

$$\downarrow\underline{I}_g^{(refl)}(\tau_1;-\mu,\phi_o-\phi) = \frac{1}{4\pi\mu}\int_o^1\int_o^{2\pi}\underline{S}(\tau_1;\mu,\phi;\mu',\phi')\uparrow\underline{I}_g(\tau_1;\mu',\phi')\,d\mu'\,d\phi' , \tag{3.14}$$

where the $\underline{S}$ matrix is defined in R.T., p. 252, Eq. (122). The radiation that is reflected from the lower boundary can be separated into three different components: the first is the reflected incident flux, the second is the

reflected diffuse radiation that has not reached the lower boundary before its first reflection, and the third is the reflected diffuse radiation that has previously been reflected from the lower boundary before being scattered back down to the lower boundary. As a consequence, the intensity matrix $\uparrow \underline{I}_g(\tau_1;\mu,\phi)$ can be expressed as the sum of these three reflected components:

$$\boxed{\uparrow \underline{I}_g(\tau_1;\mu,\phi) = \uparrow \underline{I}_{g,1}(\tau_1;\mu,\phi) + \uparrow \underline{I}_{g,2}(\tau_1;\mu,\phi) + \uparrow \underline{I}_{g,3}(\tau_1;\mu,\phi) \quad .} \tag{3.15}$$

The equations for each one of these matrices are:

$$\uparrow \underline{I}_{g,1}(\tau_1;\mu_o,\phi_o-\phi_o) = \pi \underline{R}(\mu_o)\ \underline{F}\ (-\mu_o,\phi_o) e^{-\tau_1/\mu_o} \tag{3.16}$$

where the reflection matrix $\underline{R}$ is given by Eq. (2.10) ;

$$\uparrow \underline{I}_{g,2}(\tau_1;\mu,\phi_o-\phi) = \underline{R}(\mu)\ \downarrow \underline{I}(\tau_1;-\mu,\phi_o-\phi) \tag{3.17}$$

where $\downarrow \underline{I}$ is given by Eq. (3.6) ;

$$\uparrow \underline{I}_{g,3}(\tau_1;\mu,\phi_o-\phi) = \underline{R}(\mu)\ \downarrow \underline{I}_g^{(refl)}(\tau_1;-\mu,\phi) \tag{3.18}$$

where $\downarrow \underline{I}_g^{(refl)}$ is given by Eq. (3.14). Each of these three components of reflected radiation will make separate contributions to $\downarrow \underline{I}_g^{(refl)}$:

$$\downarrow \underline{I}_g^{(refl)}(\tau_1;-\mu,\phi_o-\phi) = \downarrow \underline{I}_{g,1}^{(refl)}(\tau_1;-\mu,\phi_o-\phi) + \downarrow \underline{I}_{g,2}^{(refl)}(\tau_1;-\mu,\phi_o-\phi) + \downarrow \underline{I}_{g,3}^{(refl)}(\tau_1;-\mu,\phi_o-\phi) \quad . \tag{3.19}$$

Any of the matrices on the right side, say $\downarrow\underline{I}_{g,i}^{(refl)}$, can be obtained by substituting $\uparrow\underline{I}_{g,i}$ for $\uparrow\underline{I}_{g}$ in Eq. (3.14). When one does this, the equation for the first matrix is

$$\downarrow\underline{I}_{g,1}^{(refl)}(\tau_1;-\mu,\phi_o-\phi) = R(\mu_o)e^{-\tau_1/\mu_o}\left\{\begin{pmatrix} I_{\ell,1}^{R(o)}\left[\mu,\mu_o;q(\mu_o)\right] \\ I_{r,1}^{R(o)}\left[\mu,\mu_o;q(\mu_o)\right]\end{pmatrix}\right. \tag{3.20}$$

$$+ I_{\ell,1}^{R(1)}(\mu,\mu_o)\underline{P}^{(1)\prime}(-\mu,\phi_o-\phi)$$

$$\left. + I_{r,1}^{R(2)}(\mu,\mu_o)\underline{P}^{(2)\prime}(-\mu,\phi_o-\phi)\right\} ,$$

where

$$\begin{pmatrix} I_{\ell,1}^{R(o)}\left[\mu,\mu_o;q(\mu_o)\right] \\ I_{r,1}^{R(o)}\left[\mu,\mu_o;q(\mu_o)\right]\end{pmatrix} = \frac{3F_o\mu_o}{32(\mu+\mu_o)}\left[\underline{S}_1(\mu)\underline{S}_1'\left[\mu_o,q(\mu_o)\right]\right. \tag{3.21}$$

$$\left. - \underline{S}_2(\mu)\underline{S}_2'\left[\mu_o,q(\mu_o)\right]\right] ,$$

$$I_{\ell,1}^{R(1)}(\mu,\mu_o) = \frac{3F_o}{8(\mu+\mu_o)}\mu_o^2\left[(1-\mu^2)(1-\mu_o^2)\right]^{1/2} q^2(\mu_o)\, W^{(1)}(\mu,\mu_o) , \tag{3.22}$$

$$I_{r,1}^{R(2)}(\mu,\mu_o) = \frac{3F_o\mu_o}{32(\mu+\mu_o)}\left[1 - \mu_o^2q^2(\mu_o)\right] W^{(2)}(\mu,\mu_o) , \tag{3.23}$$

$$W^{(i)}(\mu,\mu_o) = X^{(i)}(\mu)X^{(i)}(\mu_o) - Y^{(i)}(\mu)Y^{(i)}(\mu_o), \quad i = 1,2. \tag{3.24}$$

The second component of $\downarrow \underline{I}_{g}^{(refl)}$ is given next by the equation

$$\downarrow \underline{I}_{g,2}^{(refl)}(\tau_1;-\mu,\phi_o-\phi) = \begin{pmatrix} I_{\ell,2}^{R(o)}(\mu,\mu_o) \\ I_{r,2}^{R(o)}(\mu,\mu_o) \end{pmatrix}$$

$$+ I_{\ell,2}^{R(1)}(\mu,\mu_o)\underline{P}^{(1)'}(-\mu,\phi_o-\phi) \qquad (3.25)$$

$$+ I_{r,2}^{R(2)}(\mu,\mu_o)\underline{P}^{(2)'}(-\mu,\phi_o-\phi) \quad ,$$

where

$$\begin{pmatrix} I_{\ell,2}^{R(o)}(\mu,\mu_o) \\ I_{r,2}^{R(o)}(\mu,\mu_o) \end{pmatrix} = \frac{3}{8}\int_o^1 \frac{\mu' R(\mu')}{\mu+\mu'}\left[\underline{S}_1(\mu)\widetilde{\underline{S}}_1(\mu') - \underline{S}_2(\mu)\widetilde{\underline{S}}_2(\mu')\right] \begin{pmatrix} q^2(\mu')\, I_{\ell}^{(o)}(\mu',\mu_o;1) \\ I_{r}^{(o)}(\mu',\mu_o;1) \end{pmatrix} d\mu' \quad , \qquad (3.26)$$

$$I_{\ell,2}^{R(1)}(\mu,\mu_o) = -\frac{3}{8}\mu_o(1-\mu^2)^{1/2}\int_o^1 \frac{\mu' R(\mu') q(\mu')}{\mu+\mu'}\left[1-(\mu')^2\right]^{1/2} \times \left[1-2q(\mu')(\mu')^2\right] W^{(1)}(\mu,\mu') \qquad (3.27)$$

$$\times\, I_{\ell}^{(1)}(\mu',\mu_o)\, d\mu' \quad ,$$

$$I_{r,2}^{R(2)}(\mu,\mu_o) = \frac{3}{16}(1-\mu_o^2)\int_o^1 \mu' R(\mu') \frac{\left[1-(\mu')^2 q(\mu')\right]^2}{\mu+\mu'} \times W^{(2)}(\mu,\mu') I_r^{(2)}(\mu',\mu_o)\, d\mu' \quad . \tag{3.28}$$

The third component of $\downarrow \underline{I}_g^{(refl)}$ is given by the equation

$$\downarrow \underline{I}_{g,3}^{(refl)}(\tau_1;-\mu,\phi_o-\phi) = \begin{pmatrix} I_{\ell,3}^{R(o)}(\mu,\mu_o) \\ I_{r,3}^{R(o)}(\mu,\mu_o) \end{pmatrix} + I_{\ell,3}^{R(1)}(\mu,\mu_o)\underline{P}^{(1)'}(-\mu,\phi_o-\phi) + I_{r,3}^{R(2)}(\mu,\mu_o)\underline{P}^{(2)'}(-\mu,\phi_o-\phi) \quad , \tag{3.29}$$

where

$$\begin{pmatrix} I_{\ell,3}^{R(o)}(\mu,\mu_o) \\ I_{r,3}^{R(o)}(\mu,\mu_o) \end{pmatrix} = \frac{3}{8}\int_o^1 \frac{\mu' R(\mu')}{\mu+\mu'} \left[\underline{S}_1(\mu)\tilde{\underline{S}}_1(\mu') - \underline{S}_2(\mu)\tilde{\underline{S}}_2(\mu')\right] \begin{pmatrix} q^2(\mu')\, D_\ell^{(o)}(\mu',\mu_o) \\ D_r^{(o)}(\mu',\mu_o) \end{pmatrix} d\mu' \, , \tag{3.30}$$

$$I_{\ell,3}^{R(1)}(\mu,\mu_o) = -\frac{3}{8}(1-\mu^2)^{1/2}\int_o^1 \frac{\mu' R(\mu')}{\mu+\mu'} \left[1-(\mu')^2\right]^{1/2} \times q(\mu')\left[1-2(\mu')^2 q(\mu')\right] \times W^{(1)}(\mu,\mu') D_\ell^{(1)}(\mu',\mu_o)\, d\mu' \quad , \tag{3.31}$$

$$I_{r,3}^{R(2)}(\mu,\mu_o) = \frac{3}{16}\int_o^1 \frac{\mu' R(\mu')}{\mu+\mu'}\left[1-(\mu')^2 q(\mu')\right]^2 \times W^{(2)}(\mu,\mu')\, D_r^{(2)}(\mu',\mu_o)\, d\mu' \quad . \tag{3.32}$$

The D-functions that are used above are introduced in a particular equation for $\downarrow \underline{I}_g^{(refl)}$. Because the form for the intensity matrix for radiation that has been reflected by the ground and scattered by the atmosphere back down to the ground has already been established by Eq. (3.25), the equation for $\downarrow \underline{I}_g^{(refl)}$ can be written as

$$\downarrow \underline{I}_g^{(refl)}(\tau_1;-\mu,\phi_o-\phi) = \begin{pmatrix} D_\ell^{(o)}(\mu,\mu_o) \\ D_r^{(o)}(\mu,\mu_o) \\ 0 \end{pmatrix} - D_\ell^{(1)}(\mu,\mu_o)\underline{P}^{(1)\prime}(-\mu,\phi_o-\phi) + D_r^{(2)}(\mu,\mu_o)\underline{P}^{(2)\prime}(-\mu,\phi_o-\phi) \quad . \tag{3.33}$$

When this equation is substituted into Eq. (3.19), along with Eq. (3.20), (3.25) and (3.29), then it is seen that

$$\begin{pmatrix} D_{\ell}^{(o)}(\mu,\mu_o) \\ D_r^{(o)}(\mu,\mu_o) \end{pmatrix} = e^{-\tau_1/\mu_o} R(\mu_o) \begin{pmatrix} I_{\ell,1}^{R(o)}\left[\mu,\mu_o;q(\mu_o)\right] \\ I_{r,1}^{R(o)}\left[\mu,\mu_o;q(\mu_o)\right] \end{pmatrix} + \begin{pmatrix} I_{\ell,2}^{R(o)}(\mu,\mu_o) \\ I_{r,2}^{R(o)}(\mu,\mu_o) \end{pmatrix}$$

$$+ \frac{3}{8}\int_o^1 \frac{\mu' R(\mu')}{\mu+\mu'}\left[\underline{S}_1(\mu)\widetilde{\underline{S}}_1(\mu') - \underline{S}_2(\mu)\widetilde{\underline{S}}_2(\mu')\right] \qquad (3.34)$$

$$\times \begin{pmatrix} q^2(\mu')\, D_{\ell}^{(o)}(\mu',\mu_o) \\ D_r^{(o)}(\mu',\mu_o) \end{pmatrix} d\mu' \quad ,$$

$$D_{\ell}^{(1)}(\mu,\mu_o) = -e^{-\tau_1/\mu_o} R(\mu_o)\, I_{\ell,1}^{R(1)}(\mu,\mu_o) - I_{\ell,2}^{R(1)}(\mu,\mu_o)$$

$$+ \frac{3}{8}(1-\mu^2)^{1/2}\int_o^1 \frac{\mu' R(\mu')}{\mu+\mu'}\left[1-(\mu')^2\right]^{1/2} q(\mu') \qquad (3.35)$$

$$\times \left[1 - 2(\mu')^2 q(\mu')\right] W^{(1)}(\mu,\mu') D_{\ell}^{(1)}(\mu',\mu_o)\, d\mu' \quad ,$$

$$D_r^{(2)}(\mu,\mu_o) = e^{-\tau_1/\mu_o} R(\mu_o) I_{r,1}^{R(2)}(\mu,\mu_o) + I_{r,2}^{R(2)}(\mu,\mu_o) \qquad (3.36)$$

$$+ \frac{3}{16}\int_o^1 \frac{\mu' R(\mu')}{\mu+\mu'}\left[1 - (\mu')^2 q(\mu')\right]^2 W^{(2)}(\mu,\mu') D_r^{(2)}(\mu',\mu_o)\, d\mu' \quad .$$

The integral term in Eq. (3.34), (3.35), and (3.36) accounts for the characteristics of radiation that has been reflected from the ground at least twice before being scattered back to the ground again by the atmosphere.

These equations are Fredholm integral equations of the form

$$f_n(x) = f_o(x) + \int_o^1 g(x,y) f_{n-1}(y)dy, \quad n = 1, 2, 3 \ldots \quad . \tag{3.37}$$

Equations (3.34) - (3.36) satisfy the conditions that permit a convergent solution to be obtained by successive iterations.[16] Hence, these equations will be computed by successive iterations a sufficient number of times to obtain four significant figures for $f_n(x)$.

c. Albedo and fluxes

The monochromatic albedo will be defined as the ratio of the upward to the downward radiant flux through a horizontal surface.

$$\lambda_o^F(\tau_1;\mu_o) = \frac{\uparrow \mathcal{F}^F(\tau_1;\mu_o)}{\downarrow \mathcal{F}^F(\tau_1;\mu_o)} \quad . \tag{3.38}$$

The flux can be separated into three components that correspond to the components that were introduced into Eq. (3.15). Hence, the equation for the downward flux can be written as

$$\downarrow \mathcal{F}^F(\tau_1;\mu_o) = \downarrow \mathcal{F}_1(\tau_1;\mu_o) + \downarrow \mathcal{F}_2(\tau_1;\mu_o) + \downarrow \mathcal{F}_3(\tau_1;\mu_o) \quad . \tag{3.39}$$

The equation for the first component, or the reduced solar flux is

$$\downarrow \mathcal{F}_1(\tau_1;\mu_o) = \pi F_o \mu_o e^{-\tau_1/\mu_o} \quad . \tag{3.40}$$

The equation for the second component is obtained by adding the $\downarrow I_\ell$ and $\downarrow I_r$ terms of Eq. (3.6), multiplying by μ, and then integrating over the downward hemisphere. Only the azimuth independent terms remain after the azimuthal integration, and the expression for $\downarrow \mathcal{F}_2$ becomes

$$\downarrow \mathcal{F}_2'(\tau_1;\mu_o) = 2\pi \int_o^1 \left[I_\ell^{(o)}(\mu,\mu_o;1) + I_r^{(o)}(\mu,\mu_o;1) \right] \mu \, d\mu \quad . \tag{3.41}$$

Similarly, the expression for the third component of flux is obtained from Eq. (3.19):

$$\begin{aligned} \downarrow \mathcal{F}_3(\tau_1;\mu_o) = 2\pi \, R(\mu_o) e^{-\tau_1/\mu_o} \int_o^1 \Big\{ & I_{\ell,1}^{R(o)}\left[\mu,\mu_o;q(\mu_o)\right] \\ & + I_{r,1}^{R(o)}\left[\mu,\mu_o;q(\mu_o)\right] \Big\} \mu \, d\mu + 2\pi \int_o^1 \Big[I_{\ell,2}^{R(o)}(\mu,\mu_o) \\ & + I_{r,2}^{R(o)}(\mu,\mu_o) + I_{\ell,3}^{R(o)}(\mu,\mu_o) + I_{r,3}^{R(o)}(\mu,\mu_o) \Big] \mu \, d\mu \quad . \end{aligned} \tag{3.42}$$

Another expression for $\downarrow \mathcal{F}_3$ is obtained from Eq. (3.33):

$$\downarrow \mathcal{F}_3(\tau_1;\mu_o) = 2\pi \int_o^1 \left[D_\ell^{(o)}(\mu,\mu_o) + D_r^{(o)}(\mu,\mu_o) \right] \mu \, d\mu \quad . \tag{3.43}$$

The flux $\downarrow \mathcal{F}_3$ includes only that radiation which has been reflected from the lower boundary at least once.

The equation for the upward flux is obtained from Eq. (3.15) and found to be

$$
\begin{aligned}
{}^{\uparrow}\mathcal{J}(\tau_1;\mu_o) = \frac{\pi}{2} F_o \mu_o R(\mu_o) e^{-\tau_1/\mu_o} \left[1 + q^2(\mu_o) \right] \\
+ 2\pi \int_o^1 \mu R(\mu) \left[q^2(\mu)\, I_{\ell}^{(o)}(\mu,\mu_o;1) + I_r^{(o)}(\mu,\mu_o;1) \right] d\mu \\
+ 2\pi \int_o^1 \mu R(\mu) \left[q^2(\mu)\, D_{\ell}^{(o)}(\mu,\mu_o) + D_r^{(o)}(\mu,\mu_o) \right] d\mu \quad .
\end{aligned}
\tag{3.44}
$$

3. Upper Boundary

The intensity matrix for the radiation flowing outwards from the upper surface has already been given by Eq. (3.3). This equation can be written more compactly as

$$
\boxed{ {}^{\uparrow}\underline{I}^{*}(0;\mu,\phi_o-\phi) = {}^{\uparrow}\underline{I}(0;\mu,\phi_o-\phi) + {}^{\uparrow}\underline{I}_g^{(trans)}(0;\mu,\phi_o-\phi) } \quad , \tag{3.45}
$$

where ${}^{\uparrow}\underline{I}$ represents the first term, and ${}^{\uparrow}\underline{I}_g^{(trans)}$ represents the remaining two terms on the right hand side of Eq. (3.3). This section will be divided into three parts: one for the first term and one for the second term on the right-hand side of Eq. (3.45); the third section will contain the equations for flux.

a. First term

The equation for the first term on the right-hand side of Eq. (3.45) is

$$\uparrow \underline{I}(0;\mu,\phi_o-\phi) = \frac{1}{4\mu}\,\underline{S}(\tau_1;\mu,\phi;\mu_o,\phi_o)\,\underline{F}(-\mu_o,\phi_o)$$

$$= \begin{pmatrix} I^{R(o)}_{\ell,1}(\mu,\mu_o;1) \\ I^{R(o)}_{r,1}(\mu,\mu_o;1) \end{pmatrix} \tag{3.46}$$

$$+ \frac{3\,F_o\mu_o}{32(\mu+\mu_o)} \left\{ -4\mu_o \left[(1-\mu^2)(1-\mu_o^2)\right]^{1/2} W^{(1)}(\mu,\mu_o)\underline{P}^{(1)\prime}(\mu,\phi_o-\phi) \right.$$

$$\left. + (1-\mu_o^2)W^{(2)}(\mu,\mu_o)\underline{P}^{(2)\prime}(\mu,\phi_o-\phi) \right\} .$$

b. Second term

The equation for the second term of Eq. (3.45) is

$$\uparrow \underline{I}^{(trans)}_{g}(0,\mu,\phi_o-\phi) = \uparrow \underline{I}_g(\tau_1;\mu,\phi_o-\phi)e^{-\tau_1/\mu} \tag{3.47}$$

$$+ \frac{1}{4\pi\mu}\int_0^1\int_0^{2\pi} \underline{T}(\tau_1;\mu,\phi;\mu',\phi')\uparrow \underline{I}_g(\tau_1;\mu',\phi_o-\phi')d\mu'd\phi' .$$

This equation can be separated into three parts, each part being associated with the three parts of $\uparrow \underline{I}_g(\tau_1;\mu,\phi_o-\phi)$ (Eq. (3.15)); that is,

$$\uparrow \underline{I}^{(trans)}_{g}(0;\mu,\phi_o-\phi) = \uparrow \underline{I}^{(trans)}_{g,1}(0;\mu,\phi_o-\phi) + \uparrow \underline{I}^{(trans)}_{g,2}(0;\mu,\phi_o-\phi)$$

$$+ \uparrow \underline{I}^{(trans)}_{g,3}(0;\mu,\phi_o-\phi) \quad . \tag{3.48}$$

The first part is obtained by substituting $\uparrow \underline{I}_{g,1}(\tau_1;\mu,\phi_o-\phi)$ (Eq. (3.16) for $\uparrow \underline{I}_g(\tau_1;\mu,\phi_o-\phi)$ in Eq. (3.47):

$$\uparrow \underline{I}_{g,1}^{(trans)}(0;\mu,\phi_o-\phi) = R(\mu_o)e^{-\tau_1/\mu_o}\left\{\begin{pmatrix} I_\ell^{(o)}[\mu,\mu_o;q(\mu_o)] \\ I_r^{(o)}[\mu,\mu_o;q(\mu_o)] \end{pmatrix}\right. \tag{3.49}$$

$$+ \mu_o q^2(\mu_o) I_\ell^{(1)}(\mu,\mu_o)\underline{P}^{(1)'}(\mu,\phi_o-\phi)$$

$$\left. + \left[1 - (\mu_o q(\mu_o))^2\right] I_r^{(2)}(\mu,\mu_o)\underline{P}^{(2)'}(\mu,\phi_o-\phi)\right\}.$$

When the radiation is flowing in the direction μ_o,ϕ_o, the effect of the reflected direct sunlight that passes directly through the atmosphere must be added to Eq. (3.49); this term is

$$\frac{\pi}{2} F_o R(\mu_o)e^{-2\tau_1/\mu_o}\begin{pmatrix} q^2(\mu_o) \\ 1 \\ 0 \end{pmatrix}. \tag{3.50}$$

The equation for $\uparrow \underline{I}_{g,2}^{(trans)}$ is obtained by substituting $\uparrow \underline{I}_{g,2}$ (Eq. 3.17) for $\uparrow \underline{I}_g$ in Eq. (3.47):

$$\uparrow \underline{I}_{g,2}^{(trans)}(0;\mu,\phi_o-\phi) = e^{-\tau_1/\mu} R(\mu) \left\{ \begin{pmatrix} q^2(\mu) I_\ell^{(o)}[\mu,\mu_o;1] \\ I_r^{(o)}[\mu,\mu_o;1] \end{pmatrix} \right.$$

$$- \mu_o I_\ell^{(1)}(\mu,\mu_o) q(\mu) \underline{P}^{(1)'}(-\mu q(\mu), \phi_o-\phi)$$

$$\left. + (1-\mu_o^2) I_r^{(2)}(\mu,\mu_o) \underline{P}^{(2)'}(-\mu q(\mu), \phi_o-\phi) \right\}$$

$$+ \frac{3}{8} \int_o^1 \mu' R(\mu') \underline{K}(\mu,\mu') \begin{pmatrix} q^2(\mu') I_\ell^{(o)}(\mu',\mu_o;1) \\ I_r^{(o)}(\mu',\mu_o;1) \end{pmatrix} d\mu'$$

$$- \frac{\mu_o}{F_o} \int_o^1 R(\mu') q(\mu') \left[1-2(\mu')^2 q(\mu') \right] \tag{3.51}$$

$$\times \quad I_\ell^{(1)}(\mu,\mu') I_\ell^{(1)}(\mu',\mu_o)\, d\mu'\, \underline{P}^{(1)'}(\mu,\phi_o-\phi)$$

$$+ \frac{2(1-\mu_o^2)}{F_o} \int_o^1 R(\mu') \left[1-(\mu')^2 q(\mu') \right]^2$$

$$\times \quad I_r^{(2)}(\mu,\mu') I_r^{(2)}(\mu',\mu_o)\, d\mu'\, \underline{P}^{(2)'}(\mu,\phi_o-\phi) \quad ,$$

where

$$\underline{K}(\mu,\mu') = \frac{\underline{S}_2(\mu)\underline{\tilde{S}}_1(\mu') - \underline{S}_1(\mu)\underline{\tilde{S}}_2(\mu')}{\mu - \mu'} \quad .$$

The equation for $\uparrow \underline{I}_{g,3}^{(trans)}$ is obtained by substituting $\uparrow \underline{I}_{g,3}$ (Eq. 3.18) for $\uparrow \underline{I}_{g}$ in Eq. (3.47):

$$\begin{aligned}
\uparrow \underline{I}_{g,3}^{(trans)}(0;\mu,\phi_o-\phi) = e^{-\tau_1/\mu} R(\mu) \Bigg\{ & \begin{pmatrix} q^2(\mu) D_{\ell}^{(o)}(\mu,\mu_o) \\ D_r^{(o)}(\mu,\mu_o) \end{pmatrix} \\
& - D_{\ell}^{(1)}(\mu,\mu_o) q(\mu) \underline{P}^{(1)\prime}(-\mu q(\mu), \phi_o-\phi) \\
& + D_r^{(2)}(\mu,\mu_o) \underline{P}^{(2)\prime}(-\mu q(\mu), \phi_o-\phi) \Bigg\} \\
& + \frac{3}{8} \int_o^1 \mu' R(\mu') \underline{K}(\mu,\mu') \begin{pmatrix} q^2(\mu') D_{\ell}^{(o)}(\mu',\mu_o) \\ D_r^{(o)}(\mu',\mu_o) \end{pmatrix} d\mu' \\
& - \frac{1}{F_o} \int_o^1 R(\mu') q(\mu') \left[1 - 2(\mu')^2 q(\mu') \right] \cdot \\
& \times \quad I_{\ell}^{(1)}(\mu,\mu') D_{\ell}^{(1)}(\mu',\mu_o) d\mu' \, \underline{P}^{(1)\prime}(\mu,\phi_o-\phi) \\
& + \frac{2}{F_o} \int_o^1 R(\mu') \left[1-(\mu')^2 q(\mu') \right]^2 \\
& \times \quad I_r^{(2)}(\mu,\mu') D_r^{(2)}(\mu',\mu_o) \, d\mu' \, \underline{P}^{(2)\prime}(\mu,\phi_o-\phi) \quad .
\end{aligned} \tag{3.52}$$

c. Fluxes

The downward flux on top of the atmosphere comes only from the direct flux, and the equation for this flux is

$$\downarrow\mathcal{F}(0;\mu_o) = \pi F_o \mu_o \quad . \tag{3.53}$$

The upward flux can be separated into parts: one part is the radiation that is reflected from the atmosphere before it reaches the lower boundary and the other is the part that has been reflected from the ground before emerging from the top of the atmosphere. Thus, the equation for the upward flux is

$$\uparrow\mathcal{F}(0;\mu) = \uparrow\mathcal{F}_2(0;\mu_o) + \uparrow\mathcal{F}_3(0;\mu_o) \quad . \tag{3.54}$$

The equation for the flux $\uparrow\mathcal{F}_2$ is obtained by adding I_ℓ and I_r of Eq. (3.46), then multiplying by μ, and integrating it over the upward hemisphere to get

$$\uparrow\mathcal{F}_2(0;\mu_o) = 2\pi \int_o^1 \mu \left[I^{R(o)}_{\ell,1}(\mu,\mu_o;1) + I^{R(o)}_{r,1}(\mu,\mu_o;1) \right] d\mu \quad . \tag{3.55}$$

The flux $\uparrow\mathcal{F}_3$ can be separated into three components, which correspond to the three parts of $\uparrow\underline{I}^{(trans)}_g$ (Eq. (3.48)), to obtain

$$\uparrow\mathcal{F}_3(0;\mu_o) = \uparrow\mathcal{F}_{3,1}(0;\mu_o) + \uparrow\mathcal{F}_{3,2}(0;\mu_o) + \uparrow\mathcal{F}_{3,3}(0;\mu_o) \; . \tag{3.56}$$

The equation for $\uparrow\mathcal{F}_{3,1}$ is obtained from Eq. (3.49) and (3.50) and is

$$\uparrow\mathcal{F}_{3,1}(0;\mu_o) = \frac{\pi F_o}{2}\ \mu_o R(\mu_o) e^{-2\tau_1/\mu_o}\ (q^2(\mu_o)+1)$$

$$+ 2\pi R(\mu_o) e^{-\tau_1/\mu_o} \int_o^1 \mu \left[I_\ell^{(o)}\left[\mu,\mu_o;q(\mu_o)\right] \right. \tag{3.57}$$

$$\left. + I_r^{(o)}\left[\mu,\mu_o;q(\mu_o)\right] \right] d\mu \ .$$

The equation for $\uparrow\mathcal{F}_{3,2}$ is obtained from Eq. (3.51) and is

$$\uparrow\mathcal{F}_{3,2}(0;\mu_o) = 2\pi \int_o^1 e^{-\tau_1/\mu}\ \mu\ R(\mu) \left[q^2(\mu) I_\ell^{(o)}(\mu,\mu_o;1) + I_r^{(o)}(\mu,\mu_o;1) \right] d\mu$$

$$+ \frac{3\pi}{4} \int_o^1 \mu\, d\mu \int_o^1 \mu' R(\mu') \left\{ \left[\underline{K}(\mu,\mu') \begin{pmatrix} q^2(\mu') I_\ell^{(o)}(\mu',\mu_o;1) \\ I_r^{(o)}(\mu',\mu_o;1) \end{pmatrix} \right]_\ell \right. \tag{3.58}$$

$$\left. + \left[\underline{K}(\mu,\mu') \begin{pmatrix} q^2(\mu') I^{(o)}(\mu',\mu_o;1) \\ I_r^{(o)}(\mu',\mu_o;1) \end{pmatrix} \right]_r \right\} d\mu' ,$$

where the subscripts ℓ and r indicate the first and second rows respectively of the columnar matrix that is given by the product matrix within the square brackets. The equation for $\uparrow\mathcal{F}_{3,3}$ is obtained from Eq. (3.52) and is

$$\uparrow \mathcal{F}_{3,3}(0;\mu_o) = 2\pi \int_0^1 \mu\, e^{-\tau_1/\mu} R(\mu) \left[q^2(\mu) D_\ell^{(o)}(\mu,\mu_o) + D_r^{(o)}(\mu,\mu_o) \right] d\mu$$

$$+ \frac{3\pi}{4} \int_0^1 \mu\, d\mu \int_0^1 \mu'\, R(\mu') \left\{ \left[\underline{K}(\mu,\mu') \begin{pmatrix} q^2(\mu') D_\ell^{(o)}(\mu',\mu_o) \\ D_r^{(o)}(\mu',\mu_o) \end{pmatrix} \right]_\ell \right.$$

$$\left. + \left[\underline{K}(\mu,\mu') \begin{pmatrix} q^2(\mu') D^{(o)}(\mu',\mu_o) \\ D_r^{(o)}(\mu',\mu_o) \end{pmatrix} \right]_r \right\} d\mu' \,. \qquad (3.59)$$

Because no radiant energy is absorbed in the model atmosphere that was specified in Section II,B, the flux of radiation into the atmosphere through its boundaries must equal the outgoing fluxes; that is,

$$\downarrow \mathcal{F}(0;\mu_o) + \uparrow \mathcal{F}(\tau_1;\mu_o) = \uparrow \mathcal{F}(0;\mu_o) + \downarrow \mathcal{F}(\tau_1;\mu_o) \,. \qquad (3.60)$$

The flux balance provides one check on the computed accuracy of the azimuth independent terms. The ratio of the flux balance to the incident solar flux is given by the relation

$$\epsilon(\tau_1;\mu_o) = \frac{\downarrow \mathcal{F}(0;\mu_o) + \uparrow \mathcal{F}(\tau_1;\mu_o) - \uparrow \mathcal{F}(0;\mu_o) - \downarrow \mathcal{F}(\tau_1;\mu_o)}{\downarrow \mathcal{F}(0;\mu_o)} \,. \qquad (3.61)$$

The deviation of ϵ from zero is one measure of the accuracy of the computations and will be computed for this purpose.

III. COMPUTATIONS

The steps that were followed to compute the radiation parameters will be given. The computational routine is not reproduced here, since it was developed for a Control Data Corporation Computer 3600; and this routine can not be modified by a computer for use on International Business Machines' computers. However, a copy of the routine can be obtained from R. S. Fraser. The second part of this section will discuss the accuracy of the basic input data and the accuracy of the computed data.

The computational routine was developed and the computations were done at the National Center for Atmospheric Research in Boulder, Colorado. Mr. W. H. Walker programmed the routine. Dr. J. V. Dave made many suggestions which simplified the routine. He also computed the basic data that were used for Fraser's computations. The National Center for Atmospheric Research provided without charge to this Contract (No. NAS5-3891) essentially all the computational facilities that were required. Dr. Dave's and Mr. Walker's skilled help, plus NCAR's generous assistance, removed many pitfalls that were not anticipated by the author before he commenced this study.

A. Computational Routine

1. Input data

The computations used certain input data, which were read into the computer initially. These data included Chandrasekhar's twelve scattering functions: ψ, ϕ, χ, ζ, ξ, σ, η, θ, $X^{(1)}$, $X^{(2)}$, $Y^{(1)}$, $Y^{(2)}$.

These functions were supplied by Dr. Dave. The derivatives of these functions were part of the input. Errors appeared in the numerical calculation of the derivatives and will be discussed in Section III.B., which is concerned with the accurary of the computations. The errors were detected and corrected by taking the derivatives separately. If the numerical derivations had been performed as a sub-routine of the main computational program, the errors might not have been discovered. Three other functions -- $\bar{s}(\tau_1)$, $\gamma^{(1)}(\mu)$, and $\gamma_r^{(1)}(\mu)$ -- were supplied by Dave and included in the initial input data in order to make the computations for the Lambert model. The final input datum was the index of refraction, which is required to compute the Fresnel reflection characteristics (Eq. (2.9) - (2.12)). The computational routine generated all other data that were required.

2. Computational procedure

The effect of Fresnel reflection will be discussed in terms of the total intensity and degree of polarization in the vertical plane of the sun, and also of the flux. These three quantities can be computed from I_ℓ and I_r, if these two parameters are known throughout the vertical plane of the sun. The total intensity and degree of polarization are computed from Eq. (2.3) and Eq. (2.6), respectively. The azimuth independent terms of I_ℓ and I_r are used in Eq. (3.39) - (3.41), (3.43), (3.54) - (3.59) to compute the flux quantities. Hence, I_ℓ and I_r are the basic parameters that were computed for this study.

The computations commenced by reading into the computer the basic input data for only one optical thickness (τ_1). The quantity representing the orientation of the incident flux, or the position of the sun, μ_o, was fixed. The radiation parameters at the bottom of the atmosphere were computed first; the I_ℓ - and I_r - elements of the matrix given by Eq. (3.4) were computed for this purpose. The first term of Eq. (3.4) is given by Eq. (3.5), and the necessary auxiliary equations are included within Eq. (3.6) - (3.11). The second term of Eq. (3.4) is computed from Eq. (3.33). The auxiliary equations for (3.33) are (3.34) to (3.36). The most difficult part of the entire computation is to find numerical solutions to the integral equations (3.34) to (3.36).

Equations (3.34) to (3.36) were solved by the method of successive iterations, as indicated by Eq. (3.37). The same method was used for each of the three Eq. (3.34) - (3.36) and can be illustrated with just one of them, say Eq. (3.34). The zeroth order solution was given by the sum of the two matrices that are outside the integral. The separate matrices were computed from Eq. (3.21) and (3.26). To make the first iteration, the I_ℓ - and I_r - components of the sum replaced $D_\ell^{(o)}$ and $D_r^{(o)}$, respectively, in the integrand of Eq. (3.34). The integrand then contained the quantities $I_\ell^{(o)}$ and $I_r^{(o)}$ (Eq. (3.9)), which are indeterminate at $\mu = \mu_o$, because their numerators and denominators are zero. The values of $I_\ell^{(o)}$ and $I_r^{(o)}$ at $\mu = \mu_o$ are obtained by applying L'Hospital's rule and making only one derivative of the numerator and of the denominator to obtain the expression

$$\begin{pmatrix} I_{\ell}^{(o)}(\mu_o, \mu_o; 1) \\ I_{r}^{(o)}(\mu_o, \mu_o; 1) \end{pmatrix} = \frac{3F_o\mu_o}{32} \left[\left. \frac{\partial \underline{S}_2(\mu)}{\partial \mu} \right|_{\mu = \mu_o} \underline{S}_1'(\mu_o, 1) - \left. \frac{\partial \underline{S}_1(\mu)}{\partial \mu} \right|_{\mu = \mu_o} \underline{S}_2'(\mu_o, 1) \right] .$$

Whenever functions were indeterminate at $\mu = \mu_o$, and this is the only place where they were indeterminate, the value of the indeterminate function was found by applying L'Hospital's rule just once.

The integral equations such as Eq. (3.34) were iterated until successive iterations agreed in the fourth place to the right of the decimal point. The number of iterations that were required increased slightly with increasing optical thickness and increasing nadir angle. When the index of refraction of water was used, with the result that the ground albedo was roughly 0.1, and when the optical thickness was small ($\tau_1 = 0.02$), not more than three iterations were needed; when the optical thickness was large ($\tau_1 = 2.0$), not more than four iterations were required. When the ground albedo was increased to 0.61 (with $\tau_1 = 0.50$ and $\theta_o = 66.4^o$) by increasing the index of refraction to ten, not more than six iterations were needed to get the solutions to agree in the fourth decimal place.

The downward flux at the ground for the Fresnel model was computed separately for six streams of radiation. These fluxes were added

to give the total flux (Eq. (3.39)). The six streams and their flux equations are: the reduced solar, or incident, flux - Eq. (3.40); the flux of airlight that has not been reflected from the ground - Eq. (3.41); the flux of airlight that is composed of direct sunlight and airlight that have been reflected from the ground and then scattered back to the ground by the atmosphere - Eq. (3.43); the latter stream is subdivided into three more streams, whose fluxes are given by the first integral on the right-hand side of Eq. (3.42), and also the second integral, which gives the two flux quantities

$$2\pi \int_o^1 \left[I_{\ell,i}^{R(o)} (\mu, \mu_o) + I_{r,i}^{R(o)} (\mu, \mu_o) \right] \mu \, d\mu, \quad i = 2, 3 \quad .$$

All the flux quantities, with the exception of the reduced solar flux (Eq. (3.40)), are given by integrations, which were done numerically.

The radiation parameters were computed also for the model with Lambert ground reflection. This can be done easily by replacing the second term on the right-hand side of Eq. (3.4) with the following matrix:

$$\underline{\downarrow I}_g^{(refl)L} (\tau_1; -\mu, \phi_o - \phi) = \frac{\lambda_o^F(\tau_1, \mu_o) F_o \mu_o}{4 \left[1 - \lambda_o^F \bar{s}(\tau_1) \right]} \times$$

$$\times \left[\gamma_\ell^{(1)}(\mu_o) + \gamma_r^{(1)} (\mu_o) \right] \times$$

$$\times \begin{pmatrix} \left[1 - \gamma_\ell^{(1)} (\mu) \right] \\ \left[1 - \gamma_r^{(1)} (\mu) \right] \end{pmatrix} ,$$

which is given in R.T., p. 279, Eq. (234) and (236). The ground albedo (λ_o^F), which is used in this expression, is computed for the Fresnel model (Eq. (3.38)).

Following the computations for parameters at the bottom of the atmosphere, the radiation quantities for the top of the atmosphere of the Fresnel model were computed. The I_ℓ - I_r - components of the intensity matrix were computed from Eq. (3.45). The first term of Eq. (3.45) was computed from Eq. (3.46). The second term was computed from Eq. (3.48). The three intensity matrices for the three streams of radiation indicated by Eq. (3.48) were computed and tabulated separately. The equations used to compute these three intensity matrices were Eqs. (3.49) to (3.52). The D_ℓ - and D_r - functions, which appear in Eq. (3.52), were already stored in the computer memory, since they had been computed previously for the bottom of the atmosphere.

The upward fluxes at the top of the atmosphere for six streams of radiation were computed separately for the Fresnel model. The total flux was computed from Eq. (3.54). The first term on the right of Eq. (3.54), the flux of airlight that has not been reflected from the ground, was computed from Eq. (3.55). The second term on the right of Eq. (3.54), which represents the flux of radiation that has been reflected from the ground, was computed from Eq. (3.56). The stream of radiation that is reflected from the ground can be subdivided into three components, which were computed from Eq. (3.57) to (3.59). In all cases the fluxes were

obtained by integrating the total intensity times cos $\theta = \mu$ over the upward hemisphere. The azimuthal integration eliminated the first and second harmonic terms of the intensity. Hence, the flux depended on only the azimuth independent terms of the intensity.

The flux balance error was computed from Eq. (3.61). This computation served as a check on the accuracy of the computations for the azimuth independent terms of the intensity at both the bottom and top of the atmosphere. The flux balance was not in error, when the index of refraction of water ($m \sim 1.35$) was used. However, a few computations were made for m = 2, 3, 4, 5, and 10, and with two optical thicknesses of $\tau_1 = 0.05$ and 0.50. Unexpectedly, the flux balance error increased with increasing optical thicknesses and with increasing index of refraction. The maximum value of the error was 0.01 and occurred at $\tau_1 = 0.50$, m = 10, and $\theta_o = 66.4^o$, the only solar nadir angle for which the computations were made at large index of refraction. Since the error is not present at small m, the computational routine would not seem to cause it. A small source of error may be present in the numerical values of the twelve scattering functions, which are part of the basic input into the computer. The possibility of error in these twelve scattering functions should be investigated, since these functions are frequently used by scientists who study radiative transfer in planetary atmospheres.

The radiation parameters at the top of the atmosphere for the Lambert model were needed for comparison with the Fresnel parameters,

since the comparisons were made as part of the computational routine. The Lambert intensity matrix was easily computed by replacing $\uparrow \underline{I}_g^{(trans)}$ of Eq. (3.45) with the following matrix:

$$\uparrow \underline{I}_g^{(trans)L}(0; \mu, \phi_o - \phi) = \frac{\lambda_o^F(\tau_1, \mu_o) F_o \mu_o}{4(1 - \lambda_o^F \bar{s})} \left[\gamma_\ell^{(1)}(\mu_o) + \gamma_r^{(1)}(\mu_o)\right] X$$

$$X \begin{pmatrix} \gamma_\ell^{(1)}(\mu) \\ \gamma_r^{(1)}(\mu) \end{pmatrix},$$

which is given in R.T., p. 279, Eq. (233) and (235).

After the computations were completed at the top of the atmosphere for a fixed τ_1 and μ_o, a new set of computations were commenced with the same τ_1, but with a different μ_o. After completing the computations for the set of μ_o, which were μ_o = 0.1 [0.1] 1.00, 0.96, then basic input data for a different τ_1 were read into the computer. The set of optical thicknesses was τ_1 = 0.02, 0.05, 0.10, 0.15, 0.25, 0.50, 1.00, 2.00.

The tabulated output for a single τ_1 and μ_o will be described. The radiation parameters for three models are tabulated. The three models differ according to the law of reflection at the ground. The three laws are those governing no reflection ($\lambda_o^F = 0$), Lambert reflection, and Fresnel reflection. The parameters I_ℓ, I_r, I, P are tabulated for μ = 0.01 [0.01] 1.00 and $\phi_o - \phi$ = 0 and π. At the bottom of the atmosphere these parameters apply to the downward radiation, and at the top they apply to the upward radiation. In addition, at the top both the

ℓ- and r- components of $\uparrow \underline{I}_g^{(trans)}$ and $\uparrow \underline{I}_{g,i}^{(trans)}$, i = 1, 2, 3 are tabulated. The neutral point positions, maximum degree of polarization, and position of the maximum degree of polarization are given. Also tabulated are several flux quantities and albedos for the bottom and top of the atmosphere.

B. Accuracy of Computations

1. Accuracy of scattering functions

The accuracy of the computations was determined essentially by the accuracy of 12 scattering functions, which are designated by Ψ, $\emptyset$, χ, ζ, ξ, η, ϵ, θ, $X^{(1)}$, $Y^{(1)}$, $X^{(2)}$, $Y^{(2)}$. These functions depend on X-, Y- functions, as defined in R.T. The X-, Y- functions are solutions to integral equations. Dr. Dave obtained solutions to the integral equations by an iterative process. He continued the iterations until agreement was attained in the fifth place, or higher, to the right of the decimal point for $\tau_1 \leq 1.00$ and in the third or higher decimal place for $\tau_1 = 2.00$. In order to achieve this measure of accuracy, Dave had to make 3 iterations for small τ_1, and up to 11 iterations at $\tau_1 = 2.00$.

The accuracy of the X-, Y- functions depends on the iterative procedure that is used. Two different iterative procedures can each converge to separate values, whose range is small. Hence, Dave's solutions for the X-, Y- functions may have a small error and be slightly less accurate than indicated in the previous paragraph. The accuracy of the functions was found by studying successive finite differences of the functions. This method indicated that the functions were accurate to at

least five decimal places to the right of the decimal point when $\tau_1 < 1.0$, 4 places when $\tau_1 = 1.0$, and 3 places when $\tau_1 = 2.0$.

The numerical derivatives of each of the twelve scattering functions were computed separately and were part of the basic input to the routine for computing the radiation parameters. The numerical derivatives of tabulated functions that are not exact are less accurate than are the tabulated functions. The numerical derivatives of a few of the scattering functions were so inaccurate that the functions were smoothed before differentiation by replacing the tabulated values with third degree polynomials. This procedure was followed for the following functions:

$\xi(\mu)$, $0.85 \leq \mu \leq 1.00$, $\tau_1 = 2.00$; $\gamma(\mu)$, $0.90 \leq \mu \leq 1.00$, $\tau_1 = 2.00$.

The first derivative of each of the scattering functions with respect to μ was computed by Stirling's central difference formula.[22] The formula was truncated after the seventh difference for μ in the range $0.04 \leq \mu \leq 0.96$, and for the largest number of differences that were available for μ outside of this range. The derivatives were linearly extrapolated to obtain their values at $\mu = 1.00$. The truncation error was small in comparison with the error that was caused by the least significant figure of a tabulated function. As a result, the differentiated functions had two fewer accurate decimal places than had the undifferentiated functions, since the μ- interval between the tabulated values was $\Delta\mu = 0.01$. The differentiated functions were accurate

to at least three decimal places to the right of the decimal point for $\tau_1 < 1.00$, 2 places for $\tau_1 = 1.0$, and one place for $\tau_1 = 2.0$.

2. Accuracy of computed intensity

The intensities that are independent of the ground reflection are computed from Eq. (3.6) and (3.46). A particular value of the intensity is as accurate as the least accurate of the 12 scattering functions that is used in the computation for that value of the intensity, unless $\mu = \mu_o$. Hence, the computed intensities are accurate to at least five places to the right of the decimal point for $\tau_1 < 1.00$, 4 places for $\tau_1 = 1.00$, and 3 places for $\tau_1 = 2.00$. When the value of Eq. (3.6) becomes indeterminate at $\mu = \mu_o$, L'Hospital's rule is applied and the derivatives of the scattering functions are used. As a result, the accuracy of the computed intensity of the radiation falling on the ground from the direction of the solar almuncantor ($\mu = \mu_o$) is reduced by two decimal places.

The effect of the ground reflection on the radiation field is obtained by adding another term to the intensity of the radiation that has not been reflected from the ground (Eq. (3.4) and (3.45)). The ground reflection term depends on functions that are computed by L'Hospital's rule, when the functions are indeterminate. If $\mu \neq \mu_o$, these indeterminate functions appear only in integrands. However, the integrated quantities remain at least as accurate as the intensity of the radiation not reflected from the ground.

If $\mu = \mu_o$, the error analysis becomes more complicated. The accuracy of the radiation leaving the top of the atmosphere when the index of refraction of the ground is that of water will be considered. When $\mu = \mu_o$, indeterminate functions appear outside of the integrals (Eq. (3.49), (3.51), (3.52)). These functions are evaluated by using L'Hospital's rule, and, as a consequence, their accuracy is reduced by about two decimal places. However, these functions are multiplied by the factor $e^{-\tau_1/\mu_o} R(\mu_o)$, which is less than one, since $e^{-\tau_1/\mu_o} < 1$ and $R(\mu_o) \leqslant 1$. If τ_1 is large, the effect of an error in these functions is negligible, since $e^{-\tau_1/\mu_o} \longrightarrow 0$ as $\tau_1 \longrightarrow \infty$. If τ_1 is less than about 0.1, the error in these functions becomes important, since the intensity of the radiation reflected from the ground exceeds the intensity of the radiation that is not reflected from the ground. Then the intensity may be accurate to only three decimal places to the right of the decimal point for $\tau_1 < 1.00$, 2 decimal places for $\tau_1 = 1.00$, and 1 decimal place for $\tau_1 = 2.00$. The computed data provides one internal check on its accuracy, when $\mu = \mu_o = 1$. The theory shows that $I_\ell = I_r$ in this direction. The computed data show that the relative error in I_ℓ and I_r is less than 5×10^{-5}. Hence, the accuracy of the computed data exceeds the minimum accuracy for $\mu = \mu_o = 1$, and probably for other values of μ_o as well.

The computed intensities for the Lambert model agreed with published tables of intensities[6] to at least four decimal places. The computed intensities at the bottom of the atmosphere for the Fresnel model

were compared with corresponding values that were computed by Sekera, but not published. The two sets of computations agreed to at least four decimal places.

3. Accuracy of degree of polarization

The degree of polarization for the vertical place through the sun and zenith has been computed from Eq. (2.6). The number of significant figures is determined by the numerator. When $\mu \neq \mu_o$, the computed degree of polarization is usually accurate to 0.001 for $\tau_1 < 1.00$, to 0.01 for $\tau_1 = 1.00$, and to 0.1 for $\tau_1 = 2.00$. When $\mu = \mu_o$, the accuracy of the degree of polarization is usually one decimal place less. However, the degree of polarization has not appeared to be "noisy" when plotted on graph paper.

IV. DATA ANALYSIS

A. Introduction to Analysis of Data

The radiation parameters that are computed for the model of a Rayleigh atmosphere and specular, or Fresnel, ground reflection will be compared with data computed for the same model, except that the ground reflects radiation according to Lambert's law. The two models will be distinguished in this section by referring to them as either the Fresnel or Lambert Model. The Lambert model serves as a useful reference, since most previous calculations of the radiation parameters at the top of a planetary atmosphere were made for Lambert ground reflection. The same albedo* at the ground is used in the computations for both models, when the optical thickness and solar elevation are identical for both.

The primary purpose of this research was to study the effect of specular reflection on the radiation scattered from planetary atmospheres, but the data can be usefully applied to the earth, when its atmosphere lies over a large body of water. The model of Rayleigh atmosphere and specular ground reflection comes closest to approximating the earth when the earth's atmosphere, which always contains aerosols, has a small aerosol content, the water surface is smooth, and neither the sun nor the direction of observation is very close to the horizon. The last restriction is specified in order to avoid sphericity effects. Water surfaces

---

* The albedo at a horizontal surface - either the top of bottom of the atmosphere - is defined as the ratio of the upward to the downward monochromatic flux through the surface.

are not smooth unless the air above them is calm. However, when the wind a few meters above the surface is less than 7 ms^{-1}, the water retains its specular reflecting characteristics, if the radiation incident on it has a zenith angle less than 60^{o}.[7,18]

The wavelength corresponding to a particular value of the optical thickness of the earth's atmospheric gas (no aerosol particles) is given in Table I. The relation between the optical thickness and wavelength takes into account only the scattering properties of the atmospheric gas and neglects absorption. As a result the optical thickness varies nearly as the inverse fourth power of the wavelength.

TABLE I

The optical thickness is (τ_1) for which the computations are made are listed. The corresponding wavelengths are given, when the optical thicknesses apply to the earth's atmosphere without aerosol particles.[a] The index of refraction (m) of sea water at temperature T = 20^{o}C is given for the same wavelengths.

τ_1	λ	m
0.02	0.803μ	1.3352
0.05	0.637	1.3387
0.10	0.542	1.3417
0.15	0.492	1.3440
0.25	0.435	1.3477
0.50	0.367	1.3546
1.00	0.312	1.3643
2.00	0.266	1.3789

[a] These relations were developed with data that are given in references 9 and 10.

Table I also gives the index of refraction of the ground for the Fresnel model. Only these values are used, until the final subsection (IV.F.) of this section presents a discussion of the effect of larger indices of refraction. The indices of refraction in Table I are approximate mean values for the earth's seas. The index of refraction of sea water $(m_{s,T})^*$ was calculated from the formula $m_{(s,20)}(\lambda) = m_{w,20}(\lambda) + \Delta_{20}(\lambda)$, where the subscript 20 indicates that the values are for a temperature $T = 20^{\circ}C$; the subscripts s and w refer to sea water and pure water, respectively; and Δ_{20} is the difference between the indices of sea and pure water. The value of $m_{w,20}$ was taken from Dorsey.[10] The quantity Δ_{20} is obtained from the relation $\Delta_{20}(\lambda) = \Delta_{15}(\lambda) + \delta$; Gifford's[15] experimental value of Δ_{15} was used and $\delta = 5 \times 10^{-4}$. The extreme values for the earth's seas at a given wavelength depart from those in Table I by less than 0.5 per cent.[2] Such a small variation in the index of refraction will cause only small changes in the radiation parameters at the top of the atmosphere. This will be shown in Section IV.F. where the radiation parameters are given as a function of the index of refraction.

The plan for the discussion that follows is to show first the character of the flux of radiant energy from the top of the atmosphere. Then the angular distribution of the radiant energy will be given by means of the intensity parameter. Next, the degree of polarization will be

---

* The subscripts are eliminated from the symbol m for the index of refraction in Table I and in the remainder of this report.

discussed. The neutral points will receive special attention. Finally, the radiation parameters will be given as a function of the index of refraction. The purpose here is to study how various components of the radiation field change as the intensity of the specular reflection increases.

B. Flux of Radiant Energy

1. Albedo at the ground

The albedo at the ground is computed only for the Fresnel model. This albedo is shown on Fig. 2 as a function of the total optical thickness of the atmosphere for five solar zenith angles $(\theta_o)^*$. At large optical thickness, $\tau_1 = 2.0$, the albedo is nearly independent of the solar zenith angle, the relative variation being about 5 percent from the mean value of 0.061. This is nearly the albedo of diffuse light, which is 0.067 for $\tau_1 = 2.0$. As the optical thickness decreases from $\tau_1 = 2.0$, the albedo changes from the common value of about 0.061 to the albedo of the direct sunlight, when no atmosphere exists ($\tau_1 = 0$). When the sun is rather high in the sky, $\theta_o < 46^o$, the albedo changes less than 0.01 absolute value as the solar zenith angle varies for a given optical thickness. Furthermore, the albedo is small for high sun, but increases as the optical depth of the atmosphere increases. On the other hand, when the sun is low in the sky, the albedo is much more sensitive to the optical depth of the atmosphere, as demonstrated by the curve for $\theta_o = 78.5^o$.

---

* The parameter θ_o is called the solar zenith and nadir angle at the bottom and top of the atmosphere, respectively.

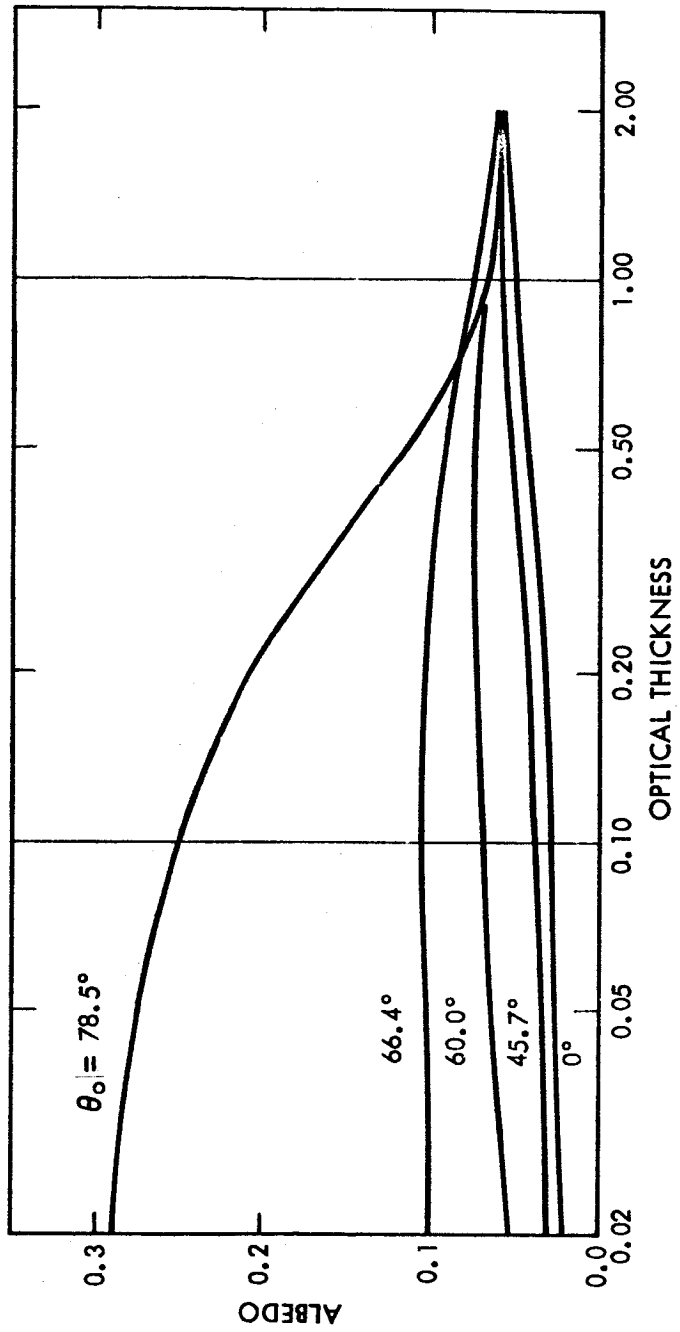

Figure 2. Albedo of the ground as a function of optical thickness.

The ground albedo can be explained in terms of the separate albedos of two streams of radiation that together comprise the total flow of radiation. One stream is the flux of reduced solar radiation, and the other is the stream of airlight. Designate the albedos of these streams with the fluxes that are introduced in Eq. (3.39) - (3.40):

$$\lambda_o^1 = {}^{\uparrow}\mathcal{F}_1 / {}^{\downarrow}\mathcal{F}_1, \quad \lambda_o^{2,3} = ({}^{\uparrow}\mathcal{F}_2 + {}^{\uparrow}\mathcal{F}_3)({}^{\downarrow}\mathcal{F}_2 + {}^{\downarrow}\mathcal{F}_3)^{-1} \quad .$$

When these quantities and Eq. (3.39) are substituted into Eq. (3.38), an expression for the resultant albedo is obtained:

$$\lambda_o^F(\tau_1, \mu_o) = \frac{{}^{\downarrow}\mathcal{F}_1}{{}^{\downarrow}\mathcal{F}^F} \lambda_o^1 + \frac{{}^{\downarrow}\mathcal{F}_2 + {}^{\downarrow}\mathcal{F}_3}{{}^{\downarrow}\mathcal{F}^F} \lambda_o^{2,3} \quad . \qquad (4.1)$$

Hence, the resultant albedo is determined by the separate albedos (λ_o^1 and $\lambda_o^{2,3}$), which are weighted according to the relative strength of the downward flux of the corresponding stream of radiation. The albedo of the reduced solar flux (λ_o^1) is given on Fig. 1. The relative weights and the albedo of the airlight require some discussion, which follows.

The ratio of only the reduced solar flux at the ground to the sum of both the reduced solar airlight and fluxes (${}^{\downarrow}\mathcal{F}^F$) that fall on the ground is given as a function of optical thickness on Fig. 3. If the sun is at the zenith, the flux of direct sunlight exceeds the flux of airlight, when the optical thickness is less than 1.1. As the solar zenith angle increases, the solar flux is more strongly attenuated, since the optical path length through the atmosphere increases. When the solar zenith angle reaches $\theta_o = 84.3^o$, most of the flux is directly from the sun,

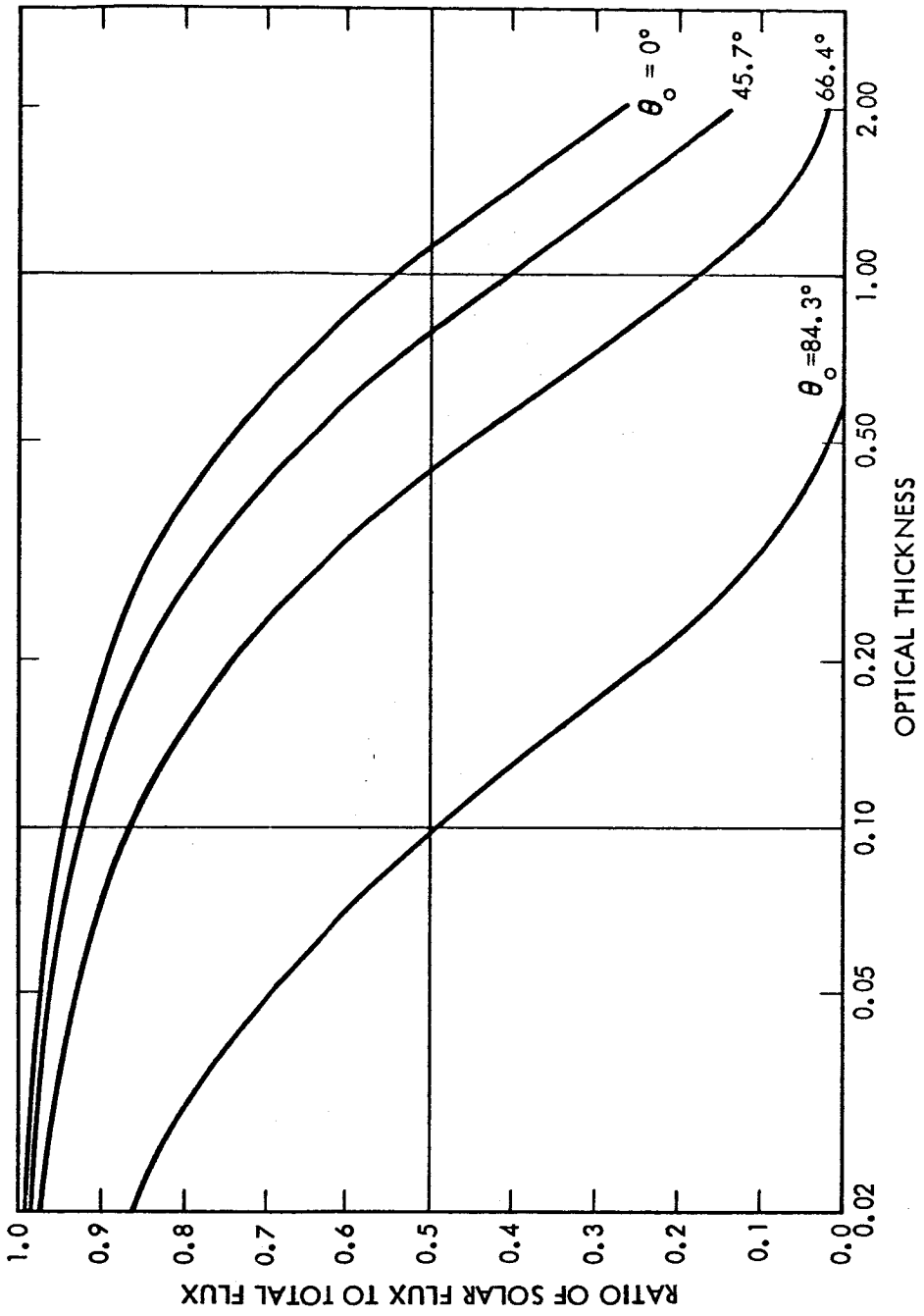

Figure 3. The ratio of the reduced solar flux to the total flux that falls on a horizontal surface at the ground as a function of optical thickness ($\tau_1(\tau^F)^{-1}$).

only if the optical thickness is less than 0.097. If the solar zenith angle is between 0^{o} and 84^{o}, then the reduced solar flux always exceeds the flux of airlight when $\tau_1 < 0.097$, and the reverse is true when $\tau_1 > 1.1$.

The albedo of the diffuse airlight is given as a function of optical thickness in Table II. The data are given for only one solar zenith angle ($\theta_o = 45.7^{o}$), since the relative albedo changes less than 15 percent as a function of θ_o and for a given optical thickness ($\theta_o \leq 84.3^{o}$). The albedo of diffuse light is largest for $\tau_1 = 0.02$, where $\lambda_o^F = 0.156$, and least for $\tau_1 = 2.0$, where $\lambda_o^F = 0.066$.

The question arises: why does the albedo of the diffuse light depend strongly on the optical thickness of the atmosphere? The reason is that the Fresnel reflection coefficient increases as the zenith angle of the incident light increases, if the index of refraction is small, as in the present study. The intensity of the skylight from near the horizons is greater than the intensity of the skylight from the zenith, when the optical thickness is small. The reverse is true for large optical thickness (see Fig. 4). Hence a larger fraction of the diffuse skylight is reflected when the optical thickness is small than when it is large.

TABLE II

The albedo at the ground of the diffuse airlight, when the ground reflects specularly. $\mu_o = 0.7$, $\theta_o = 45.7^{o}$.

τ_1	0.02	0.05	0.10	0.15	0.25	0.50	1.00	2.00
albedo	0.1560	0.1431	0.1297	0.1204	0.1077	0.0903	0.0751	0.0657

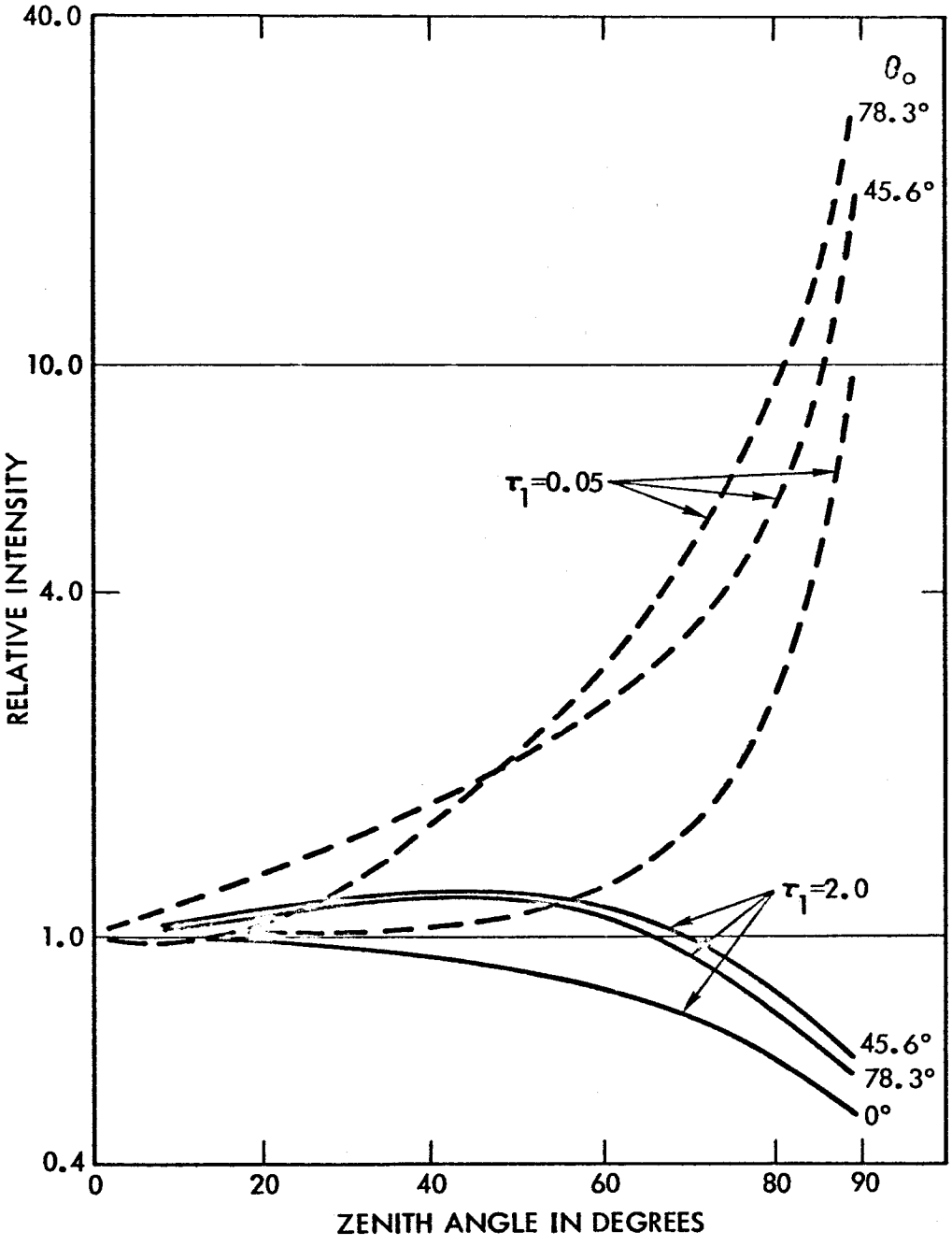

Figure 4. Darkening of the sky towards the horizon at the ground, when the ground reflects radiation specularly. The numbers at the end of the lines refer to the solar zenith angle. The azimuth is $\phi_o - \phi = 0^o$, or the vertical planes of observation and of sun coincide.

Since the albedo at the ground ($\lambda_o^F(\tau_1)$) is the same for the Fresnel and Lambert models, the flux of radiation into the bottom of the atmosphere from below is nearly the same for both models. The total upward flux at the ground can be separated into three components with a relation that is obtained by substituting Eq. (3.39) into Eq. (3.40):

$$\uparrow\mathfrak{F}^i(\tau_1, \mu_o) = \lambda_o^F(\tau_1)\left[\downarrow\mathfrak{F}_1(\tau_1) + \downarrow\mathfrak{F}_2(\tau_1) + \downarrow\mathfrak{F}_3^i(\tau_1)\right], \quad i = F, L, \tag{4.2}$$

where the superscript i indicates whether the ground reflects radiation according to Fresnel's or Lambert's law. The ratio of the upward flux for the Lambert model to the upward flux for the Fresnel model is

$$\frac{\uparrow\mathfrak{F}^L(\tau_1, \mu_o)}{\uparrow\mathfrak{F}^F(\tau_1, \mu_o)} = \frac{\downarrow\mathfrak{F}_1 + \downarrow\mathfrak{F}_2 + \downarrow\mathfrak{F}_3^L}{\downarrow\mathfrak{F}_1 + \downarrow\mathfrak{F}_2 + \downarrow\mathfrak{F}_3^F} = 1 + \frac{\downarrow\mathfrak{F}_3^L - \downarrow\mathfrak{F}_3^F}{\downarrow\mathfrak{F}_1 + \downarrow\mathfrak{F}_2}, \tag{4.3}$$

since the computed data show that $\downarrow\mathfrak{F}_3^i(\downarrow\mathfrak{F}_1 + \downarrow\mathfrak{F}_2)^{-1} << 1$. The ratio that appears on the right of Eq. (4.3) is given in Table III for both small and large optical thicknesses. The absolute value of the ratioes are less than a few per cent. Hence, the upward flux of radiant energy into the bottom of the atmosphere is nearly the same for both models.

TABLE III

The ratio that appears on the right hand side of Eq. (4.3) for small and large optical thickness.

τ_1	μ_o	$\frac{{}^{\downarrow}\mathcal{J}_3^L - {}^{\downarrow}\mathcal{J}_3^F}{{}^{\downarrow}\mathcal{J}_1 + {}^{\downarrow}\mathcal{J}_2}$
0.02	0.1	-0.037
	0.2	-0.009
	0.4	-0.001
	1.0	0.000
2.00	0.1	-0.007
	0.2	0.004
	0.4	0.004
	1.0	0.003

2. Upward flux at the top of the atmosphere

The meanings of the different flux quantities that appear on Fig. 5 will be described again. The term flux, when used here, will always refer to the flow of radiation through a horizontal surface. The downward flux incident on top of the atmosphere is $\mu_o \pi$, independent of the atmospheric optical thickness. In order to express the flux as an absolute value when the solar constant is $F_o(\lambda)$, the flux values given here must be multiplied by $\pi^{-1} F_o$. The various upward flux parameters are computed from Eq. (3.54) to (3.59). As indicated by Eq. (3.54), the

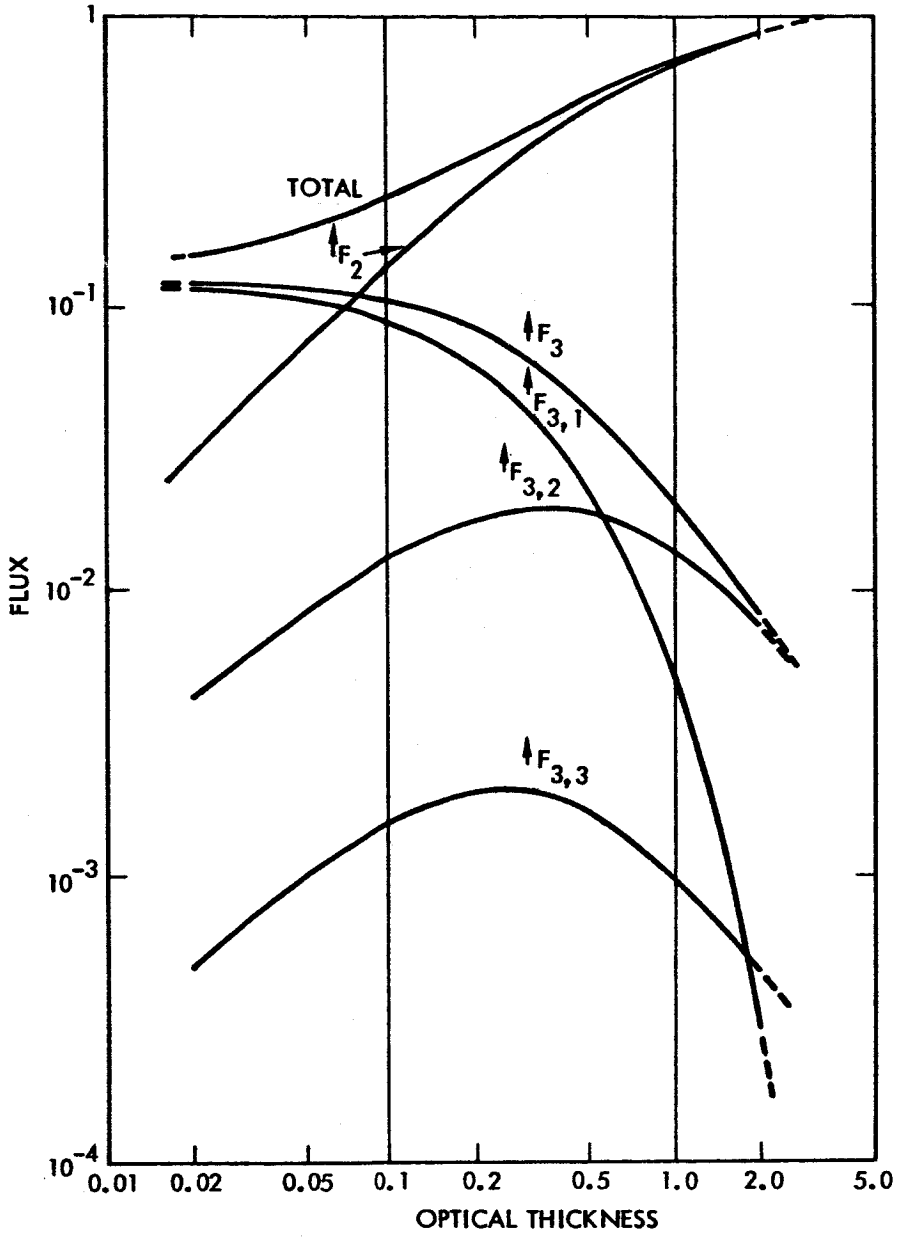

Figure 5. The upward flux from the top of the atmosphere as a function of the optical thickness. The script $\mathcal{F}$'s for flux that appear in the text are replaced by printed F's on the figures. The solar nadir angle is $\theta_o = 66.4^o$.

total upward flux at the top of the atmosphere can be separated into two streams of radiation: the first containing the light that is scattered from the atmosphere and is not reflected from the ground ($^{\uparrow}\mathcal{F}_2$), and the other stream containing all other radiation, which is reflected from the ground ($^{\uparrow}\mathcal{F}_3$). The stream of radiation reflected from the ground can be subdivided into three more streams (Eq. (3.56)). The first of these streams is the reduced solar flux that is reflected from the ground and passes either directly, or after one or more scatterings, out of the atmosphere ($^{\uparrow}\mathcal{F}_{3,1}$); the second stream consists of diffuse radiation that is reflected from the ground once, and only once ($^{\uparrow}\mathcal{F}_{3,2}$); the third stream consists of all radiation that has been reflected from the ground two or more times ($^{\uparrow}\mathcal{F}_{3,3}$).

The upward flux at the top of the atmosphere is given as a function of optical thickness on Fig. 5. When the optical thickness of the atmosphere becomes infinite, the upward flux equals the incident downward flux ($\mu_o \pi$), which equals 1.257 when $\mu_o = 0.4$; and the radiation leaving the top of the atmosphere is independent of the reflecting surface at the base of an infinite atmosphere. On the other hand, when the optical thickness of the atmosphere approaches zero, the flux of the airlight* approaches zero ($^{\uparrow}\mathcal{F}_2 \to 0, {}^{\uparrow}\mathcal{F}_{3,2} \to 0, {}^{\uparrow}\mathcal{F}_{3,3} \to 0$), and the total upward flux becomes just the reflected direct solar flux $^{\uparrow}\mathcal{F}_{3,1}$ ($^{\uparrow}\mathcal{F} = {}^{\uparrow}\mathcal{F}_3 = {}^{\uparrow}\mathcal{F}_{3,1} = 0.1234$ at $\tau_1 = 0$).

---

*Airlight does not include any light that leaves the ground and passes directly through the atmosphere without being scattered.

The flux of radiation that has been reflected from the ground ($\uparrow\mathcal{F}_3$) exceeds the flux of the stream that has not been reflected from the ground ($\uparrow\mathcal{F}_2$), when the optical thickness is less than 0.076 (for $\mu_o = 0.4$). When the $\uparrow\mathcal{F}_3$ - stream is dominant, it consists of principally the reflected direct sunlight. When the $\uparrow\mathcal{F}_2$ - stream is dominant, the $\uparrow\mathcal{F}_3$ - stream rapidly diminishes with increasing optical thickness, until it is about 0.01 of the total flux at $\tau_1 = 2.0$. It is important to note that the flux of the light that has been reflected two or more times from the ground ($\uparrow\mathcal{F}_{3,3}$) is less than 0.01 of the total; that is, this component makes a negligible contribution to the total flux, when the index of refraction is small ($m \sim 1.35$). It will be shown in the forthcoming discussions, that the effect of the twice-reflected component has a negligible effect on the total intensity and the degree of polarization of the radiation leaving the top of the atmosphere. Hence, this component (Eq. (3.52)) can be neglected for most purposes. By neglecting this component, the most difficult and extensive part of the computations, involving solutions of integral equations, is eliminated.

If the upward fluxes shown on Fig. 5 are divided by the incident flux, then one has the albedo data, which are given on Fig. 6. The albedo at the ground is also given. As the optical thickness approaches infinity, the albedo at the top approaches one. When $\tau_1 = 2.0$, the total albedo is 0.70, and the albedo is 0.69 for the stream of radiation that has not been reflected from the ground and whose flux was designated

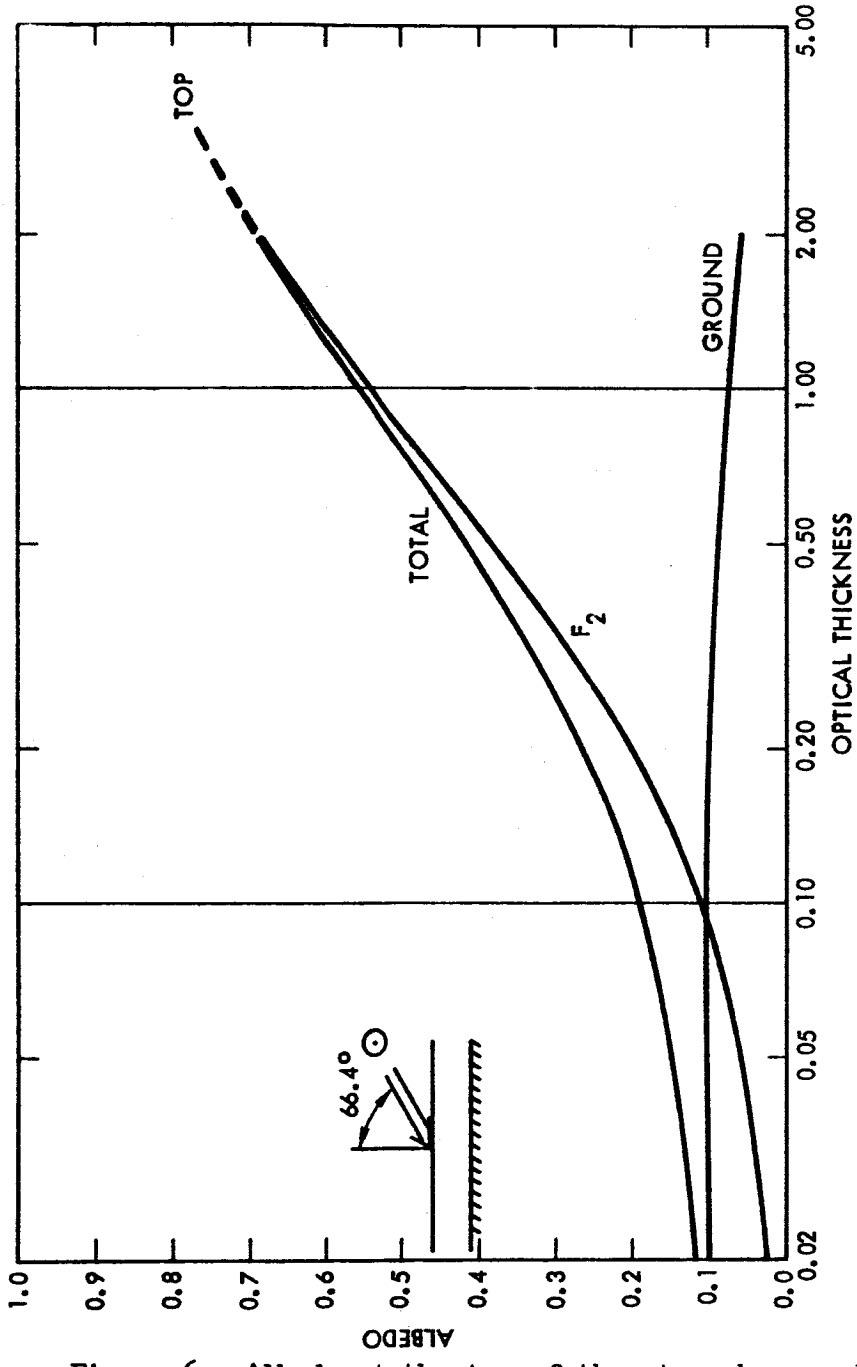

Figure 6. Albedo at the top of the atmosphere and at the ground, when radiation is reflected from the ground according to Fresnel's law. The curve labeled F_2 gives the value of the albedo at the top of the atmosphere, if the ground albedo were zero. The solar nadir angle is $\theta_o = 66.4^o$.

by $\uparrow\mathcal{F}_2$ on Fig. 5. Once again it is shown that the effect of the ground is negligibly small at $\tau_1 = 2.0$. As the optical thickness decreases, the total and $\uparrow\mathcal{F}_2$ - albedos decrease. When the optical thickness becomes zero, the albedo of the $\uparrow\mathcal{F}_2$ - stream is zero, and the albedos at the top of the atmosphere and ground are identical.

Figures 7 and 8 give more data on the total upward flux at the top of the atmosphere. Figure 7 shows that for any solar nadir angle, the upward flux increases monotonically with increasing optical thickness and approaches $\mu_o \pi$ as $\tau_1 \rightarrow \infty$. If the optical thickness is greater than 0.2, the flux decreases with increasing solar nadir angle. The dependence of the solar flux on the solar nadir angle is shown more clearly on Fig. 8. The curve for $\tau_1 = 0.05$ on Fig. 8 shows that at small optical thickness the upward flux is not a simple function of the solar nadir angle. Data not given here show that fluxes of the two streams of radiation, the $\uparrow\mathcal{F}_2$ - and $\uparrow\mathcal{F}_3$ - streams, are nearly equal at $\tau_1 = 0.05$ for high sun ($\theta_o < 53^o$), but that the component reflected from the ground ($\uparrow\mathcal{F}_3$) is dominant for larger solar nadir angles ($\theta_o > 53^o$).

The upward flux from the model with Lambert ground reflection[5] is nearly the same as that for the Fresnel model, when the solar nadir angle and the optical thickness are the same for both. This is to be expected, since the flux into the top of both models is the same, the net flux at the bottom is within a few per cent of being the same, as shown in Section IV.B.1. and no radiant energy is absorbed within the

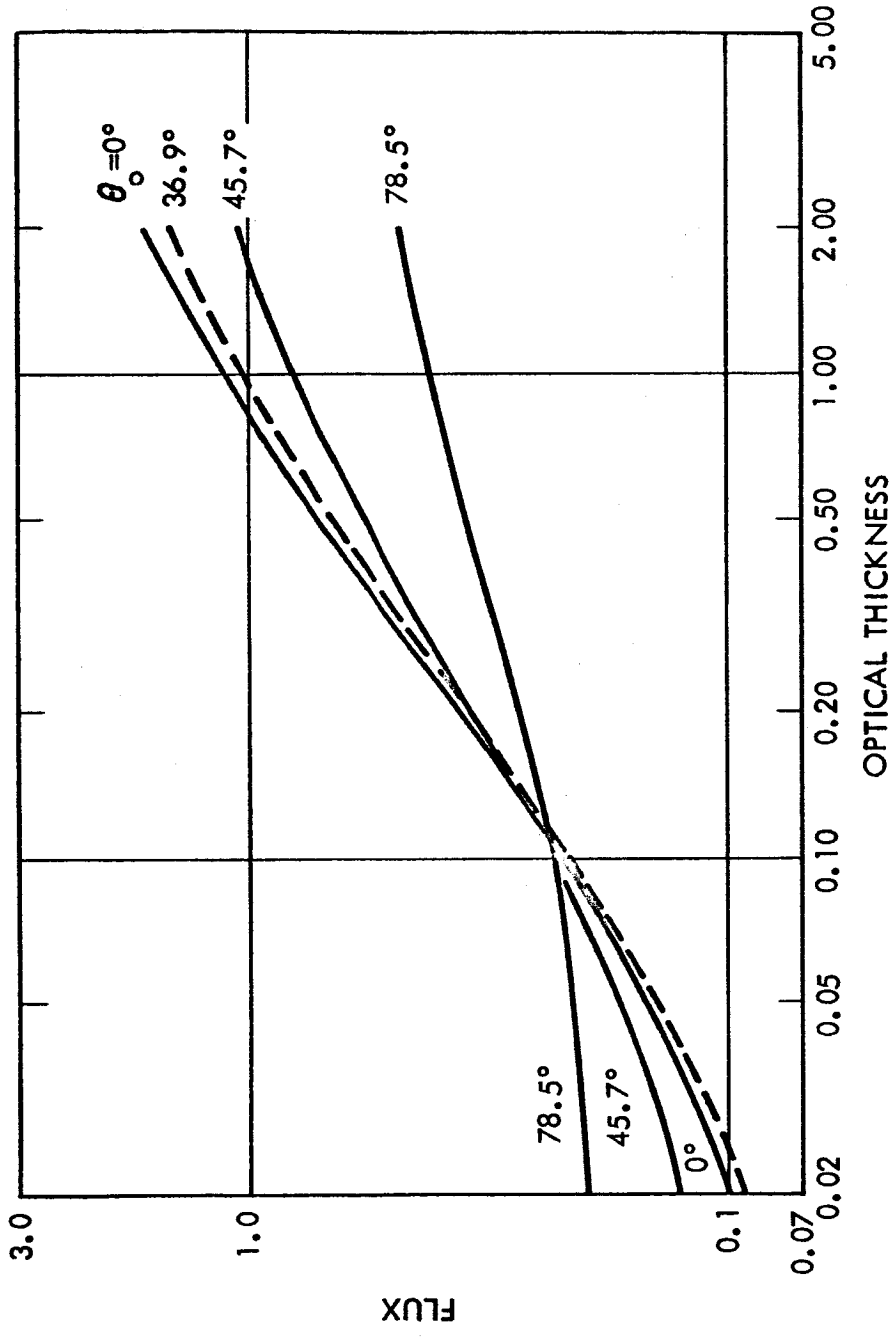

Figure 7. Upward flux at the top of the atmosphere as a function of optical thickness. The ground reflects radiation according to Fresnel's law.

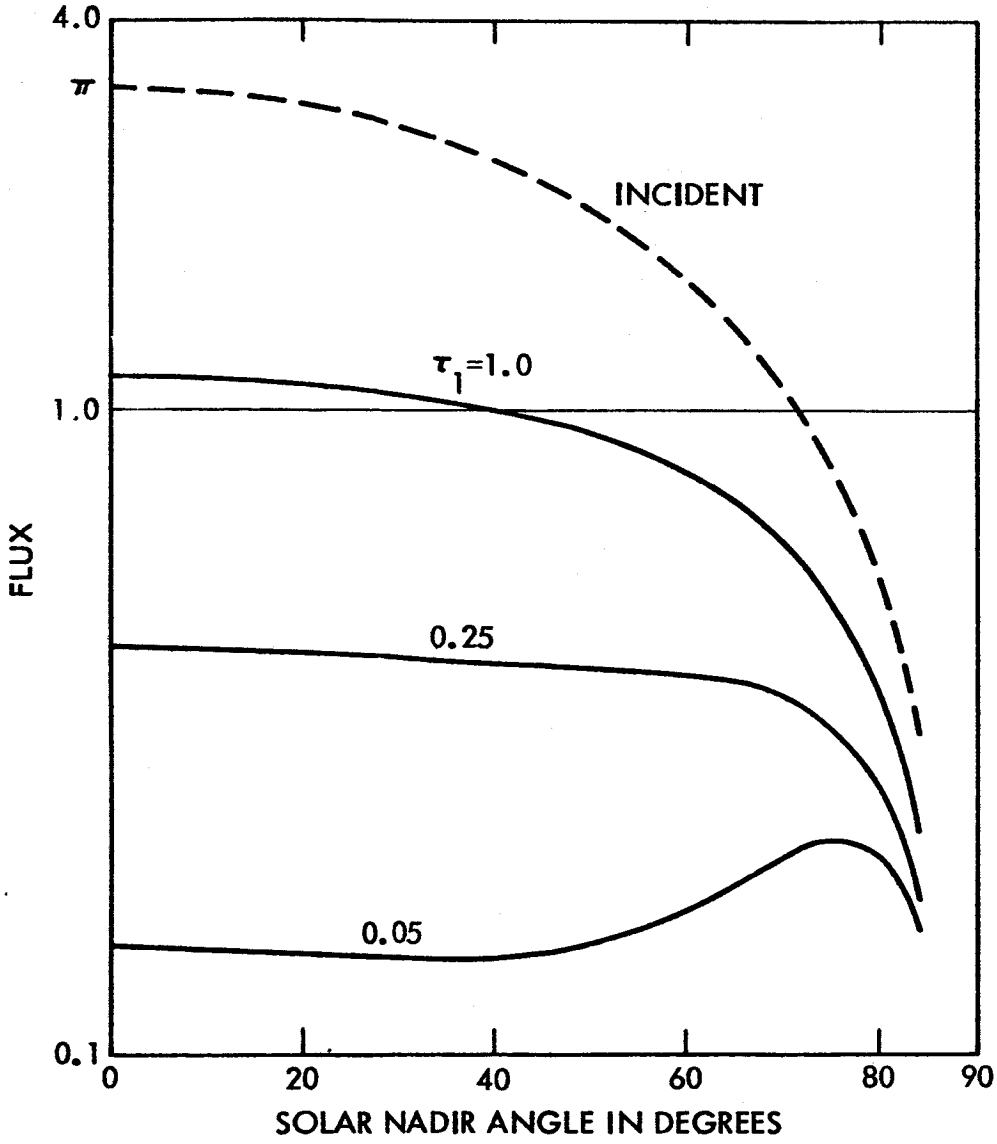

Figure 8. Upward flux at the top of the atmosphere as a function of the solar nadir angle. The ground reflects radiation according to Fresnel's law. The dashed curve gives the value of the incident solar flux ($\mu_o \pi$) on a horizontal surface at the top of the atmosphere.

model atmosphere. The ratio of the upward flux for the Fresnel model to the upward flux for the Lambert model is shown on Fig. 9. If the solar nadir angle is less than 60°, the ratio is greater than 0.98; and if the solar nadir angle $\theta_o = 78.5^{\circ}$, the ratio is greater than 0.94.

Because the upward flux at the top of the atmosphere is nearly the same for either of the two extreme models of ground reflection,* it would appear that the flux is insensitive to changes of the natural laws of ground reflection, if the ground albedo does not change. As a consequence, one can use the Lambert model, which is much simpler for making flux computations. Coulson[5] has given a simple expression for the upward flux at the top of the atmosphere and computed it for the Lambert model. Hence, by knowing only the ground albedo and the atmospheric optical thickness, one can use the Lambert model for obtaining good estimates of the upward flux at the top of the atmosphere.

C. Total Intensity

The total upward intensity at the top of a model atmosphere is first discussed in terms of the total intensity of each of the several component streams of the radiation field. The term total intensity refers to the intensity parameter that is the sum of the ℓ- and r- components of the intensity (Eq. (2.3)), and is not necessarily the sum of the intensities of all the several streams of radiation. The intensities that

---

* Later, the fluxes for the two models are shown to be nearly equal, when the index of refraction and the ground albedo are large.

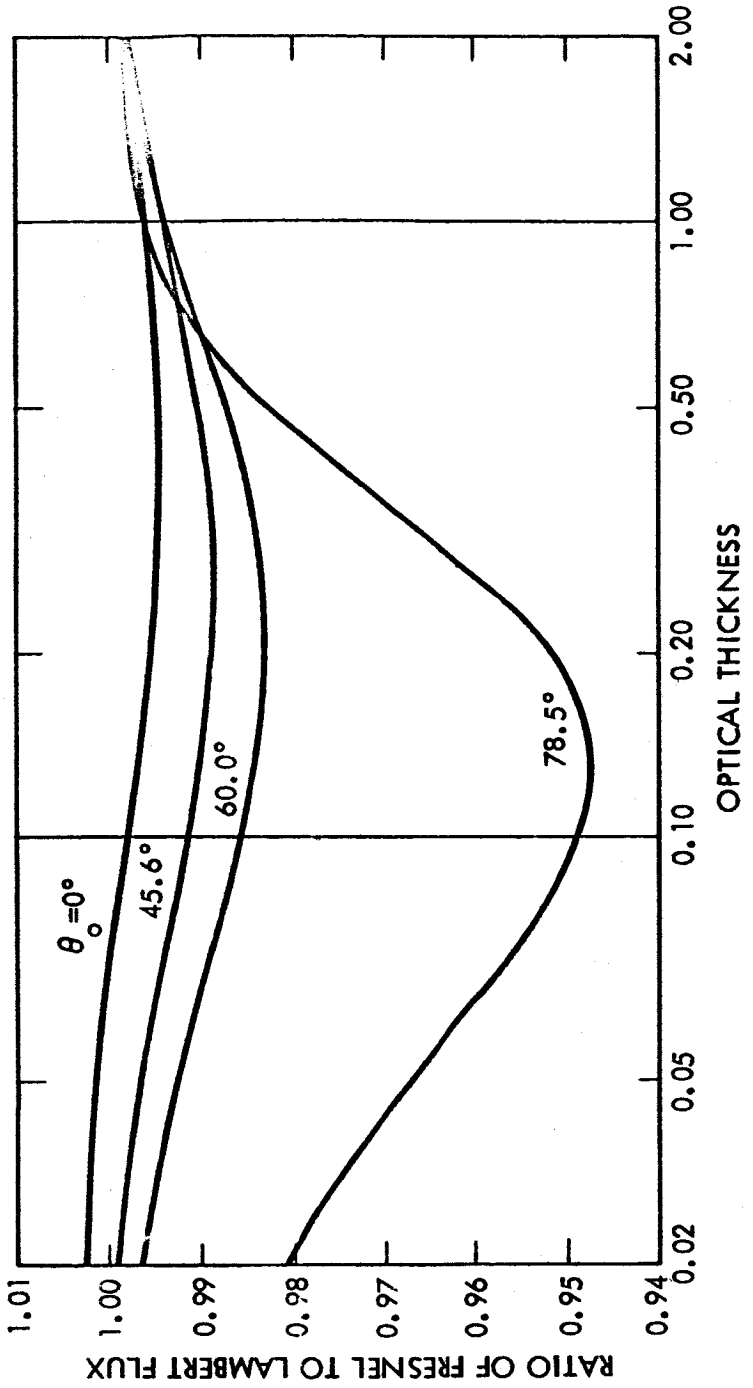

Figure 9. The ratio of the upward Fresnel flux to the upward Lambert flux at the top of the atmosphere.

appear on Fig. 10 are calculated from the following formulae: $\uparrow I^{*F}$ from Eq. (3.45), $\uparrow I$ from (3.46), $\uparrow I_g^{(trans)}$ from (3.48), $\uparrow I_{g,1}^{(trans)}$ from (3.49), $\uparrow I_{g,2}^{(trans)}$ from (3.51) and $\uparrow I_{g,3}^{(trans)}$ from (3.52). The total intensity for the Lambert model ($\uparrow I^{*L}$) is computed from R.T., Eq. (235), p. 279. These separate intensity components refer to the same streams of radiation that were used in the discussion of fluxes in Section IV.B.2. The correspondence between total intensity and flux parameters for the same stream of radiation is $\uparrow I^{*F}$ and total Fresnel flux, $\uparrow I^{*L}$ and total Lambert flux, $\uparrow I$ and $\uparrow \mathfrak{I}_2$, $\uparrow I_g$ and $\uparrow \mathfrak{I}_3$, and $\uparrow I_{g,i}$ and $\uparrow \mathfrak{I}_{g,i}$ ($i = 1, 2, 3$).

In order to express the total intensity in absolute units, the values that are given in this report must be multiplied by the factor $\pi^{-1} F_o(\lambda)$, where F_o is the monochromatic solar constant. Then the total intensity will be expressed in units of the solar constant per steradian.

The total intensity at the top of the atmosphere of radiation from the nadir is given as a function of optical thickness on Fig. 10. The total intensity equals 0.35 for an atmosphere of infinite optical thickness. When the optical thickness decreases to $\tau_1 = 2.0$, radiation reflected from the ground contributes less than 0.02 to the sum. As the optical thickness decreases to zero, the intensities for the Fresnel model ($\uparrow I^{*F}$) and for the model of zero ground albedo ($\uparrow I$) approach zero; and the intensity of the Lambert model approaches the value of μ_o times the reflection coefficient of the direct sunlight. Since the intensity of the light from the ground ($\uparrow I_g^{(trans)}$) is less than 0.16 of

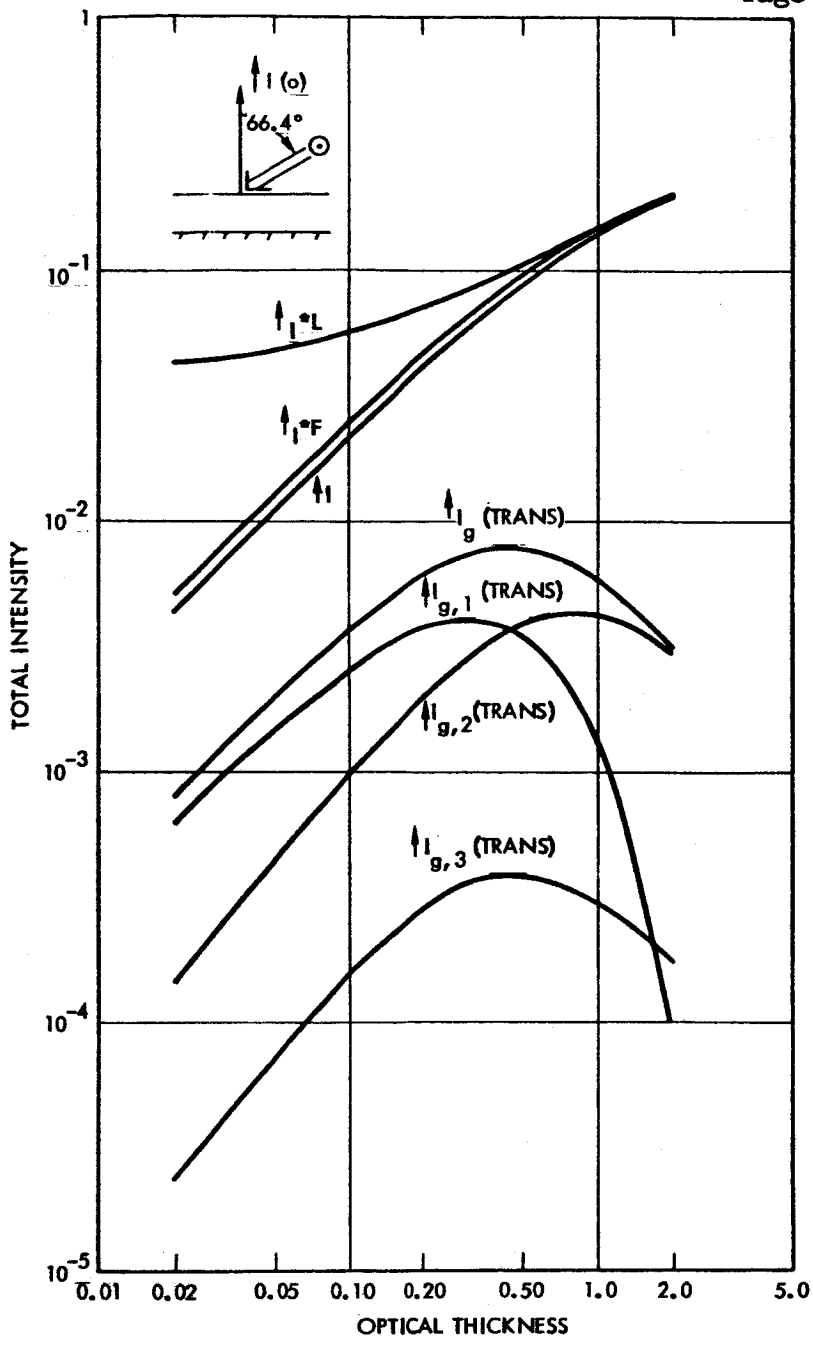

Figure 10. Total intensity of radiation at top of the atmosphere and from the nadir as a function of optical thickness. The solar nadir angle $\theta_o = 66.4^\circ$. The superscripts L and F refer to the cases where the ground reflects the incident radiation according to Lambert's and Fresnel's law, respectively.

the total Fresnel intensity ($\uparrow I^{*F}$) for all optical thicknesses, the Fresnel intensity of radiation from the nadir is not strongly affected by the light reflected from the ground. The intensity of the light that is twice, or more, times reflected from the ground ($\uparrow I_{g,3}^{(trans)}$) is less than 0.01 of $\uparrow I^{*F}$, and can be neglected for most purposes. If the reflected component $\uparrow I_{g,2}^{(trans)}$ is neglected also, the error in $\uparrow I^{*F}$ would not be more than 0.05.

The total intensity at the top of the atmosphere of radiation from the nadir is shown as a function of the solar nadir angle. (Fig. 11). The total intensity decreases as the solar nadir angle increases (except for $\uparrow I^{*L}$ at $\tau_1 = 0.05$), in part because the flux on top of the atmosphere decreases by the factor $\cos \theta_o$. The difference between a pair of $\uparrow I^{*L}$ and $\uparrow I^{*F}$ curves for the same optical thickness increases with decreasing optical thickness. The relative difference between the total intensity for the Fresnel model ($\uparrow I^{*F}$) and the total intensity ($\uparrow I$) for the model with zero ground albedo is not more than 0.2, except for small optical thickness ($\tau_1 = 0.05$) and large solar nadir angle ($\theta_o > 65^o$). The Fresnel intensity ($\uparrow I^{*F}$) is discontinuous when the sun is at the zenith ($\theta_o = 0$), because of the strong specular reflection of the direct sunlight towards the zenith.

The total intensity is given as a function of the nadir angle, when the solar nadir angle is fixed at $\theta_o = 66.4^o$, and the total optical thickness of the atmosphere is $\tau_1 = 0.50$ (Fig. 12). Because the ground

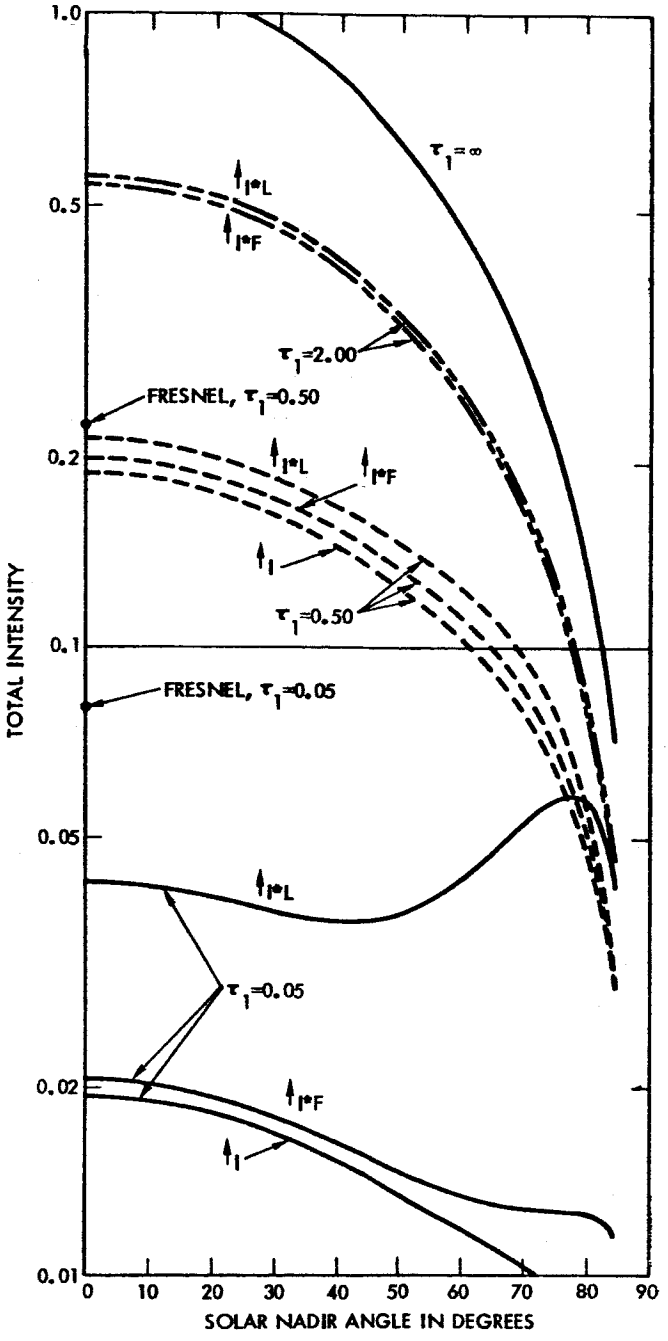

Figure 11. Intensity of radiation from the nadir at the top of the atmosphere as a function of solar nadir angle.

albedo is small (0.092), the effect of the ground on the intensity of the radiation leaving the top of the atmosphere is small for this moderate optical thickness. The Lambert intensity is the largest towards the nadir, but the Fresnel intensity is largest towards the limbs.

The Fresnel intensity is discontinuous at the angle $\theta = 66.4^{\circ}$, where the mirror image of the sun appears (Fig. 12). Although the total intensity in the direction of the image is only slightly greater than the intensity of the nearby surroundings, all of the solar energy is confined to a small solid angle of about 7×10^{-5} sterad in the case of the earth, whereas the intensity unit used on Fig. 12, gives the amount of radiant energy confined to one sterad. Hence, the sun's image is about $(7 \times 10^{-5})^{-1} \doteq 10^{4}$ as bright as a nearby spot of the same size.

The limb darkening is shown in Table IV. The ratio of the intensity in the direction $\theta = 78.5^{\circ}$ to the intensity of radiation from the nadir is used as the measure of limb darkening. The limb darkening does not differ by more than 0.02 among the three models for a given solar nadir angle θ_o, when the optical thickness is greater than or equal to two. Actual limb darkening occurs only when the sun is fairly high in the sky and $\tau_1 \geqslant 2.00$. Data not given in Table IV show that limb darkening does not occur for the models of Table IV, when $\tau_1 \leqslant 1.00$. The limb darkening, or better, brightening becomes more sensitive to the type of ground reflection, when the optical thickness is small. If the optical thickness is very small ($\tau_1 = 0.02$), the limb brightening is least for

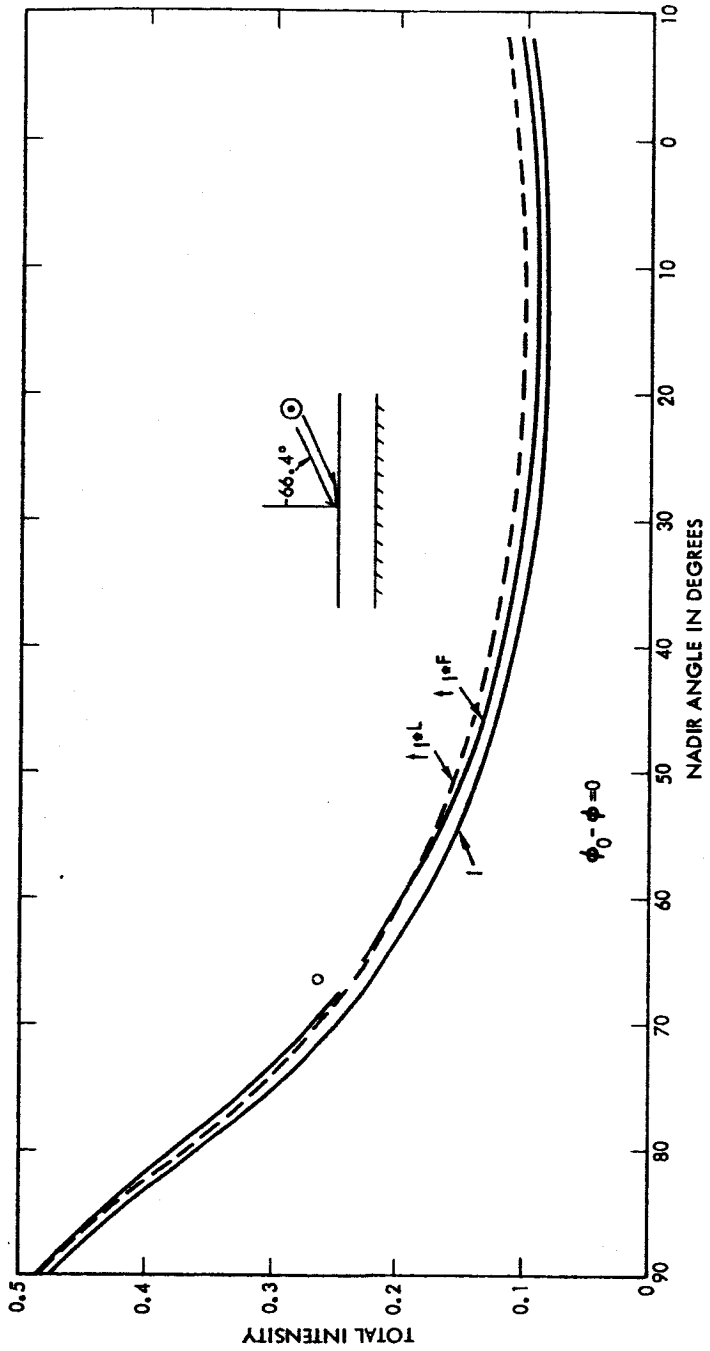

Figure 12. Total specific intensity as a function of nadir angle. The radiation comes from the side of the nadir opposite to the side of the sun; that is, $\phi_o - \phi = 0$. The optical thickness, $\tau_1 = 0.50$. The solar nadir angle $\theta_o = 66.4^o$. The albedo at the ground $\lambda_o^F(\tau_1) = 0.092$.

TABLE IV

The limb darkening from above for three atmospheric models. The two figures in parentheses give the average intensity $\left[{}^{\uparrow}I^{*F}(77.9^{\circ}) + {}^{\uparrow}I^{*F}(79.0)\right] \div 2$ rather than ${}^{\uparrow}I^{*F}(78.5^{\circ})$, in order to avoid using the high intensity of the solar image, which occurs when $\theta = \theta_o = 78.5^{\circ}$.

Optical thickness τ_1	solar nadir angle, θ_o	zero albedo $\frac{{}^{\uparrow}I(\theta=78.5^{\circ})}{{}^{\uparrow}I(\theta=0^{\circ})}$	Fresnel $\frac{{}^{\uparrow}I^{*F}(78.5^{\circ})}{{}^{\uparrow}I^{*F}(0^{\circ})}$	Lambert $\frac{{}^{\uparrow}I^{*L}(78.5^{\circ})}{{}^{\uparrow}I^{*L}(0^{\circ})}$
0.02	84.3°	9.16	11.04	1.57
	78.5	8.59	(10.4)	1.46
	60.0	6.06	7.79	1.65
	0.0	2.51	3.35	1.37
0.25	84.3	7.06	7.20	5.49
	78.5	6.26	(6.37)	4.31
	60.0	4.30	4.54	3.16
	0.0	1.79	1.95	1.56
2.00	84.3	4.22	4.17	4.16
	78.5	3.28	3.24	3.23
	60.0	1.88	1.86	1.85
	0.0	0.88	0.87	0.87
∞	84.3	2.88		
	78.5	2.20		
	60.0	1.25		
	0.0	0.67		

the Lambert model, since the light is reflected isotropically from the ground. The Fresnel and zero ground albedo models have approximately the same amount of limb brightening at small optical thickness.

D. Maximum Degree of Polarization

In order to demonstrate the usefulness of the maximum degree of polarization as a parameter of the radiation field, the degree of polarization of light leaving the top of model atmospheres and in the vertical plane of the sun is shown on Fig. 13. The general features of the degree of polarization can be considered as deviations from the degree of polarization of primary scattering. The degree of polarization of primary scattering is given by the relation $P = \sin^2 \Theta (1 + \cos^2 \Theta)^{-1}$, where Θ is the angle between the direct solar rays and the direction of observation. The primary degree of polarization is zero in the direction of the anti-solar point and reaches a maximum of one in a direction 90° from the incident solar rays. This picture is modified by multiple scattering in the atmosphere and by the ground reflection, as shown on Fig. 13. Figure 13 shows that the degree of polarization is not zero, but near zero at the solar point, that the maximum polarization occurs almost 90° from the sun, and that the maximum degree of polarization is less than one. By knowing just the value of the maximum degree for a model, one can then usually describe the general features of the degree of polarization.

The maximum degree of polarization in the sun's vertical plane is shown as a function of optical thickness on Fig. 14; the solar nadir angle

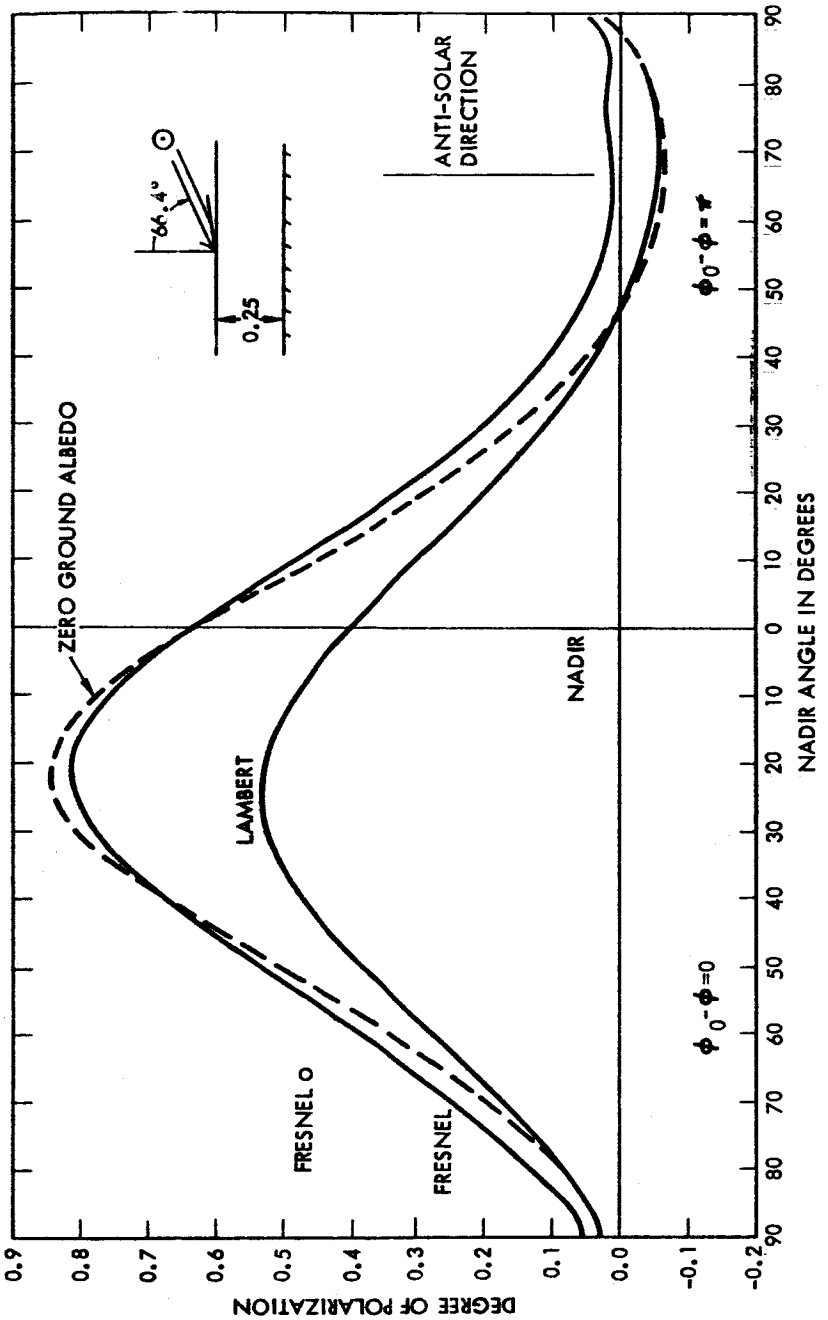

Figure 13. Degree of polarization of light leaving the top of model atmospheres and in the sun's vertical plane. The sun's nadir angle is $\theta_o = 66.4^o$. The optical thickness is $\tau_1 = 0.25$.

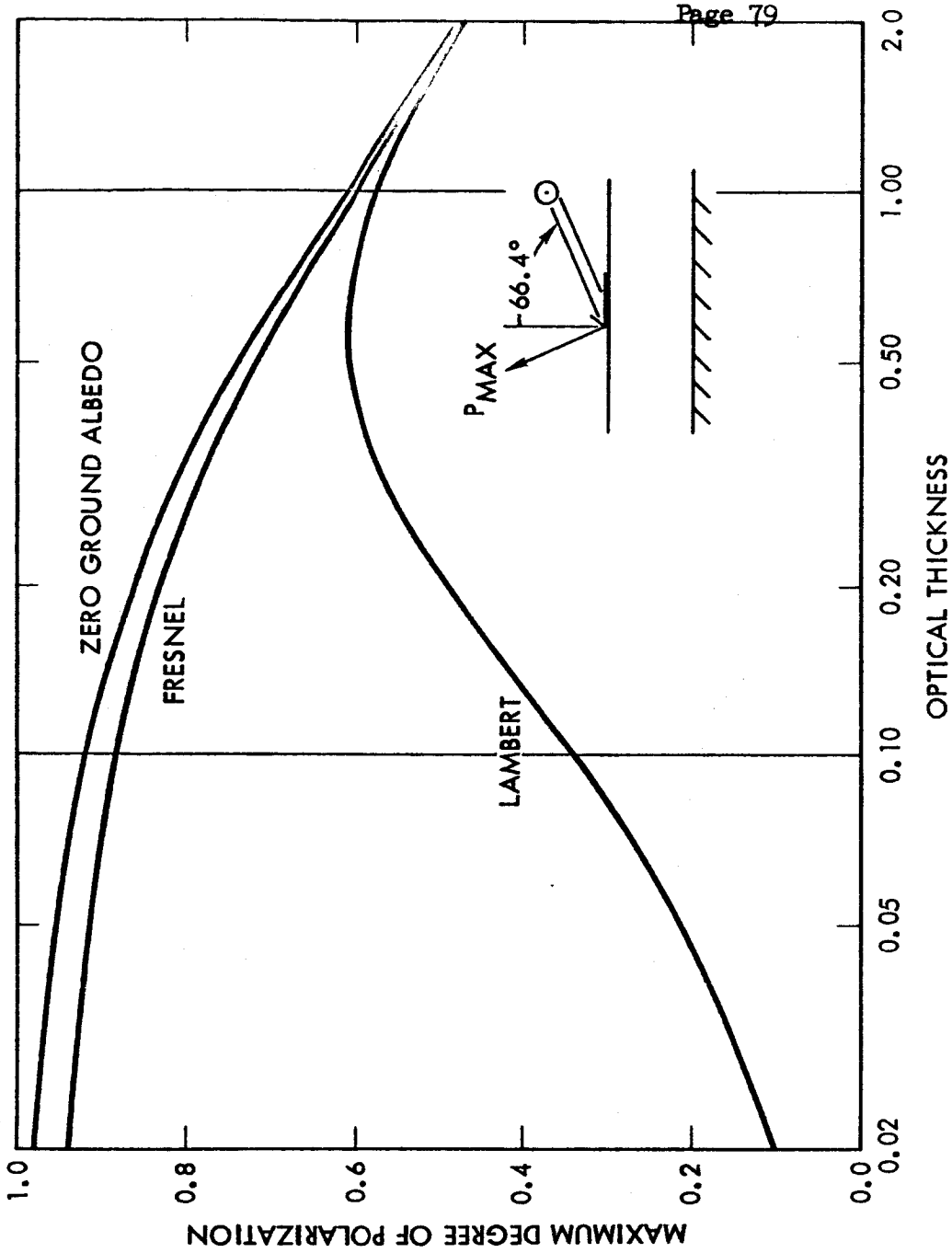

Figure 14. Maximum degree of polarization of light leaving the top of model atmospheres and in the sun's vertical plane as a function of optical thickness. The solar nadir angle is $\theta_o = 66.4^o$.

is $\theta_o = 66.4^o$ for these data. The maximum degree of polarization is 0.28 for an infinitely thick atmosphere. The maximum degree of polarization increases to a value between 0.46 to 0.48 for the three models as the optical thickness decreases to two. As the optical thickness decreases to zero, the maximum degree of polarization for the model with zero ground albedo approaches one, the value for primary scattering. The Fresnel maximum degree of polarization is only slightly less than that of the model without ground reflection, principally because the intensity of the light reflected from the ground is a small fraction of the total for the Fresnel model. The maximum degree of polarization for the Lambert model approaches zero as the optical thickness decreases to zero, since the light reflected from the ground is unpolarized for this model. Whereas the maximum degree of polarization of light received at the ground is nearly the same for both the Fresnel and Lambert models,[24] the maximum degree of polarization of light leaving the top is quite different for the two models at moderate, or smaller, optical thickness.

More data on the maximum degree of polarization leaving the top of the atmosphere are shown on Fig. 15*. The maximum degree of polarization decreases by a factor of almost two as the optical thickness increases from 0.05 to 2.00. The maximum degree of polarization for the model that does not reflect any light at the ground is slightly greater than for the Fresnel model, and the difference decreases with increasing

---

* The light from the direction of the solar image is the highest polarized at small optical thickness and large solar nadir angle, but these data are not used on Fig. 15.

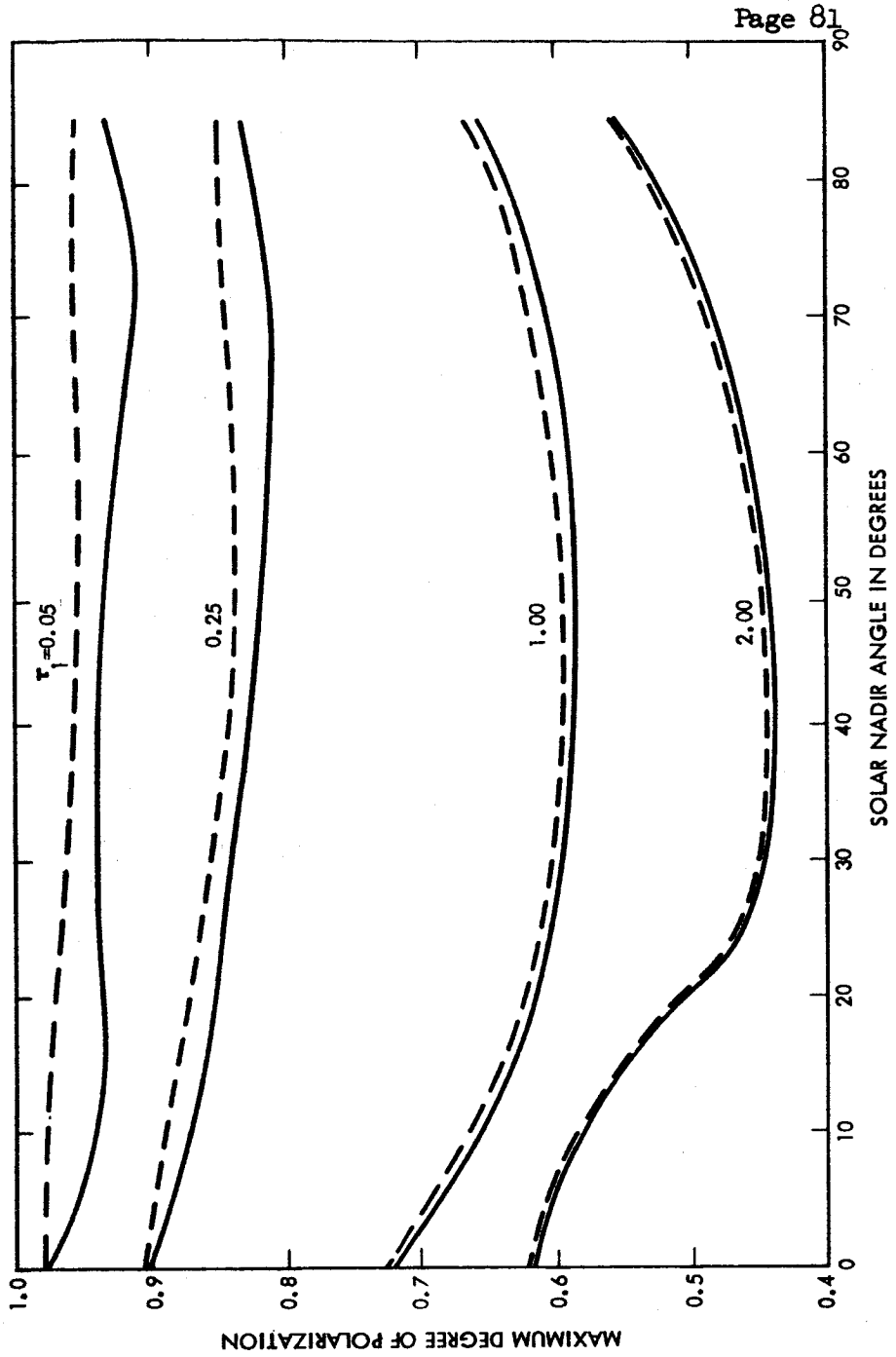

Figure 15. Maximum degree of polarization of the radiation leaving the top of the atmosphere and in the sun's vertical plane as a function of the solar nadir angle. The dashed curves apply to the zero ground albedo model, and the solid curve applies to the Fresnel model.

optical thickness. The variation of the maximum degree of polarization with solar nadir angle increases with increasing optical thickness.

The angular distance between the direction of the maximum degree of polarization of light leaving the top of the atmosphere in the vertical plane of the sun and the solar rays is shown as a function of optical thickness on Fig. 16; the sun's nadir angle is $\theta_o = 66.4^o$. The position of maximum polarization for the three models is 87^o at optical thickness 2.0. As the optical thickness approaches zero, the position shifts to 90^o for the model of zero ground albedo. The position for the Fresnel model is only slightly smaller than for the zero albedo model. The position for the Lambert model departs strongly from the 90^o position at small optical thickness, because the light from near the nadir is strongly depolarized by the relatively intense unpolarized radiation from the ground near the nadir. The maximum degree of polarization is shifted toward the limb, where the neutral light from the ground has less effect on light leaving the top of the atmosphere, because of the long optical path of the light through the atmosphere.

E. Neutral Points

The term neutral points refers to the places where the light leaving either the top or the bottom of the atmosphere is unpolarized. The neutral points are a useful parameter for studying the scattering properties of planetary atmospheres, because the neutral point positions are sensitive to changes of the scattering characteristics of a planetary

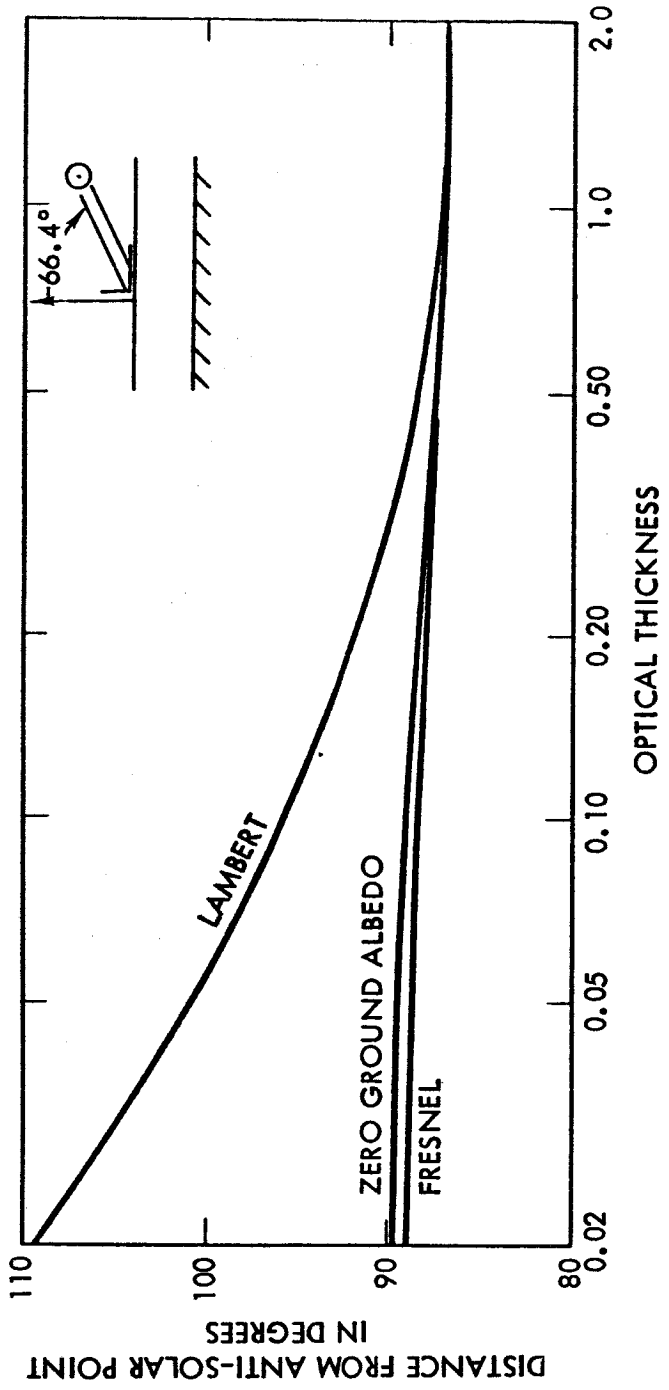

Figure 16. The angular distance along the sun's vertical plane between the solar rays and the direction of the maximum degree of polarization of light leaving the top of a model atmosphere. The sun's nadir angle is $\theta_o = 66.4^o$.

atmosphere[3,4,13,19,20,21,23] and to changes of the reflecting characteristics of the ground.[3,19,21,24,25] Furthermore, neutral point positions are easy to measure.[21,23]

Coulson[5] computed the neutral point positions at the top of the atmosphere, when the ground reflects radiation according to Lambert's law. As a result of his work, one can represent the neutral point positions schematically. The schematic positions of the neutral points shown on Fig. 17 would be expected, if the aerosol content of the atmosphere were low, and if the light were reflected from the ground according to approximately Lambert's law. Then three neutral points would appear in the vertical plane of the sun at one wavelength, but only two neutral points at any one time. When the solar nadir angle is small (left of Fig. 17), neutral point number one would appear between the anti-solar point and the horizon, and neutral point number 2 would appear between the anti-solar point and the nadir. When the solar nadir angle becomes large, neutral point one would disappear, and at about the same time, neutral point number 3 would appear near the opposite horizon. The exact positions of the neutral points depend essentially on wavelength, the aerosol content of the atmosphere, and the ground reflection characteristics.

The neutral point positions are shown as a function of optical thickness on Fig. 18; the solar nadir angle is $\theta_o = 66.4^o$. The position of neutral point one is plotted as a negative angle ($-\theta_1$ of Fig. 17), and the position of neutral point 2 is positive (θ_2 of Fig. 17). Neutral

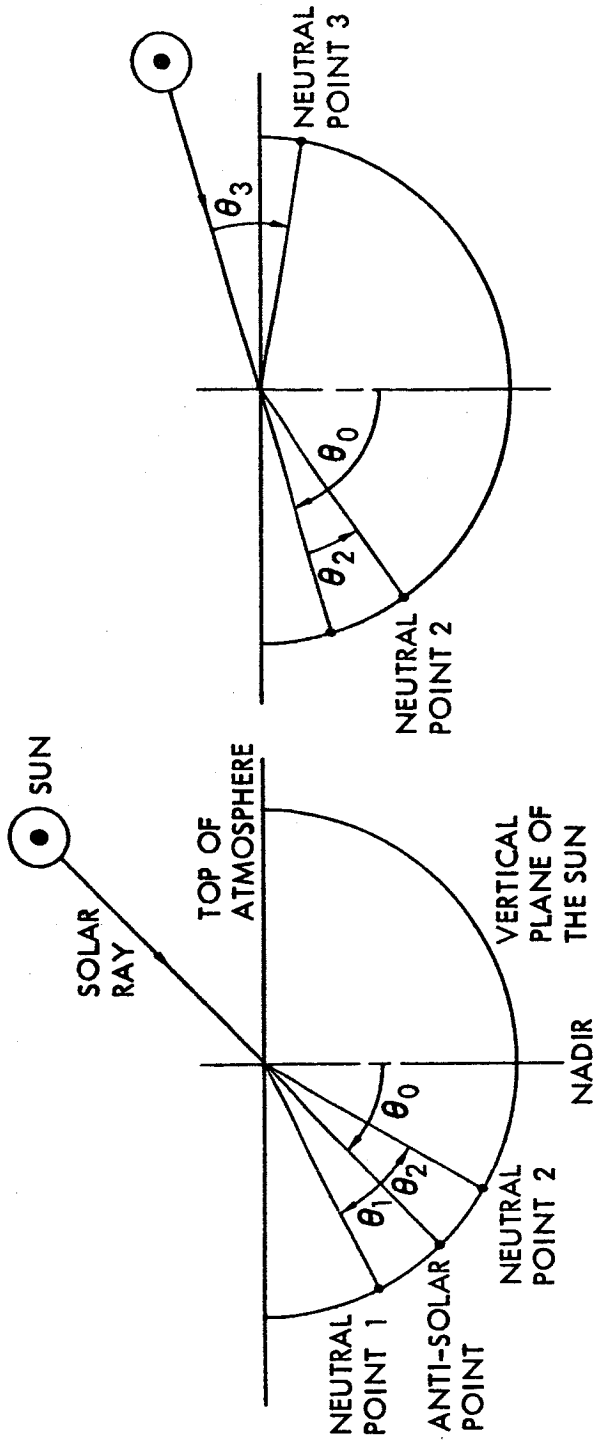

Figure 17. Schematic representation of the neutral points that would appear to an observed above a planetary atmosphere. The ground reflects radiation according to approximately Lambert's law. The left drawing shows the two neutral points that would appear when Θ_o is small. The right drawing shows the two neutral points that would appear when Θ_o is large.

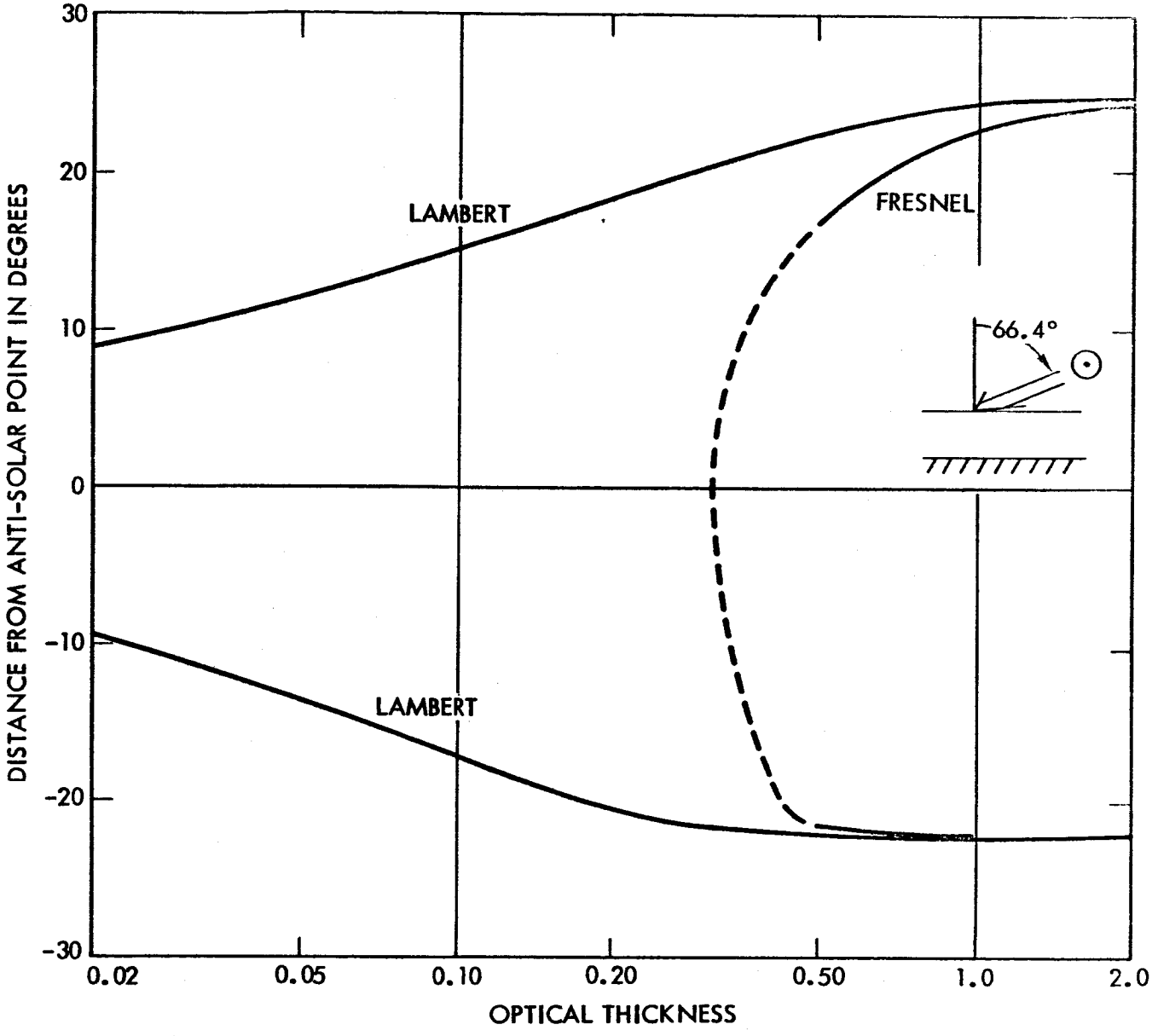

Figure 18. Distance of neutral points from anti-solar point. The distance is negative for neutral point one and positive for neutral point 2. The Fresnel curve is dashed for $0.30 < \tau_1 < 0.50$, where the neutral point positions were not calculated. The solar nadir angle is $\theta_o = 66.4^o$.

point 3 does not appear until the solar nadir angle becomes larger than about 68°. The positions of neutral points that correspond for the Fresnel and Lambert models nearly coincide, when the optical thickness $\tau_1 = 2.0$. As the optical thickness decreases, the neutral points move towards the anti-solar point, but much more rapidly for the Fresnel model. The Fresnel neutral points disappear from the sun's vertical when the optical thickness is less than about 0.3. The Lambert neutral points disappear only when the atmosphere vanishes. The neutral point positions are not shown for the model for which the ground absorbs all radiation that falls on it, since the positions for this and the Lambert model differ by only a few tenths of a degree.

The degree of polarization throughout the entire vertical plane of the sun is shown for the optical thickness ($\tau_1 = 0.25$) that is just below the threshold for the disappearance of the Fresnel neutral points (Fig. 13). The degree of polarization is nearly the same for the Fresnel and zero ground albedo models. Even though the difference is less than 0.07 near the anti-solar point, the neutral points are not present in the Fresnel model, but are present at a large distance of about 20° from the anti-solar point for both the zero ground albedo and Lambert models. If the planetary atmosphere were to contain aerosol particles of the type that are frequently found in continental areas of the earth, then the neutral points would be shifted further from the anti-solar point[13] than is shown for the Lambert model on Fig. 13. Hence, the Fresnel neutral

points are shifted closer to the anti-solar point, or even disappear from the vertical plane of the sun, while the Lambert neutral points may remain far from the sun, both for a Rayleigh atmosphere and for some model atmospheres containing aerosol particles.

The neutral point distances are given as a function of the solar nadir angle on Fig. 19. Three sets of curves for optical thicknesses of 0.25, 0.50 and 1.00 are shown. The neutral point distances of points one and two from the anti-solar point and of point three from the sun are given; these respective distances are indicated by the angles θ_1, θ_2, and θ_3 on Fig. 17. The dashed curves are for the Lambert model and the solid curves are for the Fresnel model. The differences between the Lambert and Fresnel curves are only a few degrees, when the optical thickness $\tau_1 = 1.0$. The differences increase as the optical thickness decreases to 0.50. Then the Fresnel neutral points disappear from the sun's vertical plane for $\theta_o < 24^o$ ($\tau_1 = 0.50$), whereas the Lambert neutral points do not disappear. The neutral point differences increase still more, when the optical thickness decreases to $\tau_1 = 0.25$. The Fresnel neutral point distances that were computed for $\tau_1 = 0.25$ are shown by circles. The curves are dotted where the positions are not known exactly. Fresnel neutral point two disappears for $\theta_o < 75^o$. Two Fresnel neutral points number one exist when the solar nadir angle is between 70^o and 75^o. No Fresnel points exist when the solar nadir angle is less than 70^o, but the Lambert neutral points follow the schematic behavior that was indicated on Fig. 17.

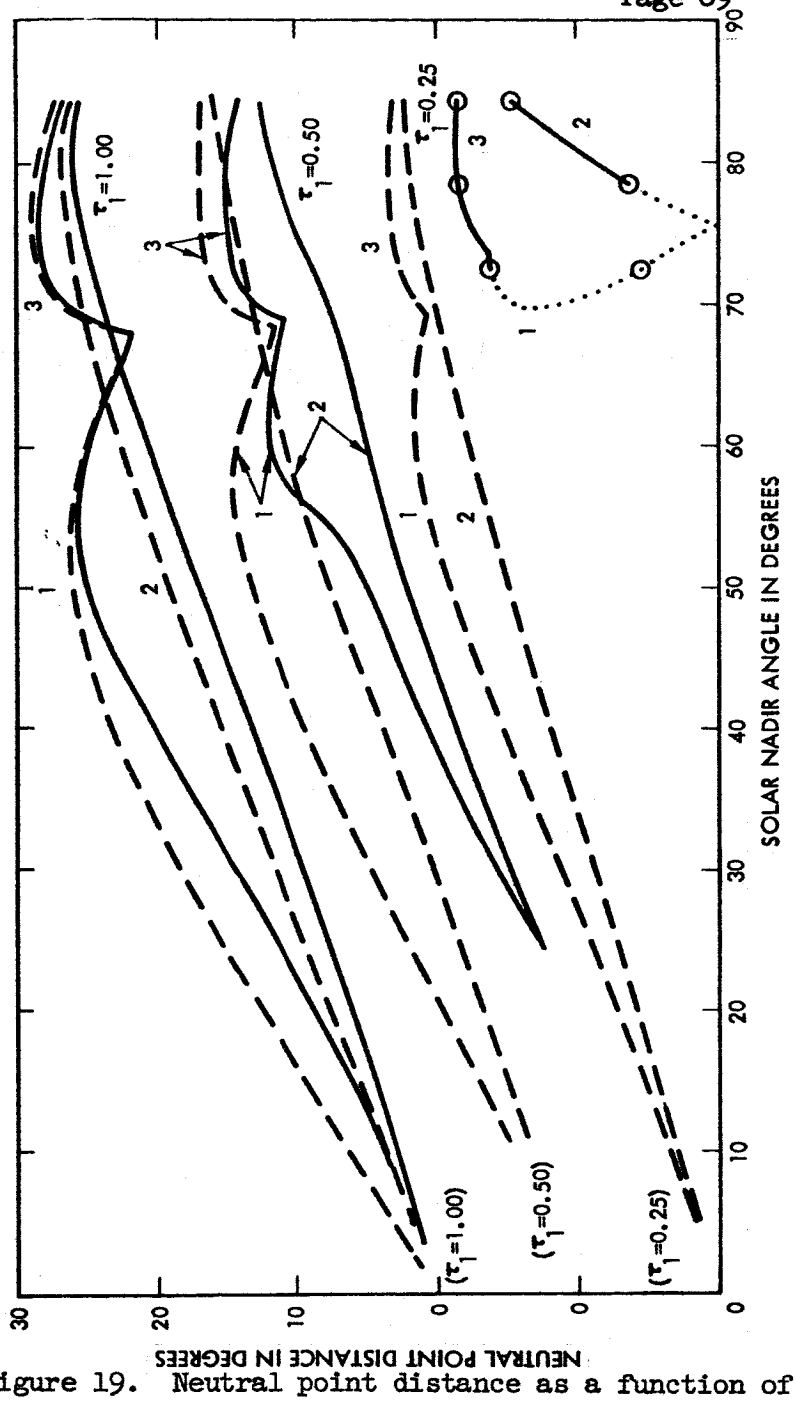

Figure 19. Neutral point distance as a function of solar nadir angle. The dashed and solid curves apply when the ground reflects according to Lambert's and to Fresnel's law, respectively. The origin for each of the three sets is indicated by the optical thickness written next to the origin. The numbers 1, 2 and 3 refer to the neutral points that are given on Fig. 17.

The stream of radiation that is reflected from the ground two or more times in the Fresnel model has a small effect on the neutral point position. For example, when the optical thickness is $\tau_1 = 0.25$, the computed neutral point positions would be shifted 0.5°, if this stream were neglected.

When the ground reflects radiation according to Lambert's law, the neutral points are nearly in the same positions at both the bottom and the top of the atmosphere. However, this is not true for the Fresnel model. The neutral point positions at the bottom and the top of the atmosphere are compared for the two models as a function of the solar nadir angle on Fig. 20. Note that the origin of the ordinate for the Lambert data is 4° above the origin for the Fresnel data. The positions on top of the atmosphere are represented by a continuous line, except that the Fresnel neutral point curves at the top are dotted where $70^\circ < \theta_o < 79^\circ$; and the neutral points at the bottom are represented by a dashed line. The neutral points on the bottom are labeled by their historical names. The Brewster point at the bottom corresponds to point one at the top, the Babinet point corresponds to point 2, and the Arago point corresponds to point 3. Neutral point positions at the bottom differ by less than a few degrees from their corresponding positions at the top for the Lambert model. On the other hand, the corresponding neutral point positions for the top and bottom differ considerably for the Fresnel model. For example, the Fresnel neutral points disappear

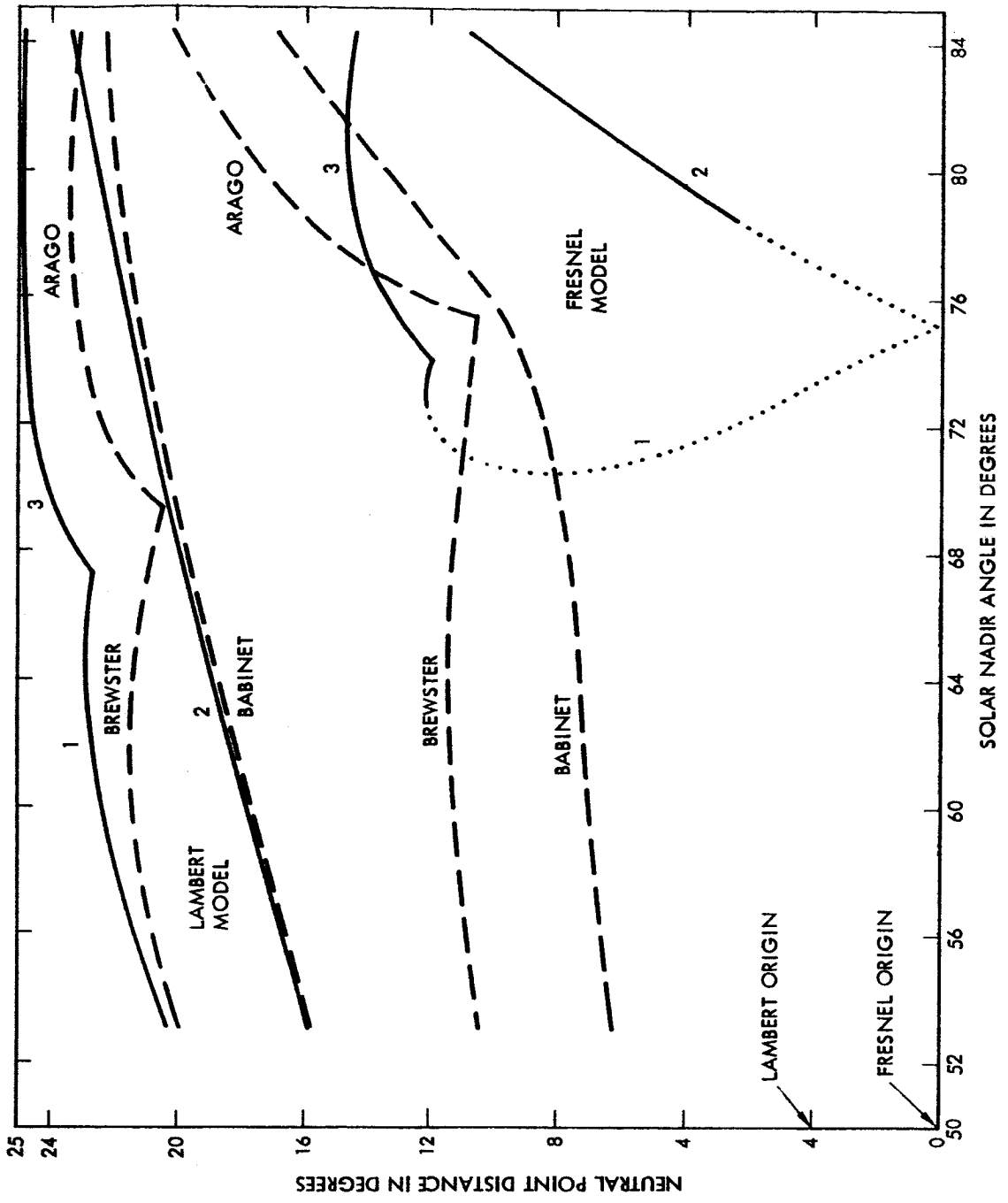

Figure 20. Comparison of neutral point positions at the bottom and at the top of the atmosphere as a function of the solar nadir angle. The Fresnel neutral points number one and two curves are dotted in the region where their positions are not accurately known. The optical thickness $\tau_1 = 0.25$. The origin of the ordinate for the Lambert model is 4° above the origin for the Fresnel model.

from top, when the solar nadir angle is less than 70°; but the Brewster and Babinet points remain at the bottom. Hence, the anomolous neutral point positions on top of an atmosphere above a specularly reflecting ground can not be predicted only with knowledge of the positions at the bottom.

When the neutral points disappear from the sun's vertical plane, physical reasoning indicates that the neutral points should still be visible near the anti-solar point. Additional computations of the neutral point positions should be made, in order to determine their behavior when they are not present in the vertical plane of the sun.

F. Dependence on Index of Refraction

The chief purpose of this section is to see how the significance of the different streams of radiation change as the albedo at the ground increases. Although the computations are made for the Fresnel law of reflection, the results will still indicate the significance of the various streams for other laws of ground reflection.

This section will also show that the radiation parameters at the top of the atmosphere change by a negligible amount for most purposes, when the index of refraction for one wavelength in the vicinity of the visible spectral band changes from a minimum to a maximum value for sea waters. For example, the index of refraction of sea water at $\lambda 5876\text{Å}$ varies from a minimum of 1.3355, when the temperature $T = 30^{\circ}C$ and the

salinity S = 20°/oo, to a maximum of 1.3418, when the temperature T = 0°C and the salinity S = 40°/oo [2] (such high salinities generally are associated with high temperatures). The relative change in the index of refraction is 0.005, which would be nearly independent of wavelength near the visible spectral band.

The albedo at the ground is given as a function of the index of refraction (m) on Fig. 21a for an optical thickness of $\tau_1 = 0.50$ and a solar nadir angle of $\theta_o = 66.4°$. If the radiation field is separated into two components -- the reduced incident solar flux and the airlight--, these two components have nearly the same albedo, which increases as the index of refraction increases. Of course the value of the albedo of both streams of radiation combined is intermediate to the values of the separate streams. As the index of refraction approaches infinity, the albedo approaches one; and when the index of refraction equals one, the albedo is zero.

In general, the albedo at the ground of the airlight and of the direct sunlight differ more than is shown on Fig. 21a. Figure 21b shows the albedos of the separate streams as a function of the solar nadir angle and for an optical thickness of $\tau_1 = 0.50$ and an index of refraction of m = 1.3546. In this case the albedos of the two streams are equal when $\theta_o = 64°$, and are nearly equal when $\theta_o = 66.4°$ as on Fig. 21a. If θ_o is less than 64°, the albedo of the airlight exceeds the albedo of the direct sunlight, and the reverse is true if θ_o is greater than 64°. The albedo of both streams together lies closer to the stream with the largest

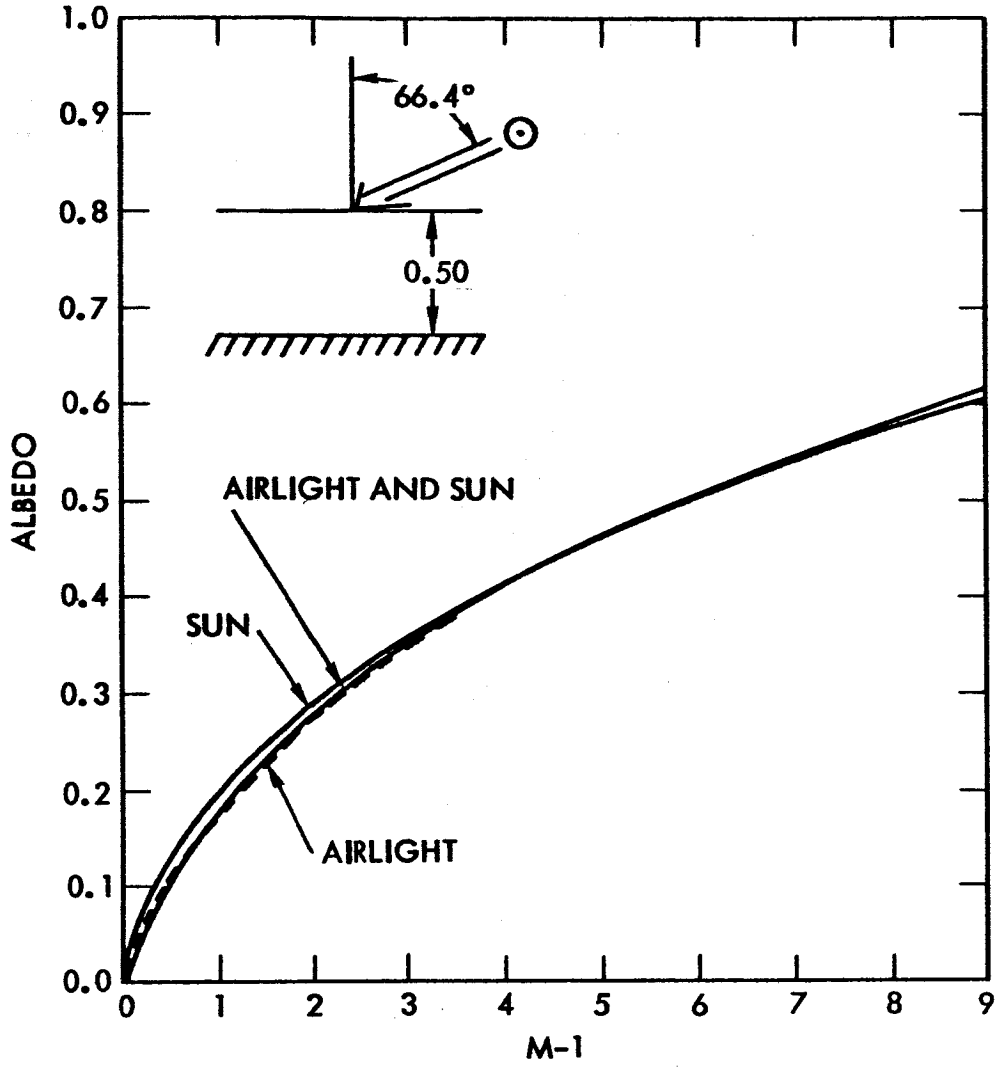

Figure 21a. Albedo at the ground as a function of the index of refraction (m). $\theta_o = 66.4^o$, $\tau_1 = 0.50$.

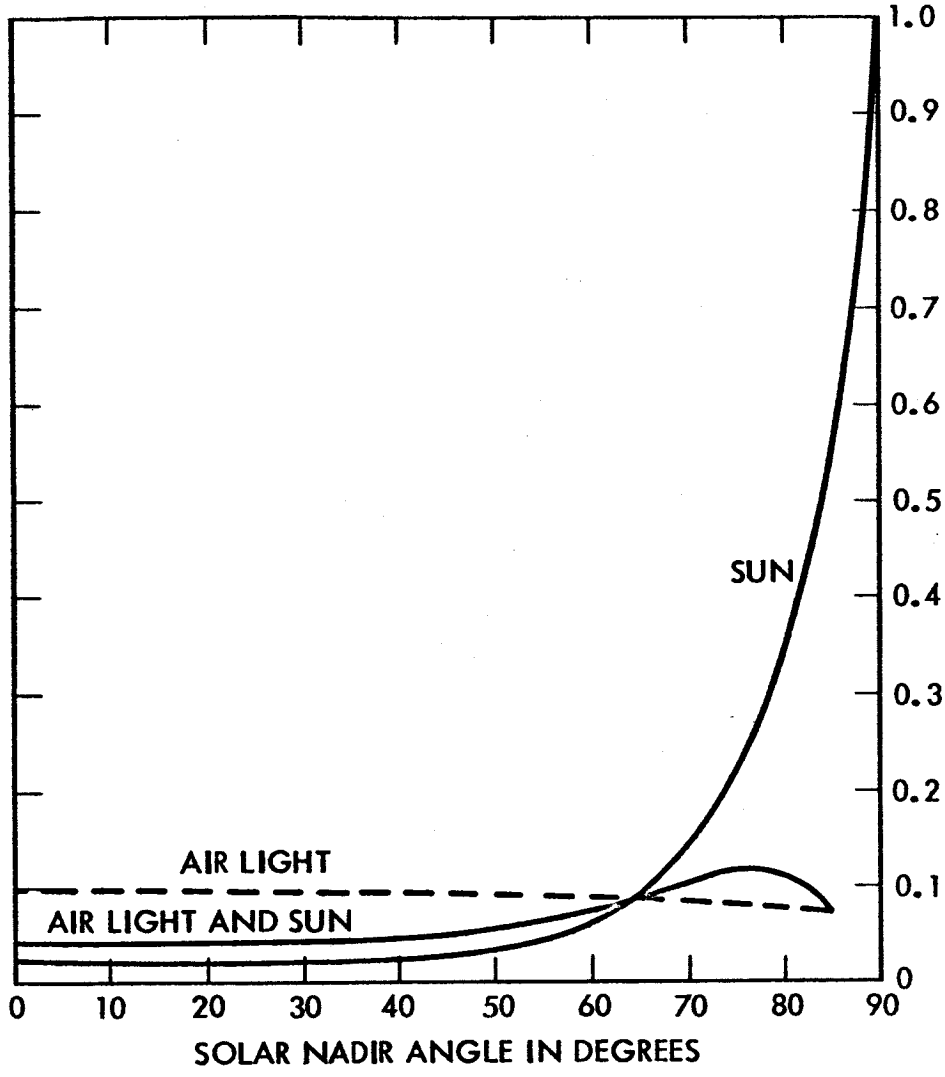

Figure 21b. The albedo of the airlight, of the reduced incident flux (curve labeled sun), and of both at the ground as a function of the solar nadir angle. $\tau_1 = 0.50$; $m = 1.3546$.

downward flux. In general, the solar nadir angle at which the albedos of the two streams are equal will depend on the optical thickness and the index of refraction, since the albedo of the airlight is a function of the optical thickness, and the albedos of both the airlight and direct sunlight are a function of the index of refraction.

The data on Fig. 21a will be used to show that the range of albedo for smooth sea water is small for the visible spectrum. The expression for the change in albedo with respect to wavelength and index of refraction is

$$d\lambda_o^F = \frac{\partial \lambda_o^F}{\partial \lambda} \frac{\partial \lambda}{\partial \tau_1} d\tau_1 + \frac{\partial \lambda_o^F}{\partial m} dm \quad .$$

Replace the differentials with finite differences, apply the formula when $\theta_o = 66.4^o$, and let τ_1 change from 0.02 to 0.50, which corresponds to the approximate limits of the visible spectral band (see Table I). The value of the first term on the right hand side of the above equation is obtained from Fig. 2 and is 0.012. The value of the second term on the right of the above equation is 0.004, since $\Delta\lambda_o/\Delta m = 0.2$ at $m = 4/3$ (Fig. 21a), and the range of the index of refraction for sea water and the visible spectrum is $m < 0.02$.[2,10] Hence, the change in the scattering characteristics of the atmosphere above the sea with a change in wavelength has a stronger effect on the sea albedo than the change of index of refraction with respect to wavelength. The change in albedo of seas with respect to variations in the index of refraction would be small in

comparison with albedo changes that depend on the optical character of the atmosphere and on the roughness of the sea.

The upward flux at the top of the atmosphere of several streams of the radiation field are shown as a function of the index of refraction on Fig. 22. When m = 1, the total flux equals the flux of the airlight that is not reflected from the ground. Since no light is reflected from the ground when m = 1, the other fluxes are zero. As the index of refraction approaches infinity, the total upward flux equals the downward flux. Even when the index is large (m = 10), and as a result the ground albedo is large ($\lambda_o^F(\tau_1) = 0.61$), the upward flux through the top of the atmosphere of radiation that has been reflected from the ground ($\uparrow\mathcal{F}_3$) is less than one-half of the total. The flux at the top of the atmosphere of radiation that has been reflected two or more times from the ground ($\uparrow\mathcal{F}_{3,3}$) is about 0.1 of the total. The total flux changes by only 2×10^{-3} at m = 4/3 as the index of refraction changes by 0.02 between the extreme values for sea water in the visible spectrum. The total upward flux for the Lambert model is not plotted on Fig. 22, since the Lambert flux is only a few per cent greater than the Fresnel flux.

The total upward flux at the top of the atmosphere, when the optical thickness is $\tau_1 = 0.05$, is shown by a dashed line on Fig. 22. This flux is less than the flux for $\tau_1 = 0.50$. The difference is large when m = 1 and decreases to zero as m increases to infinity.

The total intensity at the top of the atmosphere of radiation from the nadir is shown for several streams of radiation as a function

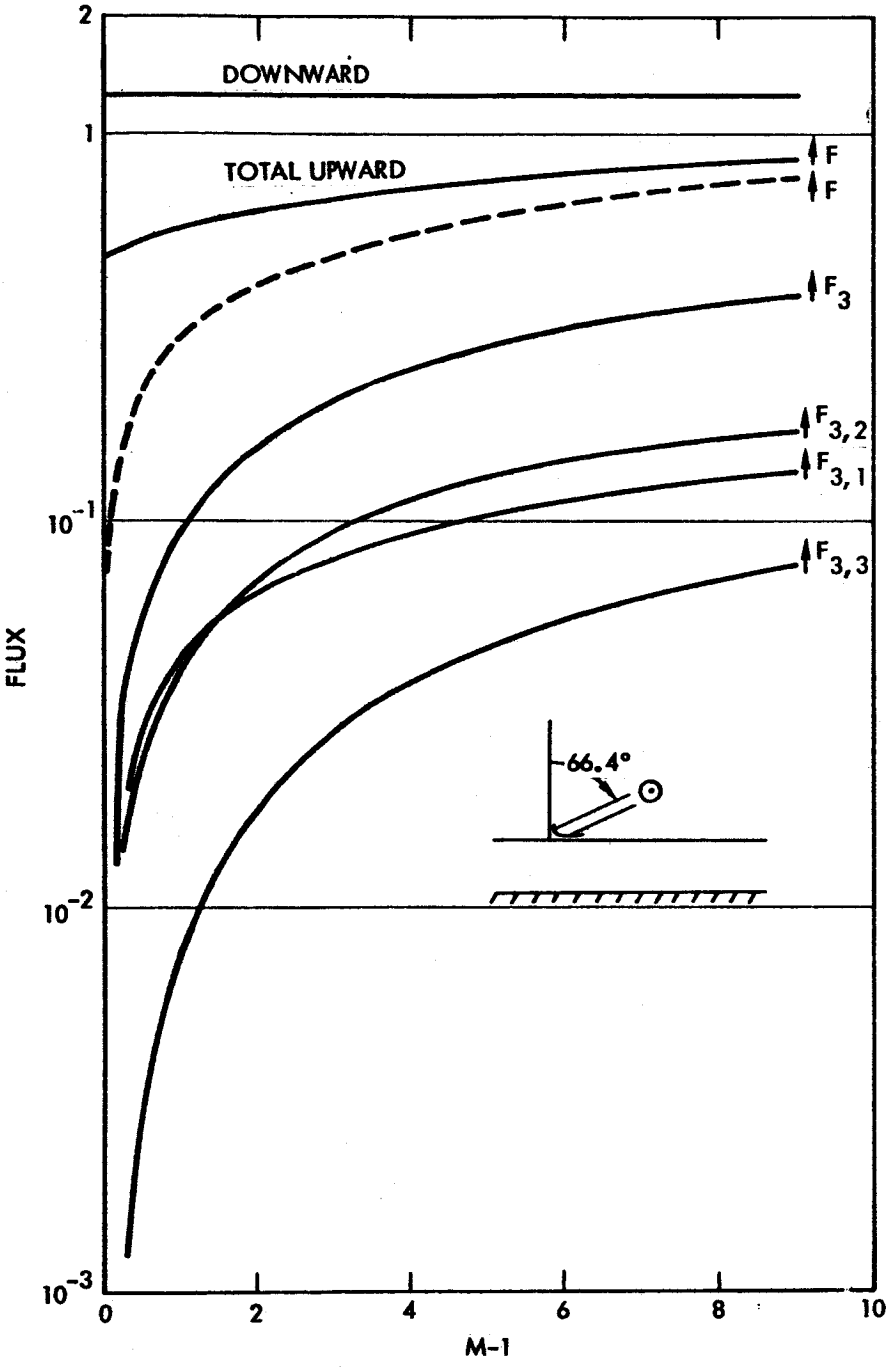

Figure 22. Fluxes at top of the atmosphere as a function of the index of refraction. The dashed curve gives the values of the total upward flux when $\tau_1 = 0.05$. See Section IV.B.2 for an explanation of the flux subscripts. The solar nadir angle is $\theta_o = 66.4^o$; and the optical thickness is $\tau_1 = 0.50$.

of the index of refraction; the solar nadir angle $\theta_o = 66.4^o$, and the optical thickness $\tau_1 = 0.50$ (Fig. 23). Of course, all the streams that are reflected from the ground disappear when m = 1. The intensity of the stream that is reflected from the ground ($\uparrow I_g$) is more than one-half of the total ($\uparrow I^{*F}$) when m is greater than 7.4. The stream of radiation that is reflected two or more times from the ground ($\uparrow I_{g,3}$) is more than one-tenth of the total for large m. Hence, if one wishes to compute intensities at the top of a moderately thick atmosphere with an error of less than 10 per cent, when the ground albedo exceeds 0.50, then, regardless of the law of ground reflection, the intensity of the stream that is reflected from the ground at least twice should be computed, in order to decide if it can be neglected.

Figure 23 also gives other interesting data. The total intensity for the Fresnel model changes in relative value by 0.4 per cent as the index of refraction varies between the extreme indices for sea water. Also, since the intensity from the nadir is greater for the Lambert model ($\uparrow I^{*L}$) than for the Fresnel model ($\uparrow I^{*F}$), the reverse is true toward the limbs, since the fluxes at the top of the atmosphere are nearly the same for both models. Figure 23 also permits a comparison of the total intensities for small (dashed curve) and moderate optical thicknesses for the Fresnel model. The total intensity for the model with the optical thickness $\tau_1 = 0.05$ is about one-tenth of the total intensity for the model with $\tau_1 = 0.50$.

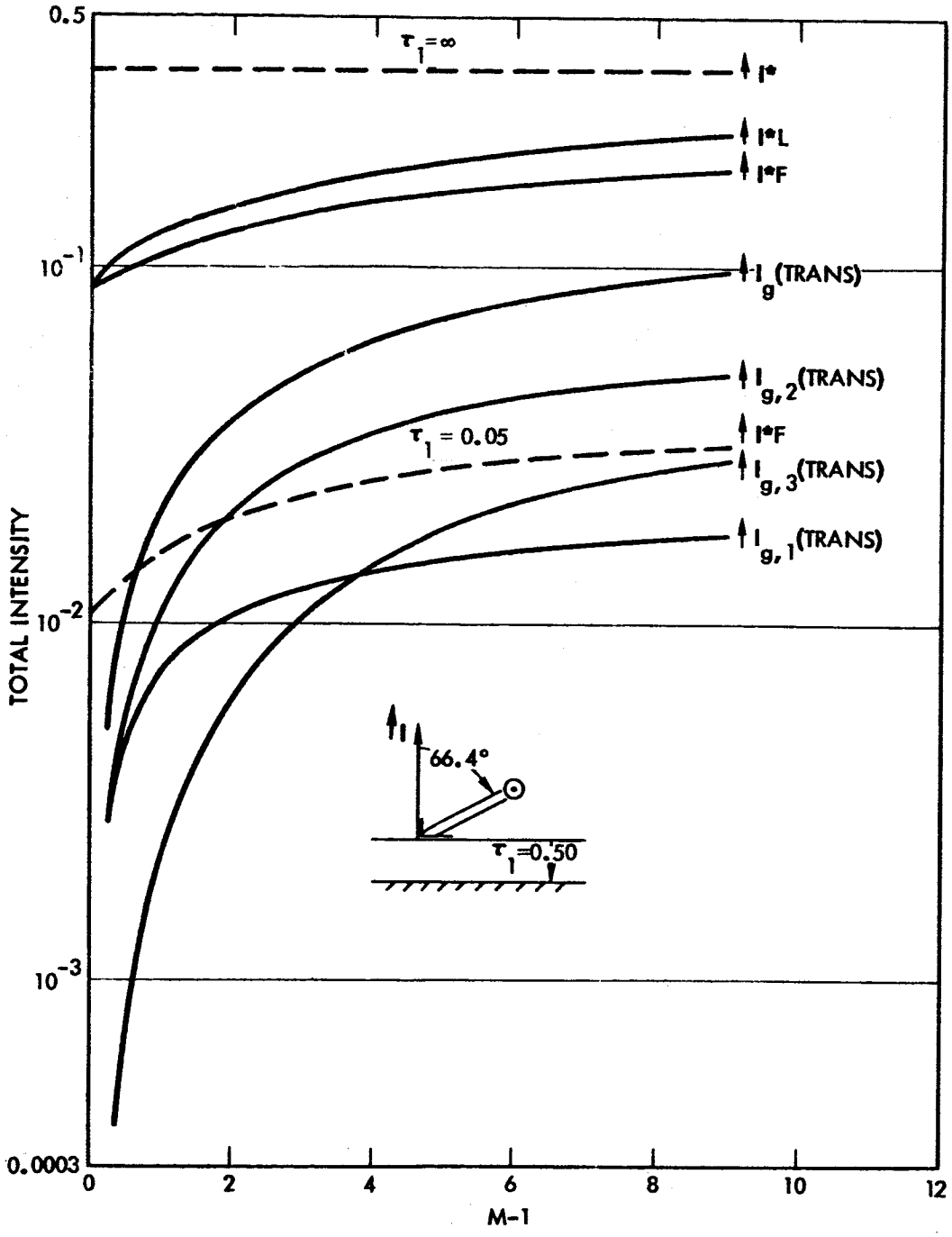

Figure 23. Specific intensity of radiation at the top of the atmosphere and from the nadir as a function of the index of refraction. The two dashed curves give the values of the specific intensity, when $\tau_1 = 0.05$ and ∞. $\theta_o = 66.4^o$; $\tau_1 = 0.50$.

When the radiation field is separated into separate streams, which are designated by subscript i, the resultant degree of polarization in the sun's vertical plane and for the models used here can be expressed in terms of the polarization of the separate streams by the relation

$$P = \frac{\sum_i (I_{r,i} - I_{\ell,i})}{\sum_i (I_{r,i} + I_{\ell,i})}$$

$$= \sum_i \frac{I_i}{I} P_i \quad , \tag{4.4}$$

where $I = \sum_i (I_{r,i} + I_{\ell,i})$, $P_i = (I_{r,i} - I_{\ell,i})(I_{r,i} + I_{\ell,i})^{-1}$, and $U_i = V_i = 0$ in the vertical plane of the sun for the models that are being used here. If Eq. (4.4) is rewritten with the notation that was used in Section IV.C., then the expression for the degree of polarization (P^{*F}) of the radiation leaving the top of the atmosphere becomes

$$P^{*F} = \frac{\uparrow I}{\uparrow I^{*F}} P + \sum_{i=1}^{3} \frac{\uparrow I_{g,i}}{\uparrow I^{*F}} P_{g,i} \quad ,$$

where $\uparrow I^{*F} = \uparrow I + \sum_{i=1}^{3} \uparrow I_{g,i}$. The first term on the right side of Eq. (4.5), for example, gives the contribution to P^{*F} by the airlight that has not been reflected from the ground. Figure 24 gives the fractional contribution of each of the streams to the maximum degree of polarization of light leaving the top of the atmosphere; the solar nadir angle is $\theta_o = 66.4^o$, and the optical thicknesses are 0.05 and 0.50. Of course, when the index of refraction m = 1, the streams that are reflected from the ground do not

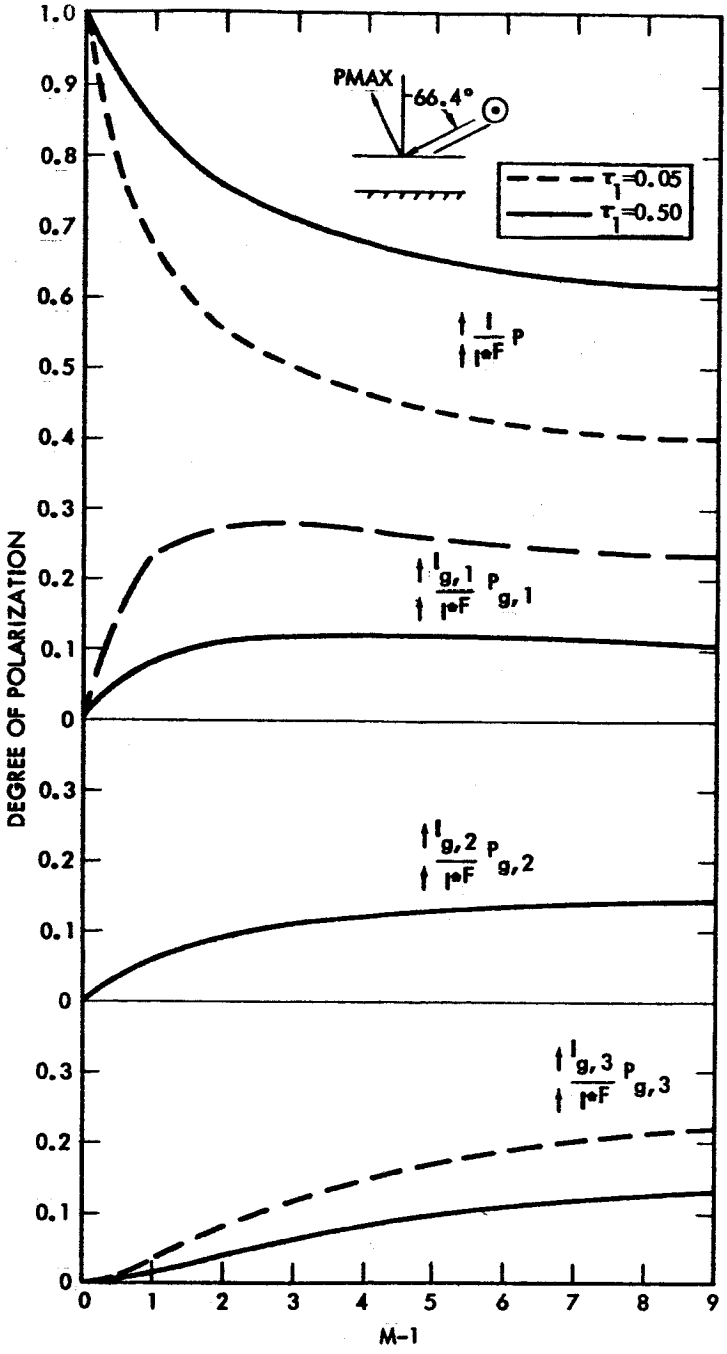

Figure 24. Fractional contributions to the maximum degree of polarization at the top of the atmosphere by different streams of the radiation field. The solar nadir angle is $\theta_o = 66.4^o$.

make any contribution to the resultant degree of polarization, which is then determined solely by the stream that is not reflected from the ground. As the index of refraction increases to m = 10, with an accompanying increase of the ground albedo to $\lambda_o^F(\tau_1) = 0.61$ for both $\tau_1 = 0.05$ and 0.50, the stream that is not reflected from the ground contributes 0.62, when $\tau_1 = 0.50$, and 0.40, when $\tau_1 = 0.05$, of the resultant maximum polarization. The streams that are reflected from the ground carry greater weight at the smaller optical thickness of $\tau_1 = 0.05$. The direct solar flux that has been reflected from the ground ($^{\uparrow}I_{g,1}\ P_{g,1}(^{\uparrow}I^{*F})^{-1}$) makes the largest contribution of any of the ground-reflected streams to the maximum of degree of polarization when the index of refraction is less than two. At larger indices of refraction all three streams that are reflected from the ground make a significant contribution to the maximum degree of polarization. A reason has not yet been found to explain why the fractional contributions of the airlight that has not been reflected from the ground, and then is reflected from the ground just once ($^{\uparrow}I_{g,2}\ P_{g,2}(^{\uparrow}I^{*F})^{-1}$), are the same within a few per cent for both optical thicknesses of 0.05 and 0.50. The similarity for the two optical thicknesses of 0.05 and 0.50 may be fortuitious, since the contribution of $^{\uparrow}I_{g,2}\ P_{g,2}(^{\uparrow}I^{*F})^{-1}$ to the maximum degree of polarization is zero when the optical thickness is either zero or infinite. In these two extreme cases $^{\uparrow}I_{g,2} = 0$.

The absolute value of the maximum degree of polarization of light leaving the top of a model atmosphere is given as a function of the index

of refraction on Fig. 25; the solar nadir angle is $\theta_o = 66.4^o$. The maximum degree of polarization decreases with increasing index of refraction. When the optical thickness $\tau_1 = 0.50$, the maximum polarization decreases more rapidly with increasing index of refraction for the Lambert model than for the Fresnel model, because the intensities of the streams of radiation that are reflected from the ground increase at about the same rate for both models, but the degree of polarization of the Lambert stream is less than that of the Fresnel stream. The maximum degree of polarization changes in relative value by 0.2 per cent as the index of refraction for the visible spectrum varies through the extremes for sea water.

The curves for the two Fresnel models of optical thicknesses 0.05 and 0.50 are nearly parallel (Fig. 25). This would seem to be a coincidence, since the maximum degree of polarization would be a constant for an atmosphere of very large optical thickness. Also, the degree of polarization of light from the nadir, where the polarization is large, does not change at the same rate for both models of $\tau_1 = 0.05$ and 0.50. The degree of polarization of radiation from the nadir increases from 0.70 to 0.74, when $\tau_1 = 0.05$, and decreases from 0.56 to 0.53, when $\tau_1 = 0.50$, as the index of refraction increases from one to ten.

The distances of the neutral points on top of the atmosphere are shown as a function of the index of refraction on top of Fig. 26; the solar nadir angle is $\theta_o = 66.4^o$. The solid and dashed lines give the distances when the optical thicknesses equal $\tau_1 = 0.50$ and $\tau_1 = 0.05$,

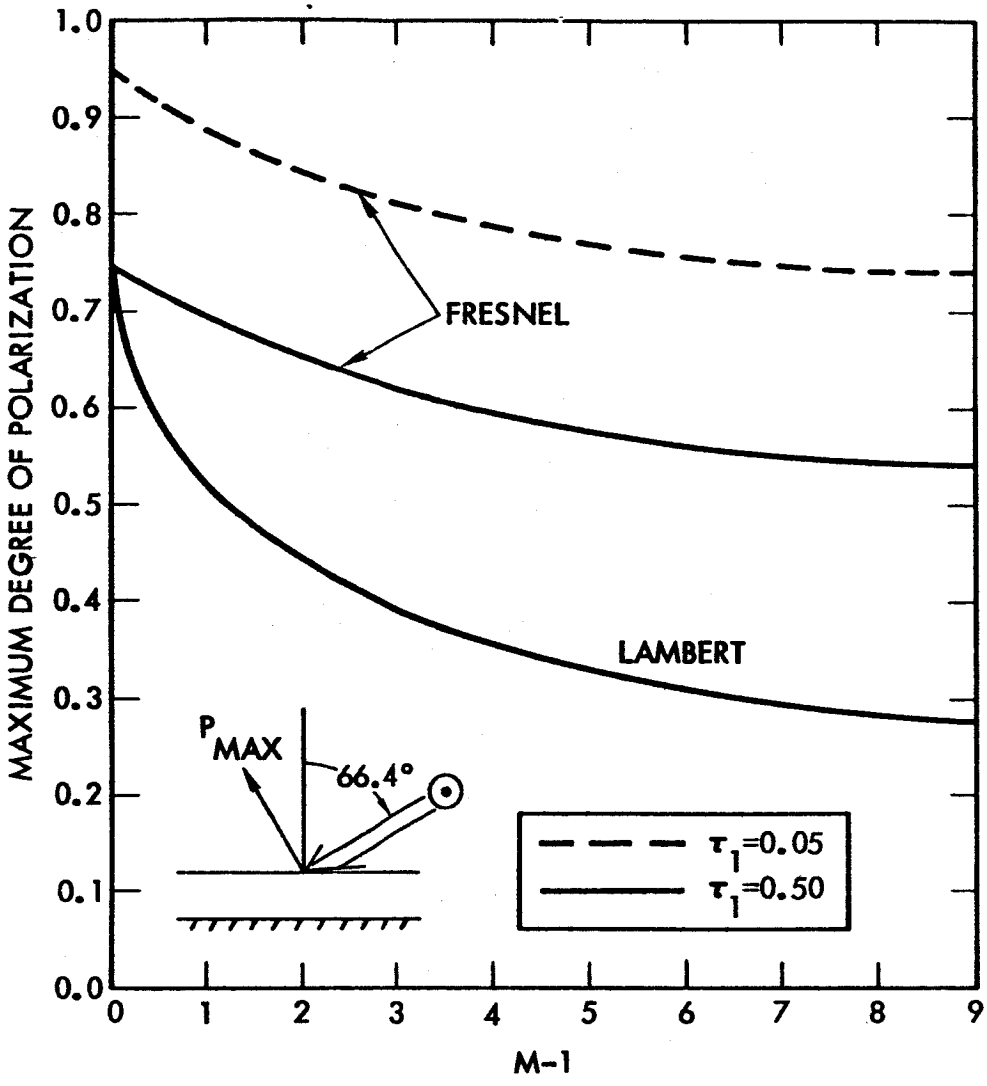

Figure 25. Maximum degree of polarization of radiation leaving the top of the atmosphere in the vertical plane of the sun as a function of the index of refraction. The solar nadir angle is $\Theta_o = 66.4^o$.

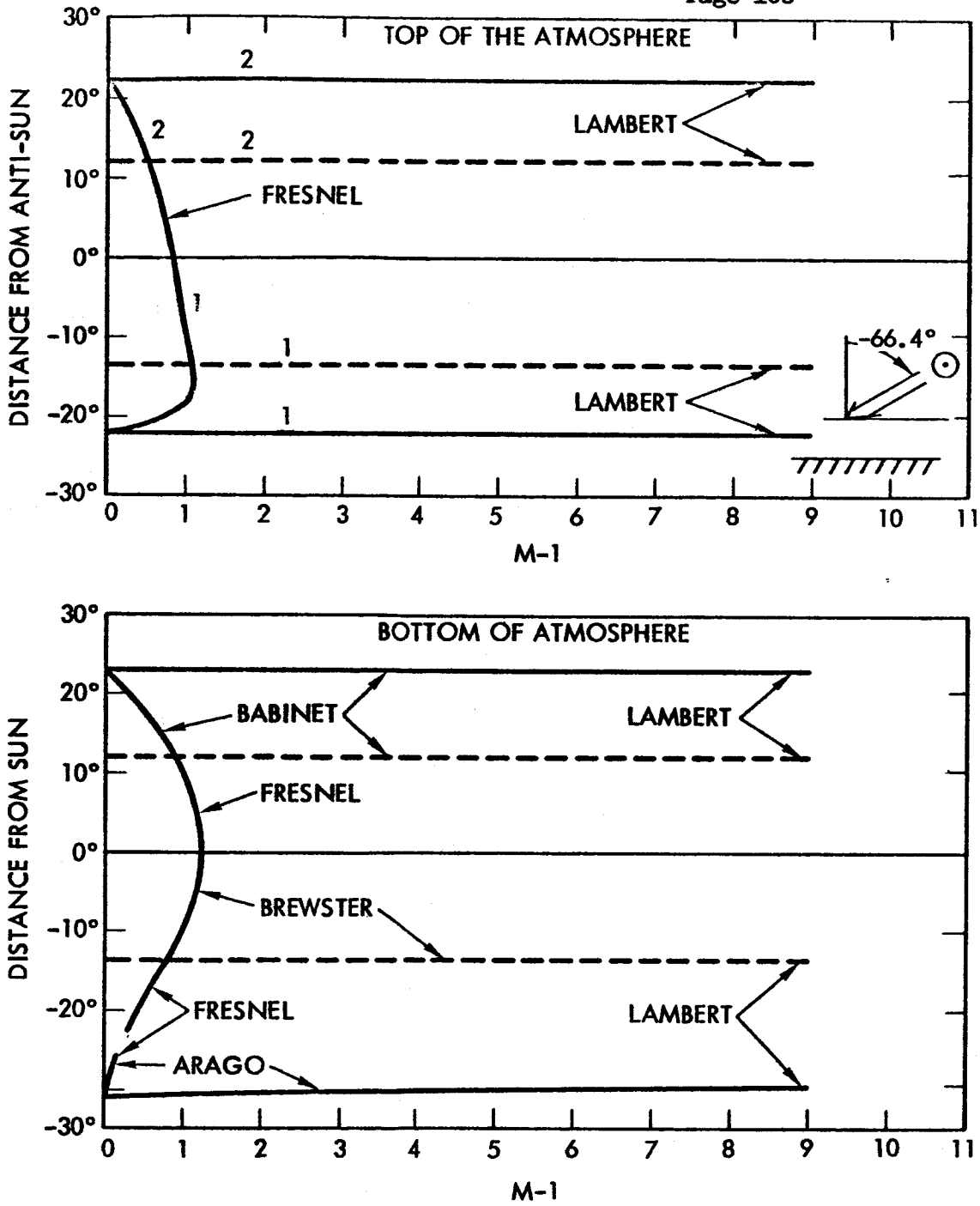

Figure 26. Neutral point distance at the top of the atmosphere as a function of the index of refraction. The solid curves are for $\tau_1 = 0.50$. The dashed curves are for $\tau_1 = 0.05$. The solar nadir angle is $\theta_o = 66.4^o$.

respectively. The neutral point distances for the Lambert model vary by only a few tenths of a degree as the index of refraction varies from one to ten, or as the ground albedo varies from zero to 0.61. The Fresnel neutral points do not even appear in the sun's vertical plane, when $\tau_1 = 0.05$ and $m > 1.34$. (No neutral point positions were calculated for values of the index of refraction between 1 and 1.34). Also, the Fresnel neutral points disappear from the sun's vertical plane for $m > 2.2$ at the moderate optical thickness of $\tau_1 = 0.50$ ($\theta_o = 66.4^o$). A neutral point anomaly is present for the Fresnel model and $\tau_1 = 0.50$. When the index of refraction is between 1.85 and 2.2, no neutral point number one, but two neutral points number two, are present in the vertical plane of the sun. As the index of refraction of sea water varies between its extremes for the visible spectrum, the Fresnel neutral points one and two would shift by 0.1^o, and 0.4^o, respectively.

Because of the interest in the neutral points at the bottom of the atmosphere, these are shown as a function of the index of refraction on the bottom of Fig. 26. The neutral points for the Lambert model are nearly independent of the index of refraction, or more specifically, the ground albedo. By comparing the Lambert neutral point positions at the bottom with those at the top, one sees that the Lambert neutral points lie within a few tenths of a degree of the same place, when the optical thickness $\tau_1 = 0.05$. However, this exact symmetry does not appear when $\tau_1 = 0.50$. Then the Babinet point lies in nearly the same place at both

the bottom and top, but an Arago point* is present at the bottom, whereas the corresponding point does not appear at the top. Instead, neutral point one is present at the top.

There is not very much similarity between the neutral point positions at the top and bottom for the Fresnel model. No Fresnel neutral points are present at the bottom in the vertical plane of sun, except at the index of refraction m = 1, and perhaps slightly larger, when $\tau_1 = 0.05$ ($\theta_o = 66.4^o$). When $\tau_1 = 0.50$, an Arago point is present at small index of refraction. The Arago point disappears as m increases, and is replaced by a Brewster point before the index of refraction reaches the value of m = 1.35. The Fresnel neutral points disappear from the vertical plane of the sun, when the index of refraction exceeds 2.2 ($\tau_1 = 0.50$). The disappearance of the neutral points from the sun's vertical at both the top and bottom for the same index of plane refraction again would seem to be fortuitious, since the neutral point positions do not coincide at the top and bottom. When the neutral points disappear from the sun's vertical plane, they are expected to continue to exist near the sun, at the bottom, and near the anti-solar point, at the top of the atmosphere.

---

* The Arago point distance is the angle between the anti-solar point and the Arago point.

V. SUMMARY

In order to make these conclusions precise, they will apply only to two models that have been used in this report. The models are based on the assumptions that the atmosphere is plane-parallel, homogeneous, non-absorbing, and scatters radiation according to Rayleigh's law, and that the ground reflects radiation according to either Fresnel's or Lambert's law. Unless stated otherwise, the ground is assumed to have the index of refraction of water. The atmosphere is illuminated on the top by parallel radiation.

The type of ground reflection will have an important influence on the characteristics of the radiation leaving the top of the atmosphere. At the ground, however, the neutral point position is the only parameter of the downward radiation that changes significantly from the Lambert to the Fresnel model. Of course, the radiation leaving the top of an infinitely thick atmosphere is unaffected by the ground. When the optical thickness decreases to less than one, the specific intensity, degree of polarization, and neutral point positions, but not the upward flux, depend significantly on whether or not the ground reflects radiation according to the Fresnel or the Lambert law. Since the relative difference in the fluxes for the two extreme models of ground reflection having the same optical thickness is less than 0.06, the flux would seem to be insensitive to other natural laws of ground reflection, as long as the ground albedo does not change. Because of this, the computations for the flux

are simplified: one can proceed on the assumption that the ground reflects radiation according to Lambert's law, instead of using the true law of reflection at the ground.

When the ground has a small index of refraction, as in the case of water, the stream of radiation which has been reflected from the ground two or more times has but small effect on the radiation field, and can be neglected. However, when the ground albedo exceeds fifty per cent, this stream becomes significant. As an example, on condition that: the atmosphere is of moderate optical thickness ($\tau_1 = 0.50$); the ground reflects according to Fresnel's law; the albedo is above 50 per cent; and the solar nadir angle is $\theta_o = 66.4$, then the twice-reflected streams contribute more than 7 per cent of the upward flux and 10 per cent to the maximum degree of polarization at the top of the atmosphere. This twice-reflected stream of radiation becomes more important for atmospheres of optical thickness smaller than 0.50. Hence, when the ground albedo exceeds 50 per cent and the atmospheric optical thickness is moderate or smaller, one can not neglect the twice-reflected stream and be confident that he can compute the radiation parameters at the top of the atmosphere with an error of less than 10 per cent.

The neutral point positions at the top of the atmosphere are completely different for the Fresnel and Lambert models, when the optical thickness is moderate or smaller. When the optical thickness is $\tau_1 = 0.50$, the neutral points are as much as 10^o closer to the sun for the Fresnel

model as for the Lambert model. At an optical thickness of $\tau_1 = 0.25$, the Fresnel neutral points disappear from the vertical plane of the sun for solar nadir angles smaller than 70°, but not the Lambert neutral points. The Fresnel neutral points disappear from the sun's vertical plane at larger solar nadir angles when the optical thickness is smaller, but the Lambert neutral points remain in the sun's vertical plane. When the Fresnel neutral points disappear from the sun's vertical plane, they are expected to continue to exist near the anti-solar point. Because the neutral point positions are sensitive to the aerosol content of an atmosphere and to the type of ground reflection, their characteristics outside of the sun's vertical plane should be investigated.

VI. ACKNOWLEDGEMENTS

As I made clear in Section III., I am extremely grateful to Dr. Dave for the assistance that he gave to me. I wish to thank the National Center of Atmospheric Research for inviting me to visit them and for their computer services.

VII. BIBLIOGRAPHY

1. Atroshenko, V. S., E. M. Feigelson, K. S. Glazova, and M. S. Malkevich, Calculation of the Brightness of Light - Part 2 (Consultants Bureau, New York, 1963), 226 p.

2. Bein, W. (1935); his data are given in G. Dietrich, General Oceanography (Interscience Publ., New York, 1957), 74-75.

3. Brewster, D., On the polarization of the atmosphere, Royal Soc. of Edinburgh Transactions, 23, 211 (1861-1864).

4. Chandrasekhar, S., Radiative Transfer (Claredon Press, Oxford, England, 1st ed., 1950), 393 p.

5. Coulson, K. L., Characteristics of the radiation emerging from the top of a Rayleigh atmosphere, Planet. Space Sci. 1, 265, 277 (1959).

6. Coulson, K. L., J. V. Dave and Z. Sekera, Tables Related to Radiation Emerging from a Planetary Atmosphere with Rayleigh Scattering (University of California Press, Los Angeles, 1960), 548 p.

7. Cox, C., and W. Munk, Some problems in optical oceanography, Jo. Marine Res. 14, 63 (1955).

8. Dave, J. V. and Z. Sekera, Private communication.

9. Deirmendjian, D., The optical thickness of the molecular atmosphere, Archiv. Meteor. Geophys. Biolkim., B, 6, 452 (1955).

10. Dorsey, N. E., Properties of Ordinary Water-Substance (Reinhold Pub. Corp., New York, 1940) 284, 295.

11. Feigelson, E. M., M. S. Malkevich, S. Ya. Kogan, T. D. Koronatova, K. S. Glazova, and M. A. Kuznetsova, Calculation of the Brightness of Light - Part 1 (Consultants Bureau, Inc., New York, 1960), 104 p.

12. Forsythe, W. E., Smithsonian Physical Tables (Smithsonian Institution, Washington, 9th ed., 1959), 532.

13. Fraser, R. S., Computed intensity and polarization of light scattered outwards from the earth and an overlying aerosol, Jo. Opt. Soc. Amer. 54, 157 (1964).

14. Fraser, R. S. and Z. Sekera, The effect of specular reflection in a Rayleigh atmosphere, Appen. E of Investigation Polarization of Skylight (University of California, Los Angeles, Dept. of Meteorology, 1955), 12 p.

15. Gifford, cited in reference 10, p. 295.

16. Hildebrand, F. B., Methods of Applied Mathematics (Prentice-Hall, Inc., New York, 1952), 421-424.

17. Hodgman, C. D. (Ed.), Handbook of Chemistry and Physics (The Chemical Rubber Publishing Co., Cleveland, 43rd ed., 1961), 3025.

18. Hulburt, E. O., The polarization of light at sea, Jo. Opt. Soc. Amer. 24, 35 (1934).

19. Jensen, C., Die Polarisation des Himmelslicht, Handbuch der Geophysik, VIII, Lieferung 2-3, 527 (1942).

20. Neuberger, H., Beiträge zur Untersuchung des atmosphärischen Reinheitsgrade, Deutsche Seewarte 56, 1 (1936).

21. Neuberger, H., Introduction to Physical Meteorology (The Pennsylvania State Collete, State College, Pa., 1951), 271 pp.

22. Scarborough, J. B., Numerical Mathematical Analysis (The John Hopkins Press, Baltimore, 1930), pp. 114-115.

23. Sekera, Z., Polarization of skylight; In: Handbuch der Physik 48, Ed. J. Bartels (Springer-Verlag, Berlin, 1957), p. 288-328.

24. Sekera, Z., The effect of sea reflection on the sky radiation, Union Geodesique et Geophysique Internationale Monogr. 10, 66 (1961).

25. Soret, J. L., Influence des surfaces d'eau sur la polarisation atmosphèrique et observation de deux points neutres à droite et à gauche de Soleil, Comptes Rendus, 107, 867 (1888).